

Additional salmon farms in Tory Channel

An assessment of effects on water-quality using a biophysical model

Prepared for Ministry for Primary Industries

14 October 2016

Prepared by:
Niall Broekhuizen
Mark Hadfield

For any information regarding this report please contact:

Niall Broekhuizen
Ecological Modeller
Coastal & Estuarine Processes
+64-7-856 1798
niall.broekhuizen@niwa.co.nz

National Institute of Water & Atmospheric Research Ltd
PO Box 11115
Hamilton 3251

Phone +64 7 856 7026

NIWA CLIENT REPORT No: HAM2015-039
Report date: 14 October 2016
NIWA Project: MPI15204 & MPI17202

Quality Assurance Statement		
	Reviewed by:	Graham Rickard
	Formatting checked by:	Alison Bartley
	Approved for release by:	Andrew Forsythe

© All rights reserved. This publication may not be reproduced or copied in any form without the permission of the copyright owner(s). Such permission is only to be given in accordance with the terms of the client's contract with NIWA. This copyright extends to all forms of copying and any storage of material in any kind of information retrieval system.

Whilst NIWA has used all reasonable endeavours to ensure that the information contained in this document is accurate, NIWA does not give any express or implied warranty as to the completeness of the information contained herein, or that it will be suitable for any purpose(s) other than those specifically contemplated during the Project or agreed by NIWA and the Client.

Contents

- Executive summary 8**
- 1 Introduction 12**
 - 1.1 Scenarios..... 13
- 2 Methods..... 16**
 - 2.1 Revised Cook Strait tidal hydrodynamic data..... 16
 - 2.2 Revised representation of the sinking of faeces, pseudo-faeces & uneaten food..... 19
 - 2.3 Farm characteristics..... 19
 - 2.4 Analysis and presentation of results..... 20
- 3 Results 23**
 - 3.1 Model performance: comparison of the ‘existing operating conditions’ scenario with field data 23
 - 3.2 Single-additional-farm scenarios relative to baseline_{f2016} (AM_AF_WD) 24
 - 3.3 Multiple-additional-farm scenarios relative to baseline_{f2016} (AM_AF_WD) 37
 - 3.4 Baseline_{f2016}+Tipi2+Motu5+Weka5 (AM_AF_WD+Tipi2+Motu5+Weka5) in comparison with operating farms (EM_EF_WD) 50
- 4 Discussion & Implications..... 60**
 - 4.1 Modelling limitations..... 61
 - 4.2 Water-quality thresholds..... 64
 - 4.3 Assessment relative to water-quality standards 65
 - 4.4 Onapua Bay..... 67
- 5 Conclusions 68**
- 6 Acknowledgements 69**
- 7 References..... 70**
- Appendix A Time-series from the single additional farm scenarios (concentration difference)..... 72**
- Appendix B Time-series from the single additional farm scenarios (relative concentration) 77**
- Appendix C Time-series from the multiple additional farm scenarios (concentration change)..... 82**

Appendix D	Time-series from the multiple additional farm scenarios (relative concentration)	87
Appendix E	Time-series of concentration difference between the baseline_{f2016}+Tipi2+Motu5+Weka5 (AM_AF_WD+Tipi2+Motu5+Weka5) and operating farms (EM_EF_WD) scenarios.....	92

Tables

Table 1-1:	Descriptions of the eight scenarios which we have considered.	13
Table 1-2:	Total feed inputs (tonne) associated with the farms of each scenario.	15
Table 2-1:	Comparison of M2 tidal sea level parameters.	17
Table 2-2:	Equilibrium flushing times for Queen Charlotte Sound.	18
Table 3-1:	Mean and standard deviation (across all five Marlborough District Council monitoring sites) of measured and simulated chlorophyll concentration.	24

Figures

Figure 1-1:	Map of Queen Charlotte Sound and Tory Channel showing the locations of the five existing farms, the three potential new farm sites and the five Marlborough District Council monitoring sites.	12
Figure 2-1:	Accumulation of tracer from the 200 m flushing simulation using the revised tidal forcing.	18
Figure 3-1:	Simulated dynamics of water-quality state-variables in the uppermost layer at station QCS-1 (inner Grove Arm) under differing single additional fish-farm scenarios.	26
Figure 3-2:	Simulated dynamics of water-quality state-variables in the uppermost layer at station QCS-2 (outer Grove Arm) under differing single additional fish-farm scenarios.	27
Figure 3-3:	Simulated dynamics of water-quality state-variables in the uppermost layer at station QCS-3 (Tory Channel) under differing single additional fish-farm scenarios.	28
Figure 3-4:	Simulated dynamics of water-quality state-variables in the uppermost layer at station QCS-4 (inner/central Queen Charlotte) under differing single additional fish-farm scenarios.	29
Figure 3-5:	Simulated dynamics of water-quality state-variables in the uppermost layer at station QCS-5 (outer Queen Charlotte) under differing single additional fish-farm scenarios.	30
Figure 3-6:	False colour maps of time-averaged, winter-time, near-surface water-quality characteristics for the AM_AF_WD and AM_AF_WD+Tipi2 scenarios.	32
Figure 3-7:	False colour maps of time-averaged, summer-time, near-surface water-quality characteristics for the AM_AF_WD and AM_AF_WD+Tipi2 scenarios.	33

Figure 3-8:	False colour maps of time-averaged, winter-time, near-surface water-quality characteristics for the AM_AF_WD and AM_AF_WD+Motu5 scenarios.	34
Figure 3-9:	False colour maps of time-averaged, summer-time, near-surface water-quality characteristics for the AM_AF_WD and AM_AF_WD+Motu5 scenarios.	35
Figure 3-10:	False colour maps of time-averaged, winter-time, near-surface water-quality characteristics for the AM_AF_WD and AM_AF_WD+Weka5 scenarios.	36
Figure 3-11:	False colour maps of time-averaged, summer-time, near-surface water-quality characteristics for the AM_AF_WD and AM_AF_WD+Weka5 scenarios.	37
Figure 3-12:	Simulated dynamics of water-quality state-variables in the uppermost layer at station QCS-1 (inner Grove Arm) under differing multiple additional fish-farm scenarios.	39
Figure 3-13:	Simulated dynamics of water-quality state-variables in the uppermost layer at station QCS-2 (outer Grove Arm) under differing multiple additional fish-farm scenarios.	40
Figure 3-14:	Simulated dynamics of water-quality state-variables in the uppermost layer at station QCS-3 (Tory Channel) under differing multiple additional fish-farm scenarios.	41
Figure 3-15:	Simulated dynamics of water-quality state-variables in the uppermost layer at station QCS-4 (inner/central Queen Charlotte) under differing multiple additional fish-farm scenarios.	42
Figure 3-16:	Simulated dynamics of water-quality state-variables in the uppermost layer at station QCS-5 (outer Queen Charlotte) under differing multiple additional fish-farm scenarios.	43
Figure 3-17:	False colour maps of time-averaged, winter-time, near-surface water-quality characteristics for the AM_AF_WD and AM_AF_WD+Tipi2+Motu5 scenarios.	45
Figure 3-18:	False colour maps of time-averaged, summer-time, near-surface water-quality characteristics for the AM_AF_WD and AM_AF_WD+Tipi2+Motu5 scenarios.	46
Figure 3-19:	False colour maps of time-averaged, winter-time, near-surface water-quality characteristics for the AM_AF_WD and AM_AF_WD+Tipi2+Motu5+Weka5 scenarios.	47
Figure 3-20:	False colour maps of time-averaged, summer-time, near-surface water-quality characteristics for the AM_AF_WD and AM_AF_WD+Tipi2+Motu5+Weka5 scenarios.	48
Figure 3-21:	False colour maps of time-averaged, winter-time, near-surface water-quality characteristics for the AM_AF_WD and AM_SF_WD+Tipi2+Motu5+Weka5 scenario.	49
Figure 3-22:	False colour maps of time-averaged, summer-time, near-surface water-quality characteristics for the AM_AF_WD and AM_SF_WD+Tipi2+Motu5+Weka5 scenario.	50
Figure 3-23:	Simulated dynamics of water-quality state-variables in the uppermost layer at station QCS-1 (inner Grove Arm) in the EM_EF_WD and AM_AD_WF+Tipi2+Motu5+Weka5 scenarios.	52

Figure 3-24:	Simulated dynamics of water-quality state-variables in the uppermost layer at station QCS-2 (outer Grove Arm) in the EM_EF_WD and AM_AD_WF+Tipi2+Motu5+Weka5 scenarios.	53
Figure 3-25:	Simulated dynamics of water-quality state-variables in the uppermost layer at station QCS-3 (Tory Channel) in the EM_EF_WD and AM_AD_WF+Tipi2+Motu5+Weka5 scenarios.	54
Figure 3-26:	Simulated dynamics of water-quality state-variables in the uppermost layer at station QCS-4 (inner/central Queen Charlotte) in the EM_EF_WD and AM_AD_WF+Tipi2+Motu5+Weka5 scenarios.	55
Figure 3-27:	Simulated dynamics of water-quality state-variables in the uppermost layer at station QCS-5 (outer Queen Charlotte) in the EM_EF_WD and AM_AD_WF+Tipi2+Motu5+Weka5 scenarios.	56
Figure 3-28:	False colour maps of time-averaged, winter-time, near-surface water-quality characteristics for the EM_EF_WD and AM_AF_WD+Tipi2+Motu5+Weka5 scenarios.	58
Figure 3-29:	False colour maps of time-averaged, summer-time, near-surface water-quality characteristics for the EM_EF_WD and AM_AF_WD+Tipi2+Motu5+Weka5 scenarios.	59
Figure A-1:	Simulated dynamics of water-quality state-variables in the uppermost layer at station QCS-1 under differing single additional fish-farm scenarios.	72
Figure A-2:	Simulated dynamics of water-quality state-variables in the uppermost layer at station QCS-2 under differing single additional fish-farm scenarios.	73
Figure A-3:	Simulated dynamics of water-quality state-variables in the uppermost layer at station QCS-3 under differing single additional fish-farm scenarios.	74
Figure A-4:	Simulated dynamics of water-quality state-variables in the uppermost layer at station QCS-4 under differing single additional fish-farm scenarios.	75
Figure A-5:	Simulated dynamics of water-quality state-variables in the uppermost layer at station QCS-5 under differing single additional fish-farm scenarios.	76
Figure B-1:	Simulated dynamics of water-quality state-variables in the uppermost layer at station QCS-1 under differing single additional fish-farm scenarios.	77
Figure B-2:	Simulated dynamics of water-quality state-variables in the uppermost layer at station QCS-2 under differing single additional fish-farm scenarios.	78
Figure B-3:	Simulated dynamics of water-quality state-variables in the uppermost layer at station QCS-3 under differing single additional fish-farm scenarios.	79
Figure B-4:	Simulated dynamics of water-quality state-variables in the uppermost layer at station QCS-4 under differing single additional fish-farm scenarios.	80
Figure B-5:	Simulated dynamics of water-quality state-variables in the uppermost layer at station QCS-5 under differing single additional fish-farm scenarios.	81
Figure C-1:	Simulated dynamics of water-quality state-variables in the uppermost layer at station QCS-1 under differing single additional fish-farm scenarios.	82
Figure C-2:	Simulated dynamics of water-quality state-variables in the uppermost layer at station QCS-2 under differing single additional fish-farm scenarios.	83
Figure C-3:	Simulated dynamics of water-quality state-variables in the uppermost layer at station QCS-3 under differing single additional fish-farm scenarios.	84
Figure C-4:	Simulated dynamics of water-quality state-variables in the uppermost layer at station QCS-4 under differing single additional fish-farm scenarios.	85

Figure C-5:	Simulated dynamics of water-quality state-variables in the uppermost layer at station QCS-5 under differing single additional fish-farm scenarios.	86
Figure D-1:	Simulated dynamics of water-quality state-variables in the uppermost layer at station QCS-1 under differing multiple-additional fish-farm scenarios.	87
Figure D-2:	Simulated dynamics of water-quality state-variables in the uppermost layer at station QCS-2 under differing multiple-additional fish-farm scenarios.	88
Figure D-3:	Simulated dynamics of water-quality state-variables in the uppermost layer at station QCS-3 under differing multiple-additional fish-farm scenarios.	89
Figure D-4:	Simulated dynamics of water-quality state-variables in the uppermost layer at station QCS-4 under differing multiple-additional fish-farm scenarios.	90
Figure D-5:	Simulated dynamics of water-quality state-variables in the uppermost layer at station QCS-5 under differing multiple-additional fish-farm scenarios.	91
Figure E-1:	Simulated dynamics of water-quality state-variables in the uppermost layer at station QCS-1.	92
Figure E-2:	Simulated dynamics of water-quality state-variables in the uppermost layer at station QCS-2 under differing single additional fish-farm scenarios.	93
Figure E-3:	Simulated dynamics of water-quality state-variables in the uppermost layer at station QCS-3 under differing single additional fish-farm scenarios.	94
Figure E-4:	Simulated dynamics of water-quality state-variables in the uppermost layer at station QCS-4 under differing single additional fish-farm scenarios.	95
Figure E-5:	Simulated dynamics of water-quality state-variables in the uppermost layer at station QCS-5 under differing single additional fish-farm scenarios.	96

Executive summary

The Ministry for Primary Industries (MPI) are investigating the possibility of introducing additional salmon farms into Tory Channel. They commissioned NIWA to examine the influence of three potential new farms (singly, and in various combinations) upon the trophic status of the Tory Channel/Queen Charlotte system using an existing biophysical model (Hadfield, Broekhuizen et al. 2014; Morrisey, Anderson et al. 2015). That model is based upon the widely used, open-source ROMS framework and the specific implementation for the Queen Charlotte / Tory system has been subject to review by Marlborough District Council, the Cawthron Institute and MPI's Aquatic Environment Working Group. The model has 200 m resolution in the horizontal and twenty layers in the vertical. It is designed to examine large bay-scale/regional scale influences upon trophic status, rather than farm-scale/near-field scale effects. It includes the effects of winds, tides and freshwater inputs upon flow. The foodweb of the model contains ammonium, nitrogen, nitrate, a single phytoplankton class and a single zooplankton class and three classes of particulate organic detritus. The phytoplankton are represented by both nitrogen abundance and chlorophyll abundance. A fixed fraction (75%) of any particulate organic detritus which settles to the seabed is assumed to be lost from the system through denitrification. The remaining 25% returns to the bottom-most layer of the water-column as ammonium. Nitrogen is the only element considered within the foodweb. The model has not been used to examine whether farms will increase the probability of hypoxia.

The proposed new farms are located in Tory Channel. One is close to Tipi Bay, one is close to Motukina Point and one is in Te Weka Bay (Figure 1-1). We examined eight different fish-farming scenarios:

Scenario name	Scenario short-hand code	Description
Operating farms (or, existing farms/conditions)	EM_EF_WD ¹	This scenario included all mussel farms that were in operation in 2010 (as revealed in an aerial survey) and the four salmon farms operating in Queen Charlotte Sound and Tory Channel at that time (namely: Ruakaka, Otanerau, Clay Point and Te Pangu). The fish farm characteristics (monthly stock size distribution and feed inputs) were those provided by New Zealand King Salmon for the period 1 January 2012 to 1 April 2014.
Baseline	AM_AF_WD ²	Currently allocated mussel- and salmon farm space. In this scenario, all water-space that has already been allocated ³ for mussel farming was assumed to be occupied. Similarly, in addition to the four already operating salmon farms, the newly approved salmon farm in Tory channel (Ngamahau) was assumed to be operating, with an annual feed input of 4000 tonne.

¹ EM: existing mussels; EF-existing fish; WD: with denitrification (see later sections).

² AM: approved mussels; AF: approved fish.

³ Based upon GIS maps provided to us by Marlborough District Council in February 2014.

Scenario name	Scenario short-hand code	Description
Baseline+Tipi2	AM_AF_WD+Tipi2	As for the baseline scenario, but with the proposed Tipi Bay farm added (with an annual feed input of 2000 tonne).
Baseline+Motu5	AM_AF_WD+Motu5	As for the baseline scenario, but with the proposed Motukina Bay farm added (with an annual feed input of 5000 tonne).
Baseline+Weka5	AM_AF_WD+Weka5	As for the baseline scenario, but with the proposed Te Weka Bay farm added (with an annual feed input of 5000 tonne).
Baseline+Tipi2+Motu5	AM_AF_WD+Tipi2+Motu5	As for the baseline scenario, but with the proposed Tipi Bay and Motukina farms added (with annual feed inputs of 2000 tonne and 5000 tonne respectively).
Baseline+Tipi2+Motu5+Weka5	AM_AF_WD+Tipi2+Motu5+Weka5	As for the baseline scenario, but with the proposed Tipi Bay, Motukina and Te Weka Bay farms added (with annual feed inputs of 2000 tonne, 5000 tonne and 5000 tonne respectively).
Swapped farms	AM+SF ⁴ +Tipi2+Motu5+Weka5	As for Baseline +Tipi2+Motu5+Weka5, but <i>without</i> Ruakaka and Otanerau. This can also be thought of as ‘approved mussel farms + Te Pangu+Clay Point Ngamahau+Tipi2+Motu5+Weka5 salmon farms’.

All scenarios included mussel farms (for the first (EM_EF_WD) we included only those that had backbones in the water during an aerial survey period in 2012; for the remaining seven, we included all presently approved mussel farms).

We made a single simulation for each farming scenario. Each simulation spanned a 500 day period (May 2012 – October 2013). We assessed the influence of the new farms by calculating (a) instantaneous differences (between the new farm scenario and the baseline scenario (approved farms), (b) time-averaged instantaneous and relative differences and (c) by reference to water-quality standards.

The key findings from this work are:

- Farms in Tory Channel placed close to the Cook Strait entrance will induce smaller changes in the water-quality of Tory Channel and Queen Charlotte Sounds than farms close to the junction with Queen Charlotte. There are two reasons for this. Firstly, the farm which is closest to Cook Strait (Tipi Bay) is the smallest of the three proposed (2000 tonne annual feed versus 5000 tonne for the other two). Secondly, on the ebb

⁴ SF: implying ‘swapped farms’ or ‘substituted farms’ [but noting that the ‘lost’ farms (Ruakaka and Otanerau) have lower permitted maximum annual feed inputs than considered here for the three new farms (Tipi, Motukina and Te Weka)].

tide, water flows out of Tory Channel into Cook Strait and little of this water returns on the subsequent incoming tide. A farm close to the Cook Strait end of Tory Channel exports a larger fraction of its nitrogen waste into Cook Strait.

- For ammonium, the largest farm-effects arise in the immediate farm vicinities. For nitrate and seston, the largest effects arise in Grove Arm and side bays of Tory Channel (especially Onapua Bay). Again, the explanation is straight-forward. Fish farms are net sources of ammonium (directly excreted by the fish), and of particulate organic nitrogen (faeces and waste feed) – which degrades into ammonium. It takes some time for the phytoplankton to fully incorporate the farm-derived ammonium into new biomass. During that time, the water (containing the additional nitrogen and seed phytoplankton population) has been transported away from the source farm and subject to dispersive mixing. A similar argument holds with respect to conversion of ammonium into nitrate by bacterial activity. The combination of dispersive mixing, and gradual uptake by phytoplankton and bacteria implies that ammonium concentration increases must decline with increasing distance from the farm. Conversely, population increases by phytoplankton etc., take time to fully develop, so phytoplankton and seston concentration increases tend to be greatest at some distance (travel time) away from the farms.
- The farms are predicted to have little effect upon phytoplankton, zooplankton and detritus during the winter-months. During those months, algal growth is limited by light rather than nutrients. Thus, the additional nitrogen can only be slowly incorporated into additional biomass. Much of it is exported from the system before it can be utilized.
- Regardless of which farms are added, the largest summertime changes in phytoplankton abundance tend to arise in Onapua Bay and Grove Arm. The changes in Onapua Bay tend to exceed those in Grove Arm.
- During the summer (nutrient limited) period, phytoplankton and detritus concentrations are predicted to increase by circa 1–6% in Onapua Bay and Grove Arm (relative to the summertime baseline) in the single-farm addition scenarios. The Te Weka farm tends to induce the largest changes. The Tipi Bay farm tends to induce the smallest.
- The smallest (by total annual feed load) ‘multiple farms scenario’ (AM_AF_WD+Tipi2+Motu5) yields summertime chlorophyll and detritus concentration increases of circa 3-5% within Grove Arm and Onapua Bay (smaller elsewhere).
- The intermediate (by total annual feed load) ‘multiple farms scenario’ (AM_SF_WD+Tipi2+Motu5+Weka5) yields summertime chlorophyll and detritus increases of circa 5-6% (relative to the baseline scenario) in Grove Arm and Onapua Bay (smaller elsewhere).
- In the largest multiple-farms scenario (AM_AF_WD+Tipi2+Motu5+Weka5), the summertime chlorophyll and detritus increases in Grove Arm and Onapua Bay are predicted to be 8–10% of the baseline concentration (increases of circa 0.3-0.5 mg chl m⁻³). Relative to the simulated existing operating conditions scenario, the

increases amount to 0.5-0.7 mg chl m⁻³ (10-15% relative to the existing operating conditions).

- The existing operating conditions simulation over-predicts summertime chlorophyll (and phytoplankton) concentrations relative to field-data. Implications from this are:
 - the summertime concentrations predicted for the various 'added farms' probably also over-predict absolute summertime chlorophyll (and phytoplankton) concentrations
 - the relative (percentage) chlorophyll changes quoted above were calculated relative to a baseline simulation which is likely overly high. If the relative change is instead expressed relative to the historically measured summertime chlorophyll concentrations, the relative changes are larger (circa 40% increase) relative to historical summertime chlorophyll concentrations.
- Instantaneous chlorophyll concentrations will, perhaps, exceed 5 mg m⁻³ more often than they do now (even in the single farm additions), but we believe that such events will remain rare. Indeed, we believe they will usually remain below 3.5 mg m⁻³. 5 mg m⁻³ is a consent-condition threshold governing the three recently approved NZKS farms (two in Pelorus Sound, and Ngamahau in Tory Channel). NZKS and Marlborough District Council have agreed that chlorophyll concentrations in excess of 3.5 mg m⁻³ will trigger investigations as to whether fish-farming was the cause and, if so, will require that NZKS will undertake mitigation measures to bring chlorophyll back below 3.5 mg m⁻³.

1 Introduction

For a number of years, Queen Charlotte Sound and Tory Channel have each supported two salmon farms (Ruakaka and Otanerau in Queen Charlotte Sound; Clay Point and Te Pangu in Tory Channel). A third farm in Tory Channel (Ngamahau) has recently been approved, but it is not yet in operation.

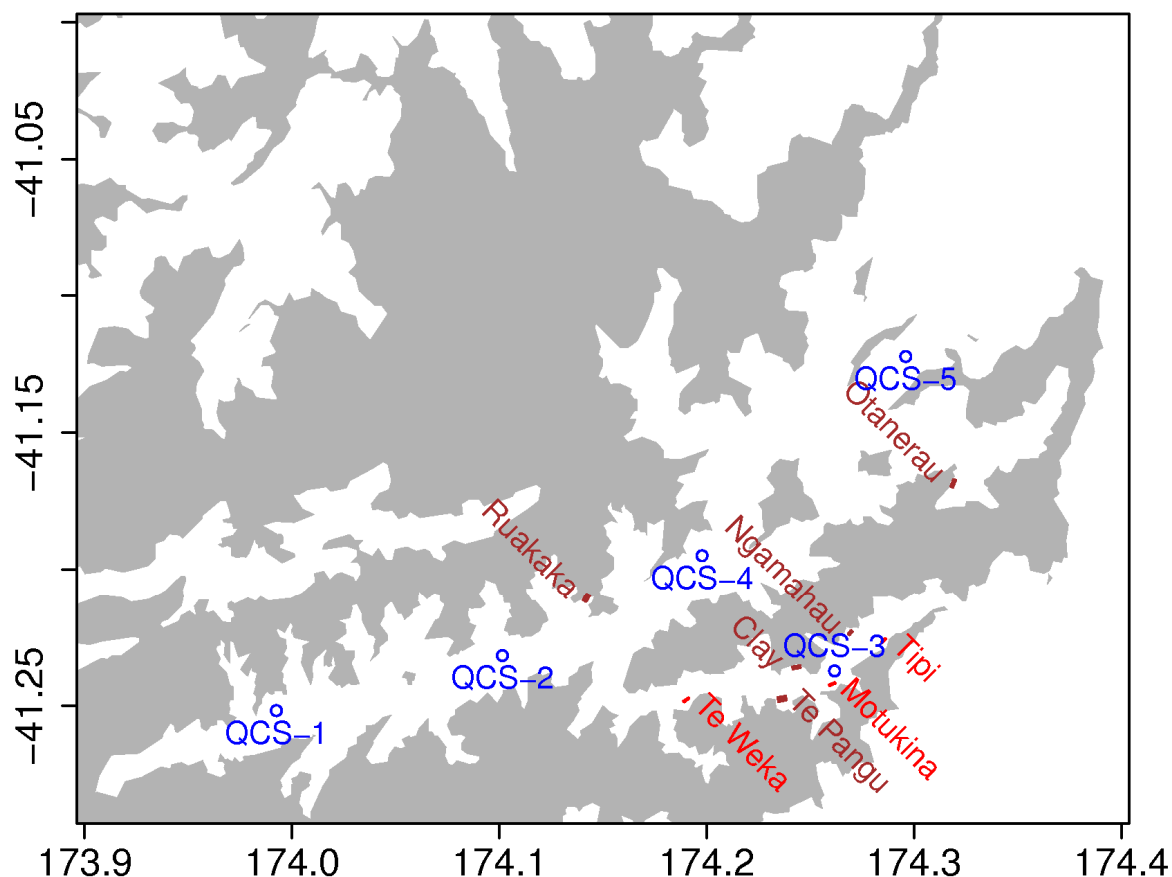


Figure 1-1: Map of Queen Charlotte Sound and Tory Channel showing the locations of the five existing farms, the three potential new farm sites and the five Marlborough District Council monitoring sites. The existing sites (Otanerau, Ruakaka, Clay Point, Te Pangu and Ngamahau) are shown in brown. The three potential new sites (Tipi Bay, Motukina Point and Te Weka Bay) are shown in red. The Marlborough District Council water-quality sampling sites are marked by blue circles and labelled QCS-1 to QCS-5. We will refer to site QCS-1 as being within ‘inner Grove Arm’, site QCS-2 as being in ‘outer Grove Arm’, QCS-3 as being in Tory Channel, site QCS-4 as being in ‘inner/central Queen Charlotte’ and site QCS-5 as being in ‘outer Queen Charlotte’.

The Ministry of Primary Industries are now seeking to determine whether the Queen Charlotte Sound/Tory Channel (QCS/Tory) system has a capacity to support additional salmon farms. As a part of their investigations, they commissioned NIWA to examine the effects that three proposed new farms (Figure 1-1) may have upon water-quality, using a slightly modified version of our biophysical model of the QCS/Tory system (Hadfield, Broekhuizen et al. 2014). The reader should consult Hadfield, Broekhuizen et al. (2014) for a description of the original QCS/Tory model. The minor modifications made since that report are described in sections 2.1 and 2.2 of this report. Other relevant background material is presented in Broekhuizen, Hadfield et al. (2015), which is a companion report (of Hadfield, Broekhuizen et al. (2014)) describing the corresponding Pelorus Sound model. The Queen Charlotte/Tory and Pelorus biophysical models were developed with

support from Marlborough District Council, MPI and Government CORE funding. They represent the best tools currently available to determine the water-column effects of aquaculture in these water bodies. They have been subject to external peer review through Council and Aquatic Environment Working Group processes.

1.1 Scenarios

For this work, we simulated a total of eight different farming scenarios. In all scenarios, we adopted the ‘with denitrification’ assumption. That is, we assumed that 75% of any particulate organic nitrogen which settles to the seabed is lost from the system (denitrified). The remaining 25% is instantaneously mineralized to ammonium and returned to the water immediately above the seabed.

Table 1-1: Descriptions of the eight scenarios which we have considered.

Scenario name	Scenario short-hand code	Description
Operating farms (or, existing farms/conditions)	EM_EF_WD ⁵	This scenario included all mussel farms that were in operation in 2010 (as revealed in an aerial survey) and the four salmon farms operating in Queen Charlotte Sound and Tory Channel at that time (namely: Ruakaka, Otanerau, Clay Point and Te Pangu). The fish farm characteristics (monthly stock size distribution and feed inputs) were those provided by New Zealand King Salmon for the period 1 January 2012 to 1 April 2014.
Baseline	AM_AF_WD ⁶	Currently allocated mussel- and salmon farm space. In this scenario, all water-space that has already been allocated ⁷ for mussel farming was assumed to be occupied. Similarly, in addition to the four already operating salmon farms, the newly approved salmon farm in Tory channel (Ngamahau) was assumed to be operating, with an annual feed input of 4000 tonne.
Baseline+Tipi2	AM_AF_WD+Tipi2	As for the baseline scenario, but with the proposed Tipi Bay farm added (with an annual feed input of 2000 tonne).
Baseline+Motu5	AM_AF_WD+Motu5	As for the baseline scenario, but with the proposed Motukina Bay farm added (with an annual feed input of 5000 tonne).
Baseline+Weka5	AM_AF_WD+Weka5	As for the baseline scenario, but with the proposed Te Weka Bay farm added (with an annual feed input of 5000 tonne).

⁵ EM: existing mussels; EF-existing fish; WD: with denitrification (see later sections).

⁶ AM: approved mussels; AF: approved fish.

⁷ Based upon GIS maps provided to us by Marlborough District Council in February 2014.

Scenario name	Scenario short-hand code	Description
Baseline+Tipi2+Motu5	AM_AF_WD+Tipi2+Motu5	As for the baseline scenario, but with the proposed Tipi Bay and Motukina farms added (with annual feed inputs of 2000 tonne and 5000 tonne respectively).
Baseline+Tipi2+Motu5+Weka5	AM_AF_WD+Tipi2+Motu5+Weka5	As for the baseline scenario, but with the proposed Tipi Bay, Motukina and Te Weka Bay farms added (with annual feed inputs of 2000 tonne, 5000 tonne and 5000 tonne respectively).
Swapped farms	AM+SF ⁸ +Tipi2+Motu5+Weka5	As for Baseline +Tipi2+Motu5+Weka5, but <i>without</i> Ruakaka and Otanerau. This can also be thought of as ‘approved mussel farms + Te Pangu+Clay Point Ngamahau+Tipi2+Motu5+Weka5 salmon farms’.

The ‘operating farms’ scenario (EM_EF_WD) was not a required scenario within our contract, but we felt that this scenario would be useful since this is the one which best corresponds to the farming conditions that have prevailed during the time-period for which water-quality data are available from Queen Charlotte Sound (Marlborough District Council have sampled at monthly intervals since July 2011 at four stations in Queen Charlotte Sound and one in Tory Channel). The EM_EF_WD scenario allows an assessment of model performance (against recent field data) to be made. This scenario is also relevant when seeking to address the question: ‘relative to the water-quality evident in the recent past, how might the proposed three new farms change future water-quality?’ (cf the question ‘relative to the water-quality that is anticipated once all the currently approved farms come into operation, how might the proposed three new farms change future water-quality?’).

⁸ SF: implying ‘swapped farms’ or ‘substituted farms’ [but noting that the ‘lost’ farms (Ruakaka and Otanerau) have lower permitted maximum annual feed inputs than considered here for the three new farms (Tipi, Motukina and Te Weka)].

Table 1-2: Total feed inputs (tonne) associated with the farms of each scenario. The unbracketed figures are totals for the period 1 May 2012 - 31 October 2013. The bracketed figures are those numbers rescaled to 365 days. The values for Otanerau, Ruakaka, Clay Point and Te Pangu are based upon historical data supplied by New Zealand King Salmon. The values for the remaining farms are based upon annual total feed inputs stipulated by the Ministry for Primary Industries.

Farm	Scenario							
	EM_EF_WD (baselin e _{f2012})	AM_AF_WD (baselin e _{f2016})	AM_AF_WD + Tipi2	AM_AF_WD +Motu 5	AM_AF_WD +Weka 5	AM_AF_WD +Tipi2+ Motu5	AM_AF_WD +Tipi2+Motu5 +Weka5	AM_SF_WD +Tipi2+Motu5 +Weka5
Otanerau	2430 (1616)	2430 (1616)	2430 (1616)	2430 (1616)	2430 (1616)	2430 (1616)	2430 (1616)	
Ruakaka	3124 (1904)	3124 (1904)	3124 (1904)	3124 (1904)	3124 (1904)	3124 (1904)	3124 (1904)	
Clay Point	6569 (4368)	6569 (4368)	6569 (4368)	6569 (4368)	6569 (4368)	6569 (4368)	6569 (4368)	6569 (4368)
Te Pangu	6146 (4086)	6146 (4086)	6146 (4086)	6146 (4086)	6146 (4086)	6146 (4086)	6146 (4086)	6146 (4086)
Ngamahau		6016 (4000)	6016 (4000)	6016 (4000)	6016 (4000)	6016 (4000)	6016 (4000)	6016 (4000)
Tipi Bay			2740 (2000)			2740 (2000)	2740 (2000)	2740 (2000)
Te Weka Point					6849 (5000)		6849 (5000)	6849 (5000)
Moutukina				6849 (5000)		6849 (5000)	6849 (5000)	6849 (5000)
Total	18269 (11974)	24285 (15974)	27025 (17974)	31134 (20974)	33874 (22974)	31134 (20974)	40723 (27974)	35169 (24454)

2 Methods

We used a spatially explicit, three dimensional, coupled biophysical model to simulate the hydrodynamics and water-quality of the QCS/Tory system. The model is an updated version of the one described by Hadfield, Broekhuizen et al. (2014). As in that work, we again simulated a 500-day period from May 2012 to October 2013. We forced the model with the same time-series of winds, surface fluxes and boundary data (except that tidal hydrodynamic boundary data were changed).

The modifications are as follows:

- Revised Cook Strait tidal boundary data (Section 2.1 below).
- An improved representation of the fact that the waste organic matter from mussel farms (faeces and pseudo-faeces) and from fish farms (faeces and uneaten feed) sink very much more rapidly than does the organic detritus that stems from dead phytoplankton etc., (section 2.2 below).

2.1 Revised Cook Strait tidal hydrodynamic data

As explained in the previous report, the QCS/Tory model was forced with tidal boundary data (i.e., tidal oscillations in sea level and velocity) from the NIWA tidal model, which covers the New Zealand EEZ and has a spatial resolution of 1–3 km in Cook Strait. The modelled tidal variations in sea level were compared with measurements at two locations, one in outer Queen Charlotte Sound and the other in Tory Channel (Hadfield, Broekhuizen et al. 2014, Section 3.2 and Table 3.1), with the result that the modelled amplitude of the largest tidal constituent (the M2, or lunar, semi-diurnal constituent) was too high by 19% at the former site and 22–26% at the latter. The report speculated that this might be a problem with the tidal forcing from the EEZ-scale model. Since then, we have reviewed the performance of both the QCS/Tory and Pelorus Sound models and concluded that results are better when these are forced by tides from a model of Cook Strait at 500 m resolution, itself embedded in the NIWA EEZ tidal model.

Table 2-1: Comparison of M2 tidal sea level parameters. M2 tidal sea level parameters from ADCP pressure data and model. Here “ratio” means model value divided by observed value and “difference” means model value minus observed value.

ADCP Site/Deployment	Amplitude (m)			Phase (°)		
	Obs.	Model	Ratio	Obs.	Model	Difference
QCS Outer Deployment 1	0.508	0.469	0.92	254.5	259.1	4.7
QCS Outer Deployment 2	0.515	0.473	0.92	256.1	259.5	3.4
Tory Channel Deployment 1	0.375	0.332	0.88	244.4	250.7	6.2
Tory Channel Deployment 2	0.369	0.334	0.91	245.5	251.2	5.7

Table 2-1 is similar to Table 3-1 from Hadfield, Broekhuizen et al. (2014), but based on the present model with the revised tidal forcing. The modelled tidal amplitudes are now 8% too low at the Queen Charlotte Sound measurement site and 9–12% too low at the Tory Channel site. This is significantly better agreement than we had previously, though with some room for improvement with further tuning⁹.

Most of the hydrodynamic analyses carried out for the previous model have been repeated for the revised model. The overall result is that agreement with measurements is improved in some respects and unchanged in others, and the tidal forcing at the lunar, semi-diurnal frequency is significantly reduced.

To assess what the change in tidal forcing means for predictions of transport of dissolved and suspended material in Queen Charlotte Sound and Tory Channel, we repeated the idealised flushing simulations described in Section 3.7 of Hadfield, Broekhuizen et al. (2014). The results are summarised in Figure 2-1, which shows time series of the accumulated amount of each of the six tracers. This graph is very similar to its counterpart, namely Figure 3-24 in Hadfield, Broekhuizen et al. (2014), with the same variation in time and between release sites and release heights. For a more quantitative look at tracer accumulation, Table 2-2 presents equilibrium flushing times from the previous and present variants of the model boundary conditions. When comparing Figure 2-1 and Table 2-2, note that ‘normalized mass (days)’ is mathematically equivalent to ‘flushing time (days)’. An explanation of what the term “flushing time” means in this context, and why it depends on the source position, is given in Section 3.7 of Hadfield, Broekhuizen et al. (2014). For the Grove Arm (or Inner Queen Charlotte Sound) sources, the flushing times are very slightly increased in the present model: this may reflect a decrease in the strength of tidal flushing arising from the reduced tidal forcing. For the Outer Queen Charlotte Sound sources, the flushing time is reduced slightly: this is likely to have occurred because reduced vertical mixing by the tides allows the overturning circulation in the outer sound to increase in strength. (It is not surprising that a reduction in tidal forcing can increase flushing times in some situations and reduce them in others, as competition between these two effects is often seen in tidal estuaries).

The most significant and relevant change for the present purposes is at the Tory Channel source, where the reduced tidal forcing in the present simulations allows the flushing time to increase by 22%, from 10.9 to 13.3–13.4 days. As mentioned in the previous report, because of the large tidal

⁹ Note also that there is an error in the phase values in Table 3-1 from Hadfield, M., Broekhuizen, N., Plew, D. (2014) A biophysical model of the Marlborough Sounds: part 1: Queen Charlotte & Tory Channel. *NIWA Client Report (for Marlborough District Council)*: 183. <http://www.marlborough.govt.nz/Environment/Coastal/Hydrodynamic-Models-of-the-Sounds.aspx>, relating to the sign convention for tidal phase. To correct a value in Table 3-1, subtract it from 360°: thus the observed tidal phase of 105.5° for QCS Outer Deployment 1 is corrected to 254.5° in Table 2-1.

excursion amplitudes in Tory Channel, when a tracer is released in central Tory Channel into an ebb flow, a significant fraction can reach Cook Strait within the first tidal period. The reduced tidal forcing of the present simulation reduces this fraction and therefore increases flushing time. Since our revised tidal boundary conditions yield larger flushing times in Tory Channel, we anticipate that material released from farms within Tory Channel will be exported into Cook Strait more slowly (relative to the results from the earlier model variant). As a corollary, we anticipate that the magnitudes of concentration change (for farm-derived nutrient increment) within Tory Channel will increase.

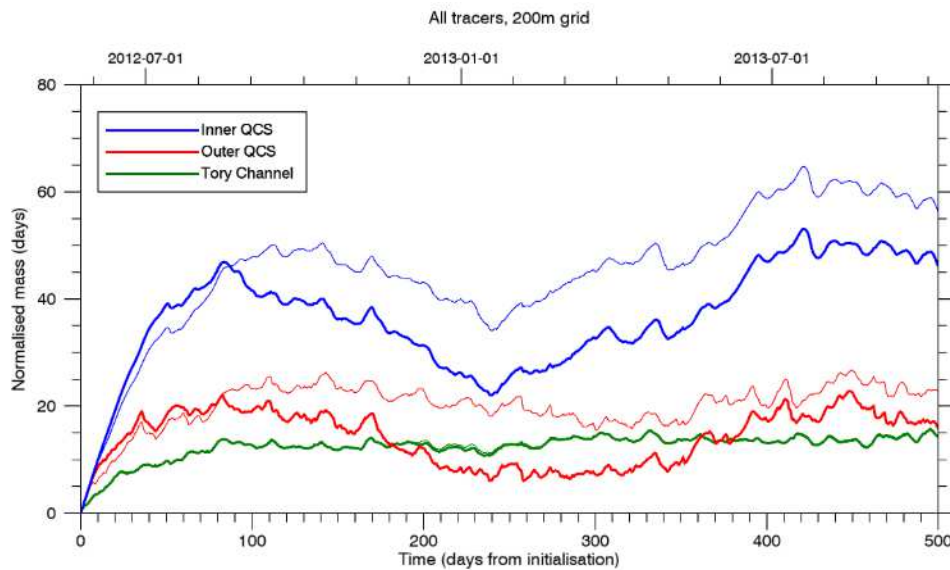


Figure 2-1: Accumulation of tracer from the 200 m flushing simulation using the revised tidal forcing. Normalised mass of tracer within Queen Charlotte Sound versus time in the 200 m flushing simulation for near-surface (thick line) and near-bottom (thin line) sources at the three tracer release sites: Inner QCS, blue; Outer QCS, red, Tory Channel, dark green.

Table 2-2: Equilibrium flushing times for Queen Charlotte Sound. Flushing times for the previous and present models evaluated from tracer accumulation data (e.g., Figure 2-1, above), averaged over the last 365 days of the 200 m flushing simulations.

Site	Flushing time T_e (days)	
	Previous model	Present model
Grove Arm near-surface	34.9	37.4
Grove Arm near-bottom	46.1	49.3
Outer QCS near-surface	15.6	13.2
Outer QCS near-bottom	22.0	21.0
Tory Channel near-surface	10.9	13.3
Tory Channel near-bottom	10.9	13.4

2.2 Revised representation of the sinking of faeces, pseudo-faeces & uneaten food

The water-quality component of our model is based upon that of Fennel, Wilkin et al. (2006). That model has two classes of organic detritus: slow-sinking (or small) and fast-sinking (or large) detritus. In our original QCS/Tory model (Hadfield, Broekhuizen et al. 2014), mussel and fish faeces, mussel pseudofaeces and uneaten fish feed passed into the large detritus class.

Unfortunately, the sinking speed of even the so-called fast sinking class (3 m d^{-1}) is several orders of magnitude smaller than that of fish faeces and pseudo-faeces ($\sim 5 \text{ cm s}^{-1}$, or $\sim 4320 \text{ m d}^{-1}$). In consequence, in the original model, particulate organic matter emitted from farms (i.e., faeces and pseudofaeces) would have remained in the water-column for far too long. This may be dynamically significant because the model provides that a fraction of any particulate organic nitrogen that settles to the seabed will be denitrified, i.e., converted to N_2 gas, rendering it biologically inert. In contrast, the particulate organic nitrogen that remains in the water column will ultimately mineralize to ammonium (NH_4^+), which is biologically active. Thus, the original model may have under-estimated denitrification and over-estimated the ‘fertilizing effect’ of the nitrogen emissions from fish-farms.

In our subsequent Pelorus model (Broekhuizen, Hadfield et al. 2015) we overcame the aforementioned deficiency by introducing a third class of particulate organic detritus (which we called extra-large detritus (henceforth, XLdetritus)), and assigned an appropriately large sinking speed to this XLdetritus. All faeces, pseudo-faeces and waste feed (and nothing else) passed into that class. While this worked moderately well, the combination of rapidly sinking detrital material and horizontal advection was numerically challenging and necessitated the use of a more sophisticated and computationally expensive horizontal advection scheme. Consequently, the run-time for each simulation was very long.

To mitigate this run-time problem, we implemented a scheme in which XLdetritus generated in the fish and mussel farms is instantly delivered to the seabed (i.e., it never has an explicit presence within the water-column). While this precludes any horizontal transport of XLdetritus, we believe it is an acceptable approximation because the real-world horizontal transport will be very small in comparison with the spatial extent of the Sounds¹⁰. Upon appearing at the seabed, a fraction (25%) of the material instantly mineralizes to NH_4^+ and is returned to the bottom-most layer of the overlying water-column. The remaining nitrogen is lost from the system (implicitly, denitrified). This is consistent with the treatment of XLdetritus in the Pelorus model, except that the concentration in the water column is implicitly assumed to be zero¹¹.

2.3 Farm characteristics

Mussel-farm perimeters were derived from GIS maps provided to us in February 2013 by Marlborough District Council. Fish farm pen perimeter locations were provided to us by New Zealand King Salmon (Ruakaka, Otanerau, Clay Point, Te Pangu, Ngamahau) and the Ministry for Primary Industries (Tipi Bay, Motikina Point, Te Weka Bay).

¹⁰ Let us assume that: (i) the regions around the farms are approx. 30 m deep, (ii) all material is released from the sea-surface and sinks at 5 cm s^{-1} . It will take 600 seconds to reach the seabed. If the current speed is 40 cm s^{-1} (high for most parts of the system), the material will travel just 240 m. Our model has a horizontal resolution of 200 m. Thus, in reality, most material should remain within the notional grid-cell in which it originated.

¹¹ Indeed, we made preliminary simulations using both our ‘explicit XLdetritus’ and our ‘teleporting XLdetritus’ model variants. The results from each variant were almost indistinguishable at graphical scale.

Details of mussel farm stocking characteristics and fish-farm stocking characteristics are provided in Hadfield, Broekhuizen et al. (2014). That report also describes the manner in which fish-farm stocking and feed input characteristics were derived. In brief, New Zealand King Salmon Ltd. provided monthly records for their existing farms (Ruakaka, Otanerau, Clay Point, Te Pangu) spanning the calendar period of interest. Data included: estimates of the numbers of living fish and average size of those fish within each cohort in each farm at the beginning and end of each calendar month together with an accompanying cohort-and-farm specific total feed input over the course of the month. We used those data directly (for the existing farms) and also used them as a basis for synthesizing plausible characteristics for the farms that do not yet exist (Ngamahau, Tipi Bay, Motukina Point, and Te Weka Bay). Specifically, we assumed that Ngamahau and Te Weka Bay would have stocking characteristics like Clay Point, whereas Tipi Bay and Motukina would have stocking characteristics like Te Pangu. We therefore took the relevant 'template-farm' (Clay or Te Pangu) characteristics and rescaled the monthly fish numbers and feed-inputs, so that the implied annual feed-loads would match the maximum feed input rates for the four farms (per annum: Ngamahau: 4000 tonne; Tipi Bay: 2000 tonne; Te Weka Bay: 5000 tonne; Motukina Point: 5000 tonne).

2.4 Analysis and presentation of results

We carried out our biophysical simulations on a 200 m resolution horizontal grid. At this resolution, the detailed structures of individual fish farms and mussel farms are not resolved. However, we believe that, at distances beyond about 1 km, natural mixing will have eroded the farm-derived steep gradients to sufficient degree that the grid spacing will have ceased to be significant. Thus, in the far-field the simulated concentrations will be much less subject to bias. In short, the model has been designed with the intent that it be used to derive an understanding of the regional (and large-bay scale) influences of farming rather than the farm-scale/small bay-scale influences.

Simulation results at the locations of each of the five Marlborough District Council sampling sites (Figure 1-1) were stored at approximately 6 minute resolution. In addition, the 12-hour averaged concentrations for every control-volume were stored.

We treat the AM_AF_WD scenario as our 'baseline' scenario (baseline_{f2016}). We illustrate the predicted influences which the various alternative scenarios have upon water-quality (relative to the baseline_{f2016} one), in two ways. First, we present the simulated time-series of the various water-quality variables as simulated at each of the five Marlborough District Council water-quality sampling sites (Figure 1-1). We will present two groups of plots. In the first group, we will show results from the baseline_{f2016} (AM_AF_WD) scenario and each of the three 'one additional farm' scenarios (i.e., $\text{baseline}_{f2016}+\text{Tipi2}$, $\text{baseline}_{f2016}+\text{Motu5}$, $\text{baseline}_{f2016}+\text{Weka5}$). In the second group, we show results from the baseline_{f2016} scenario and each of the 'multiple new farms' scenarios (i.e., $\text{baseline}_{f2016}+\text{Tipi2}+\text{Motu5}$, $\text{baseline}_{f2016}+\text{Tipi2}+\text{Motu5}+\text{Weka5}$, Swapped farms).

Secondly, we will show a series of false-colour figures. Each figure will contain six rows and each row will contain three panels (maps). Each panel is a map of the model's horizontal domain. Pixel colour at any location within the map is indicative of the numerical value of the property¹² in question at the pixel-location (yellow/red being 'high', and blue being 'low'). The colour-scheme is designed to yield 'pleasing' colours that allow differences to be distinguished readily. The colours should *not* be interpreted as indicative of whether or not the magnitude of change might be deemed 'acceptable'. For example, 'green' should not be deemed to imply 'safe/acceptable' and 'red' should not be

¹² In this context, *property* is used as a convenient short-hand to refer to the time-averaged absolute or relative concentration for a particular state-variable.

interpreted as meaning ‘unsafe/unacceptable’. The numerical range spanned by the colour-scale differs for each variable that we plot. Thus, when comparing maps of different properties, one must recognise that any specific colour does not necessarily equate to the same numerical value in both maps.

Each row corresponds to a different model state-variable (i.e., ammonium, nitrate, etc., – as indicated in the title above the left-hand-most panel of each row). Specifically, the left-hand most panel will show a time-averaged concentration for the state-variable under a reference scenario (usually, the baseline_{f2016} scenario, AM_AF_WD). The panels within the central column illustrate the time-averages of relative concentration R_p for other scenarios. For example, the central column may show results from the $\text{baseline}_{f2016} + \text{Motu5}$ scenario relative to the baseline_{f2016} one. The time-average of relative concentration is calculated as:

Equation 2-1: Definition of relative concentration

$$R_p = 1 + \frac{1}{N} \sum_{n=1}^N \frac{P_n^a - P_n^{\text{ref}}}{\epsilon + P_n^{\text{ref}}}$$

where N is the number of time-levels involved in the time-average, $\epsilon = 10^{-100}$ (present to avoid the possibility of a division by zero), while P_n^{ref} and P_n^a represent the simulated 12-hour average concentration P at time-level n in the reference (P_n^{ref}) and alternative (P_n^a) scenarios. In other words, the relative concentration is 1 plus the average fractional difference from the reference. If, on average, the alternative scenario gives lower concentrations than the reference one, the relative concentration will be less than 1; if higher it will be greater than 1. Note that the percentage change can be derived from the relative concentration, by subtracting 1.0. Thus, $R_p = 1.1$ implies that the concentration in the ‘alternative’ scenario exceeds that in the ‘reference scenario’ by 10%. Conversely, $R_p = 0.9$ implies that the concentration in the alternative scenario is 90% of that of the reference scenario (ie a 10% reduction relative to the reference scenario).

The right hand column of panels presents maps of the time-average of the instantaneous concentration differences. Zero indicates no change, negative values indicate that the alternative scenario is yielding lower concentrations than the reference simulation (left-hand most image) and positive values indicate the alternative simulation is yielding larger concentrations. Header text above each figure serves as a reminder to the reader of what each of the three panels within each row represent.

As defined above, both the relative concentrations and the concentration differences are calculated by comparison to a reference simulation rather than by comparison to a reference condition that has been established from field measurements. One implication is that if the model over-predicts (under-predicts) the concentration of a property in the reference (relative to defined by field data from a corresponding real-world field situation), then the magnitude of any resultant relative change associated with an alternative scenario will be under-estimated (over-estimated) [assuming that the model correctly predicts the magnitude of concentration change induced by the farms of the alternative scenario].

In terms of the applied farming scenarios, it is the 'operating farms' (EM_EF_WD) scenario rather than the baseline_{f2016} (AM_AF_WD) scenario that is appropriate to the period from which Marlborough District Council's field data stem from. With that in mind, we note that, relative to the existing Marlborough District Council field data for Queen Charlotte Sound, the model's 'operating farms (EM_EF_WD, baseline_{f2012})' scenario does overestimate summertime phytoplankton and chlorophyll concentrations (Table 3-1). Given that baseline_{f2016} scenario (AM_AF_WD) scenario includes the farms of the existing conditions (EM_EF_WD scenario), it seems probable that the baseline_{f2016} (AM_AF_WD) scenario also over-predicts summertime phytoplankton and chlorophyll concentrations.

3 Results

3.1 Model performance: comparison of the ‘existing operating conditions’ scenario with field data

The ‘existing operating conditions’ scenario (EM_EF_WD) purports to represent the farming systems that operated during the time-period that Marlborough District Council’s monitoring data stem from.

Hadfield, Broekhuizen et al. (2014) conclude that our model of Queen Charlotte Sound and Tory Channel appears to over-predict summertime (and under-predict winter-time) chlorophyll concentrations under ‘existing conditions’. The updated model version that we have used for the present project (i.e., the one that delivers faecal material directly to the seabed with no intervening residence in the water-column) also does so (Table 3-1). The model appears to over-predict spring/summer chlorophyll concentrations by approximately $1.5 \text{ mg chl m}^{-3}$ and under-predict winter-time ones by approximately $0.5 \text{ mg chl m}^{-3}$.

In part, the over-prediction can be attributed to the fact the phytoplankton (and chlorophyll) variables in the model are intended to correspond to real-world ‘total phytoplankton’ (summed across all size-classes), whereas the field data correspond to phytoplankton larger than approximately $1\text{-}2 \mu\text{m}$ (as captured on a GF-C filter, or readily identified and measured by microscope). We know of no data concerning phytoplankton $<1\text{-}2 \mu\text{m}$ in Queen Charlotte Sound and Tory Channel. Limited data from Beatrix Bay indicate that phytoplankton $<1\text{-}2 \mu\text{m}$ constituted an average of 29% (max. 65%) of the total phytoplankton biomass (Safi and Gibbs 2003). If similar ratios apply in the Queen Charlotte system, real-world total chlorophyll concentrations may be about 40% ($100/(1-0.29)$), or more, higher than those that have been measured using the GF-C filter. Nonetheless, even after discounting our simulated total chlorophyll by 29%, the real-world summertime average chlorophyll concentrations remain below the discounted simulated chlorophylls in our ‘operating farms (EM_EF_WD)’ scenario (Table 3-1). This has two implications:

- The summertime chlorophyll concentrations predicted for each of the various ‘proposed additional farm’ scenarios are likely to be over-predicted – because of the underlying over-prediction in the ‘existing operating farms’ scenario.
- It is probable that the quantum of relative change that we have calculated (in most cases, relative to the ‘approved farms’ scenario (AM_AF_WD)) for the summer time-period may be an under-estimate of the change that could arise (because the denominator in Equation 2-1 will have often been too large). Conversely, the quantum of relative change predicted for the winter may be over-estimated (because the denominator was often too small).

Depth & Time period	MDC field data mean & standard deviation (mg Chl m ⁻³)	Simulation mean & standard deviation (mg Chl m ⁻³)	Inferred simulated GF-C chl
Surface, Oct–Feb	1.33 (0.74)	3.05 (1.08)	2.1
Surface, May–Jul	1.19 (0.05)	0.53 (0.25)	0.4
Near bed, Oct–Feb	1.05 (0.8)	1.32 (0.46)	0.90
Near bed, May–Jul cl)	0.74 (0.69)	0.48 (0.23)	0.32

Table 3-1: Mean and standard deviation (across all five Marlborough District Council monitoring sites) of measured and simulated chlorophyll concentration. The MDC chlorophyll data comprise monthly near-surface and near-bed samples from July 2011 to February 2015. Samples were filtered through a GF-C filter. The simulation data span the period May 2012 to October 2013, for the ‘operating farms’ (EM_EF_WD) scenario. The inferred simulated GF-C chlorophyll was calculated by multiplying the simulated total chlorophyll by 0.71 (average of GF-C chlorophyll/total chlorophyll in the data of Safi & Gibbs (2003)) and rounding the result.

3.2 Single-additional-farm scenarios relative to baseline_{f2016} (AM_AF_WD)

Within the sub-sections of this section, we show results from the scenarios in which the three candidate new farms are introduced individually. Specifically, within Section 3.2.1 we show the predicted time-series of state-variable concentrations at each of the five Marlborough District Council water-quality monitoring stations (Figure 1-1). Within 3.2.2, we show maps of the time-averaged relative concentration change and time-averaged concentration differences associated with each scenario.

3.2.1 Time-series from the one-additional farm scenarios

Figure 3-1 - Figure 3-5 illustrate the time-series of simulated concentrations of each model state-variable in the upper-most layer of each water-column at each of the five Marlborough District Council water-quality sampling stations, for the baseline_{f2016} scenario and the 3 ‘one additional farm’ scenarios. The same simulation results are also presented in Figure A-1 to Figure B-5, but in those appendix-figures, it is concentration difference¹³ (Appendix A) or relative concentration (Appendix B) that is plotted.

Inspection of the plots reveals that, individually, each of the three individual farms:

- Have little or no influence upon seasonal-scale or high-frequency patterns of oscillation (phases of seasonal cycles are not changed and no new short-term fluctuations are generated).

Each additional farm induces an increase in ammonium concentrations throughout the year. At station QCS-3 (central Tory Channel) the increase is up to 20% (Figure 3-3). Elsewhere it is smaller, typically less than 10% (Figure 3-1a - Figure 3-5a, but excluding Figure 3-3a).

¹³ Concentration difference is calculated as: $D_p = \frac{1}{N} \sum_{t=1}^N (P_n^a - P_n^{\text{ref}})$. A positive difference implies that, in the time-average, the alternative scenario yields a higher concentration than the reference scenario.

The additional farms have almost no perceptible influence upon the winter-time concentrations of seston (chlorophyll, phytoplankton, zooplankton, small and large detritus) (Figure 3-1(c-f) - Figure 3-5(c-f)). In the summer, seston concentrations do increase with the additional farms, but the increases are small (for example, for chlorophyll, the maximum increase is circa 6% relative to the baseline_{f2016}).

The magnitude of effect (as measured at the monitoring sites) associated with each of the three proposed new farms increases with increasing distance of the farm from Cook Strait (Figure 3-1 - Figure 3-5). In part, this will be because the innermost farm, Te Weka, is one of the two 5000 tonne feed input farms. Nonetheless, its influence is larger than that of the other 5000 tonne farm, Motukina Point, which is closer to Cook Strait.

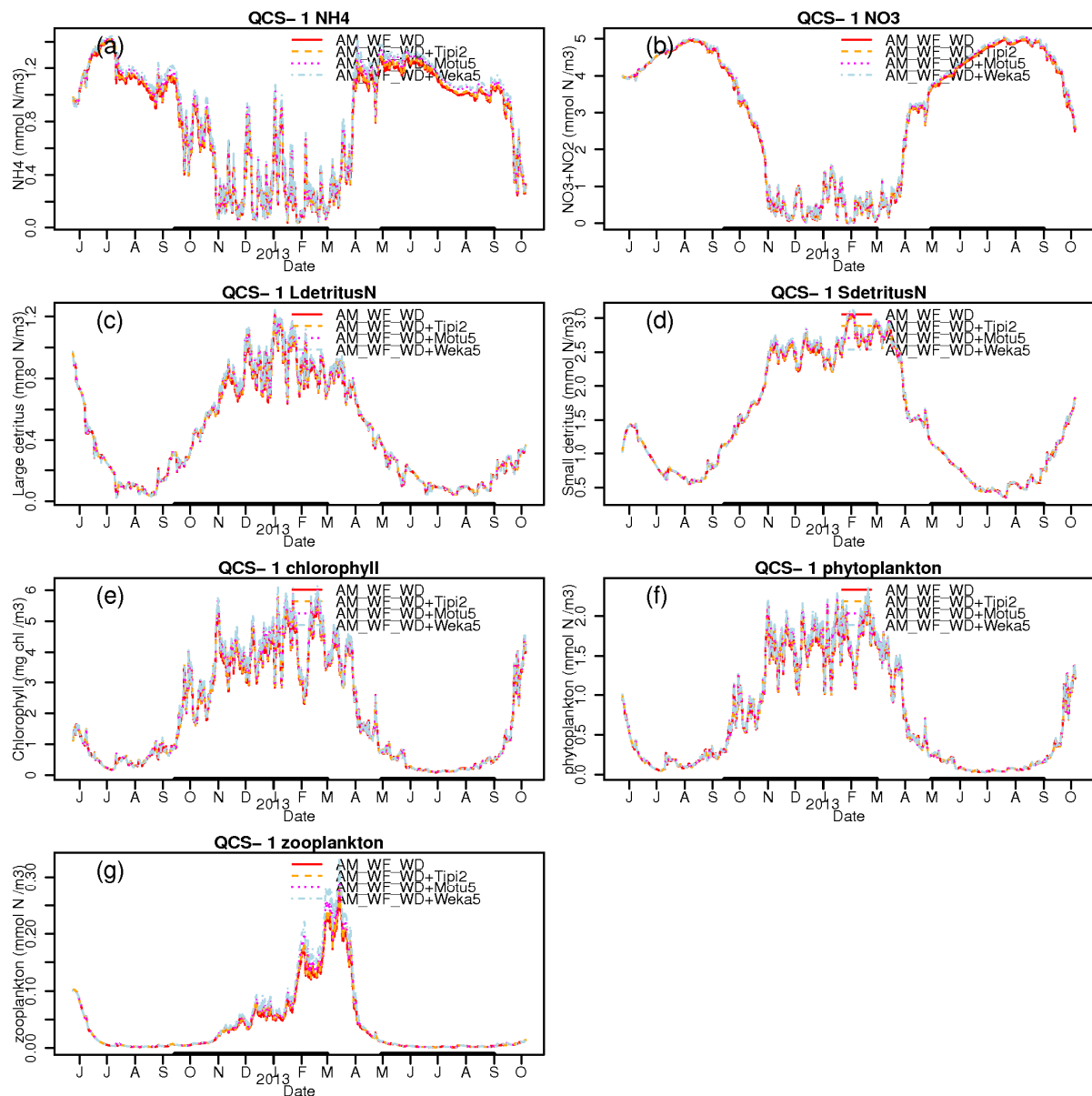


Figure 3-1: Simulated dynamics of water-quality state-variables in the uppermost layer at station QCS-1 (inner Grove Arm) under differing single additional fish-farm scenarios. The thick, black horizontal lines denote the winter (May-Aug) and spring/summer (Oct-March) time-averaging periods. The red line corresponds to the baseline_{f2016} scenario (AM_AF_WD), the dashed orange line to the ‘baseline_{f2016} farms plus Tipi Bay at 2000 tonne annual feed’ scenario, the dotted pink line to the ‘baseline_{f2016} farms plus Motukina point at 5000 tonne annual feed’, and the dashed-blue line to the ‘baseline_{f2016} farms plus Te Weka Bay at 5000 tonne annual feed.’

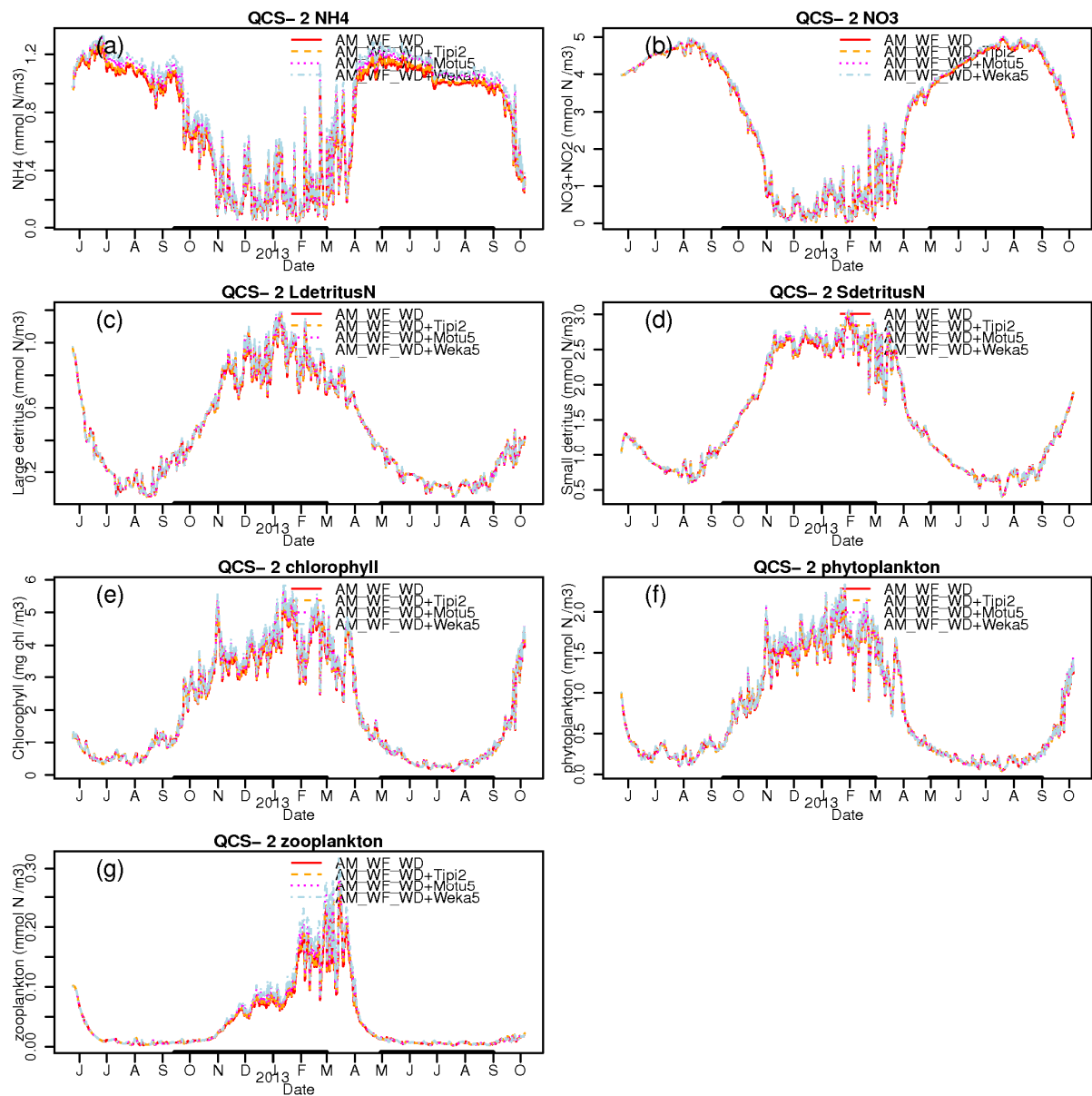


Figure 3-2: Simulated dynamics of water-quality state-variables in the uppermost layer at station QCS-2 (outer Grove Arm) under differing single additional fish-farm scenarios. Graph format as for Figure 3-1.

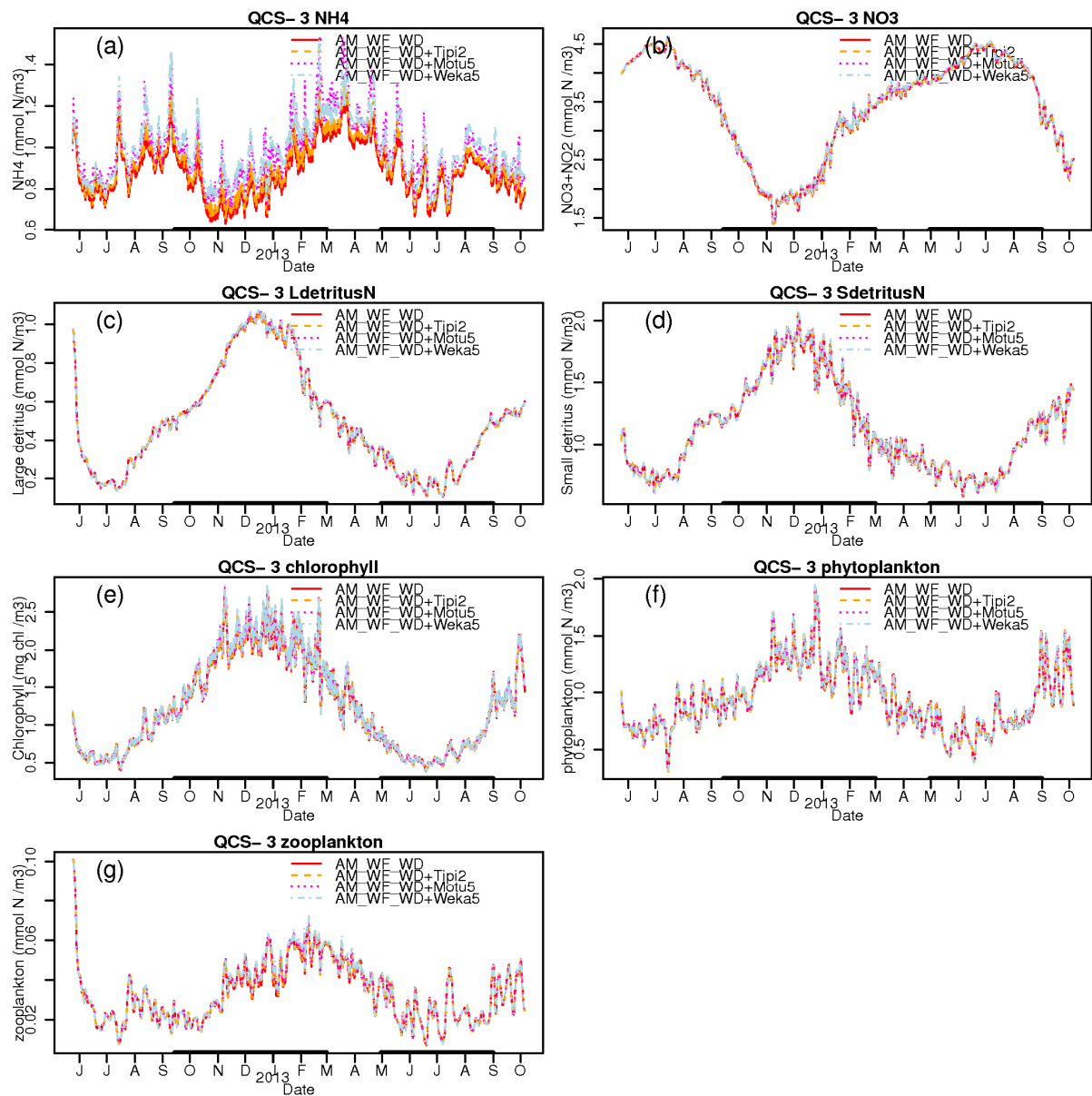


Figure 3-3: Simulated dynamics of water-quality state-variables in the uppermost layer at station QCS-3 (Tory Channel) under differing single additional fish-farm scenarios. Graph format as for Figure 3-1.

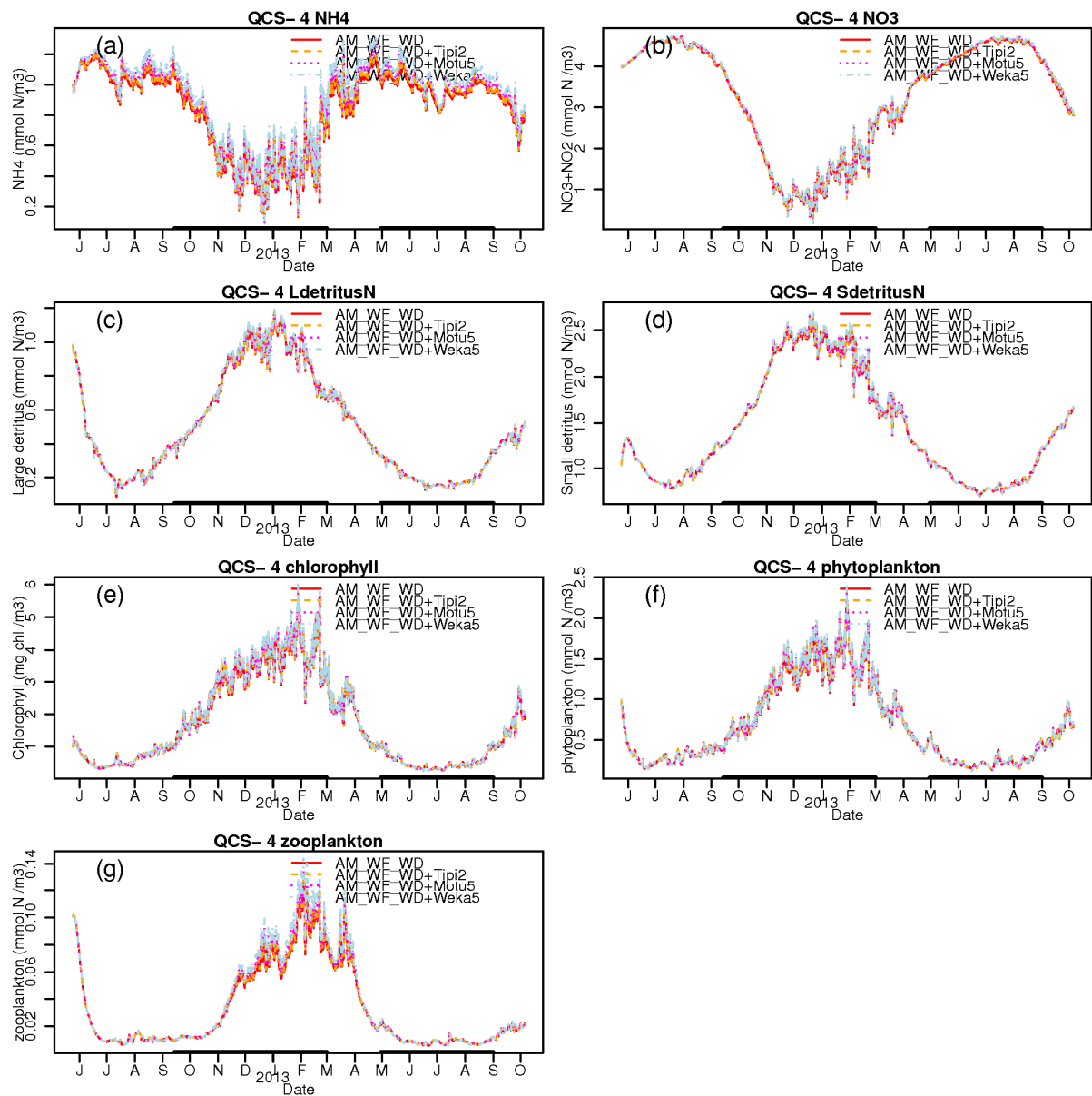


Figure 3-4: Simulated dynamics of water-quality state-variables in the uppermost layer at station QCS-4 (inner/central Queen Charlotte) under differing single additional fish-farm scenarios. Graph format as for Figure 3-1.

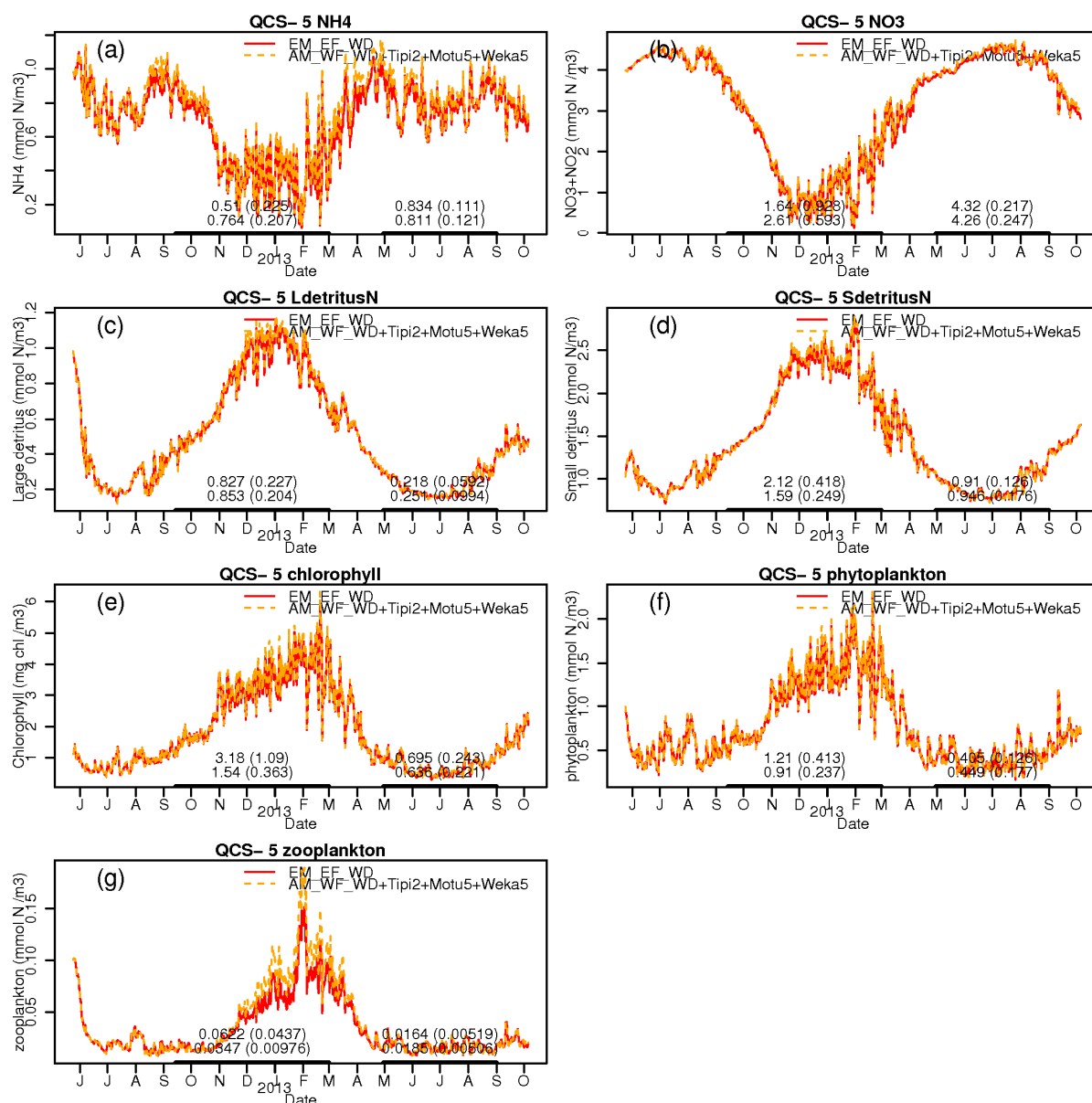


Figure 3-5: Simulated dynamics of water-quality state-variables in the uppermost layer at station QCS-5 (outer Queen Charlotte) under differing single additional fish-farm scenarios. Graph format as for Figure 3-1.

3.2.2 Change maps from the one additional farm scenarios

The false-colour maps (Figure 3-6 - Figure 3-11) reveal that:

- As one might anticipate, the largest absolute and relative near-surface ammonium concentration changes arise close to the new farms (within Tory Channel, and especially along the southern side (cf the northern/Arapawa Island side) of the channel – where the proposed new farms are).
- Somewhat elevated near-surface ammonium concentrations are evident in Grove Arm, central Queen Charlotte and Onapua Bay (e.g., Figure 3-6a).

- During the winter time-averaging period, seston concentration changes are very small throughout the system (e.g., Figure 3-6c - Figure 3-6g). During the summer, they become larger (e.g., Figure 3-7c - Figure 3-7g; see below for magnitudes).
- Changes (increases) in seston concentration are smallest in outer-most Queen Charlotte, intermediate in Tory Channel and greatest in Grove Arm and especially Onapua Bay.
- The inner-most new farm (Te Weka Bay) induces the largest changes (relative and absolute concentration increments) to seston concentration (for example, compare e.g., Figure 3-6 and Figure 3-7 (Tipi Bay winter & summer periods) with Figure 3-10 and Figure 3-11 (Te Weka Bay winter & summer periods)). During the spring/summer period, these changes in phytoplankton and chlorophyll concentration in the Te Weka Bay scenario increase by about 6% to the baseline_{f2016} scenario simulation (0.15–0.2 mg chl m⁻³ concentration increase). Relative concentration changes to other components of seston are smaller than that.
- For some state-variables (notably small detritus in the Tipi Bay and Motukina winter time-averages) there appears to be an ‘arc’ of concentration increment out in Cook Strait. It is possible that this is an artefact (i.e., generated by a small degree of numerical instability arising close to the domain boundaries). Nonetheless, even if a genuine farm effect, the relative and absolute increments are negligibly small.

Change maps from the AM_AF_WD+Tipi2 scenario

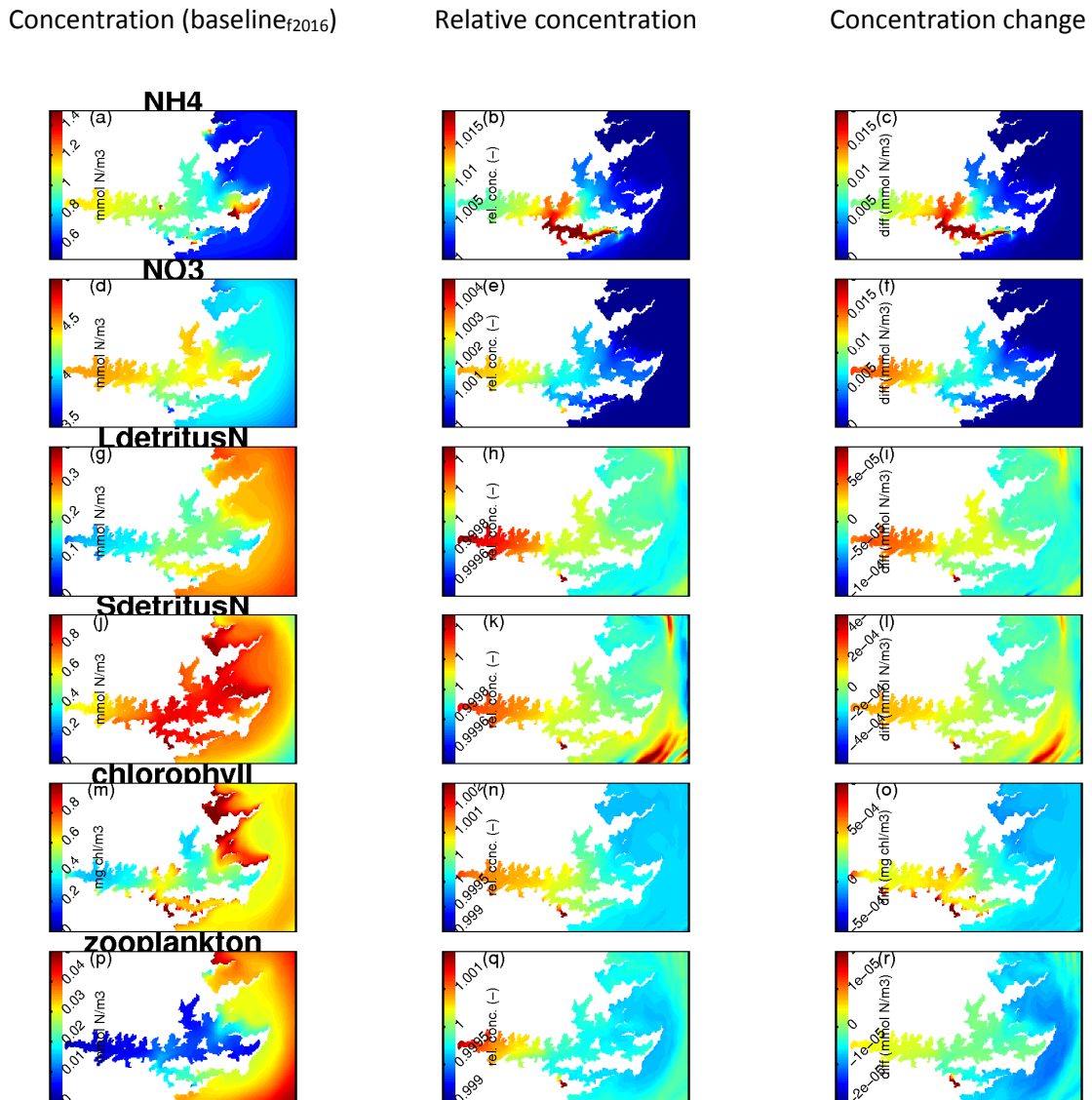


Figure 3-6: False colour maps of time-averaged, winter-time, near-surface water-quality characteristics for the AM_AF_WD and AM_AF_WD+Tipi2 scenarios. Left-hand images: time-average concentration in the AM_AF_WD scenario. Central images: relative concentration (AM_AF_WD+Tipi2 relative to AM_AF_WD). Right-hand images: concentration change (AM_AF_WD+Tipi2 minus AM_AF_WD). Each row shows results for a different state-variable (as indicated in the title of the left-hand-most image of each row).

Concentration (baseline_{f2016})

Relative concentration

Concentration change

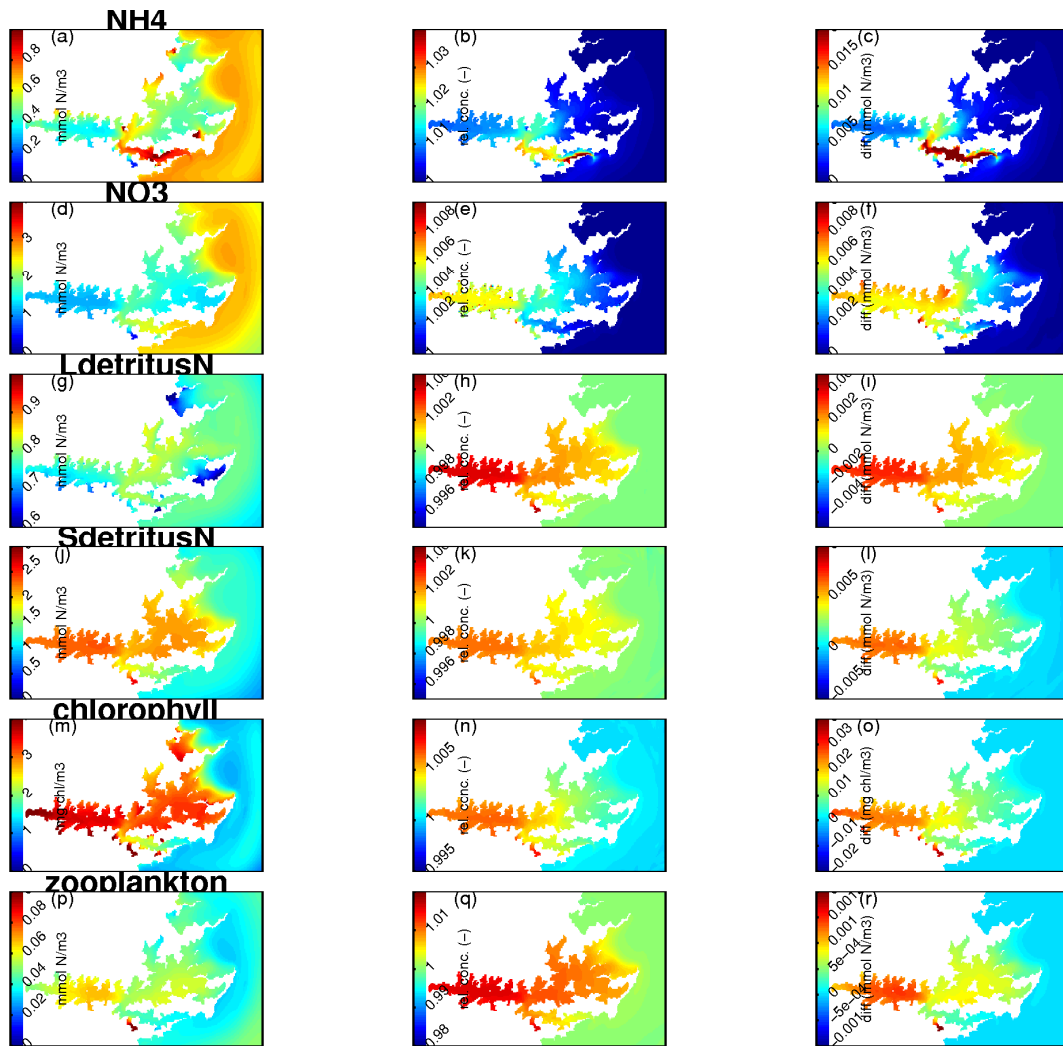


Figure 3-7: False colour maps of time-averaged, summer-time, near-surface water-quality characteristics for the AM_AF_WD and AM_AF_WD+Tipi2 scenarios. Organisation of the images follows that of Figure 3-6.

Change maps from the AM_AF_WD+Motu5 scenario

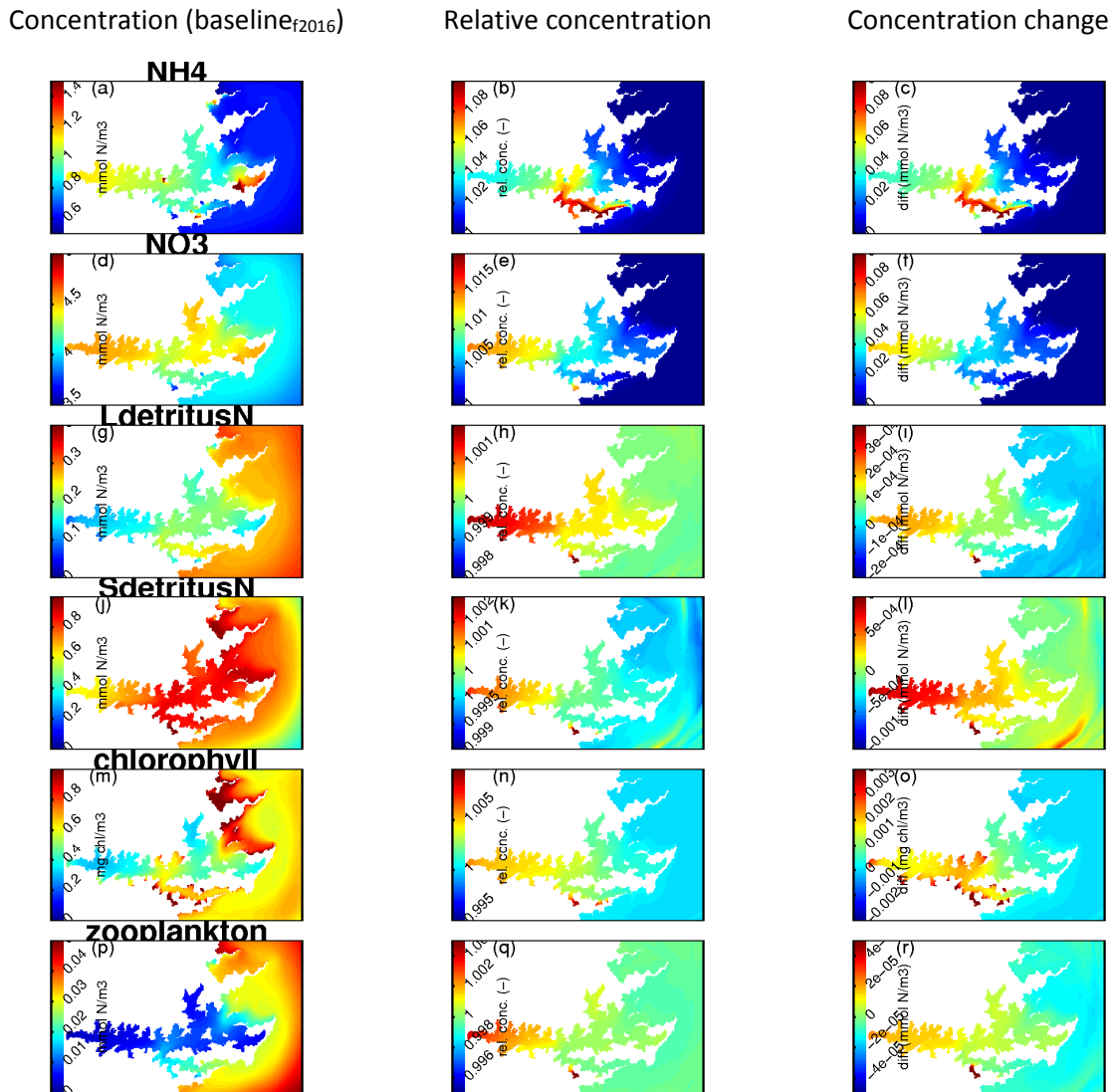


Figure 3-8: False colour maps of time-averaged, winter-time, near-surface water-quality characteristics for the AM_AF_WD and AM_AF_WD+Motu5 scenarios. Organisation of the images follows that of Figure 3-6.

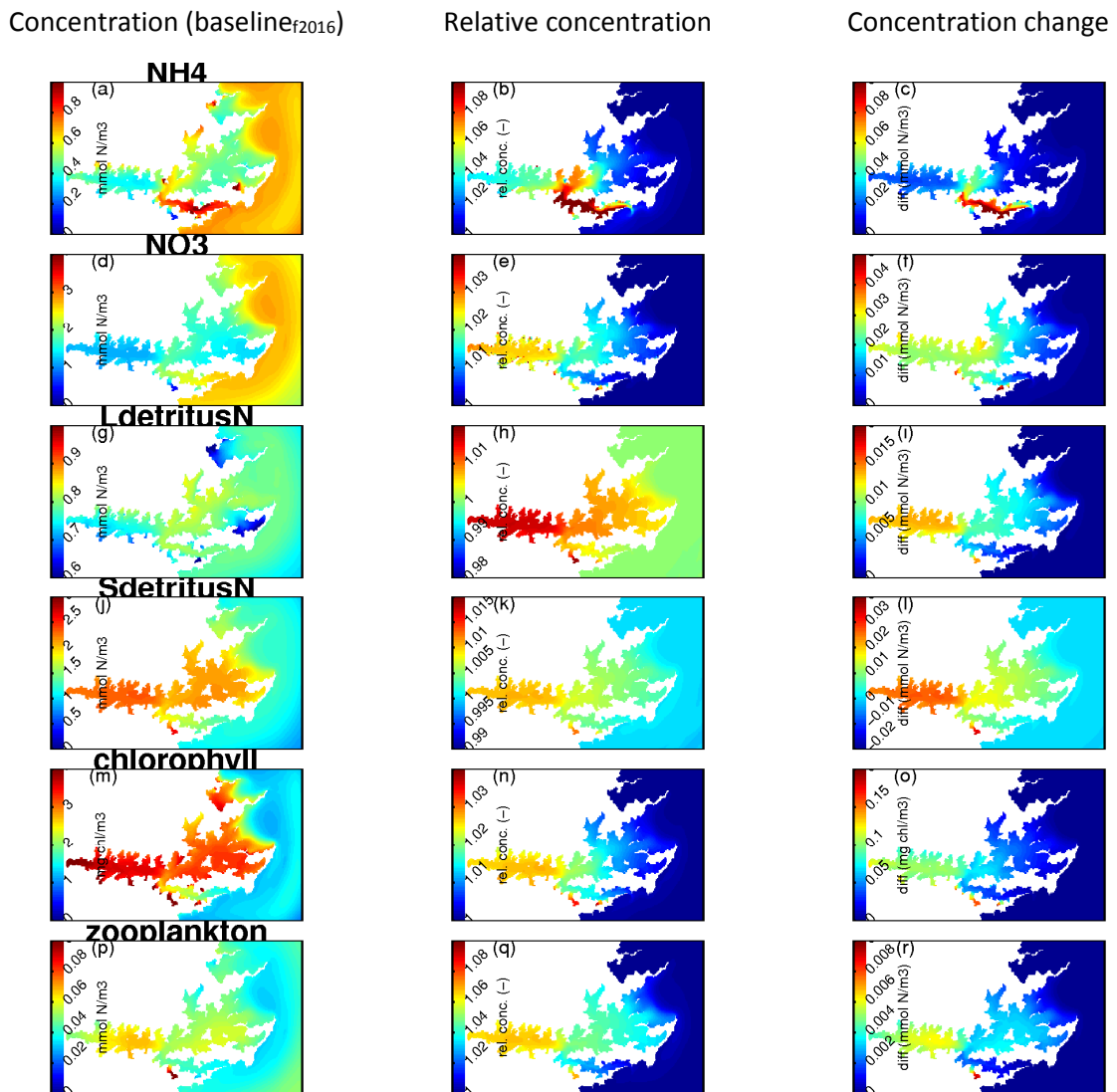


Figure 3-9: False colour maps of time-averaged, summer-time, near-surface water-quality characteristics for the AM_AF_WD and AM_AF_WD+Motu5 scenarios. Organisation of the images follows that of Figure 3-6.

Change maps from the AM_AF_WD+Weka5 scenario

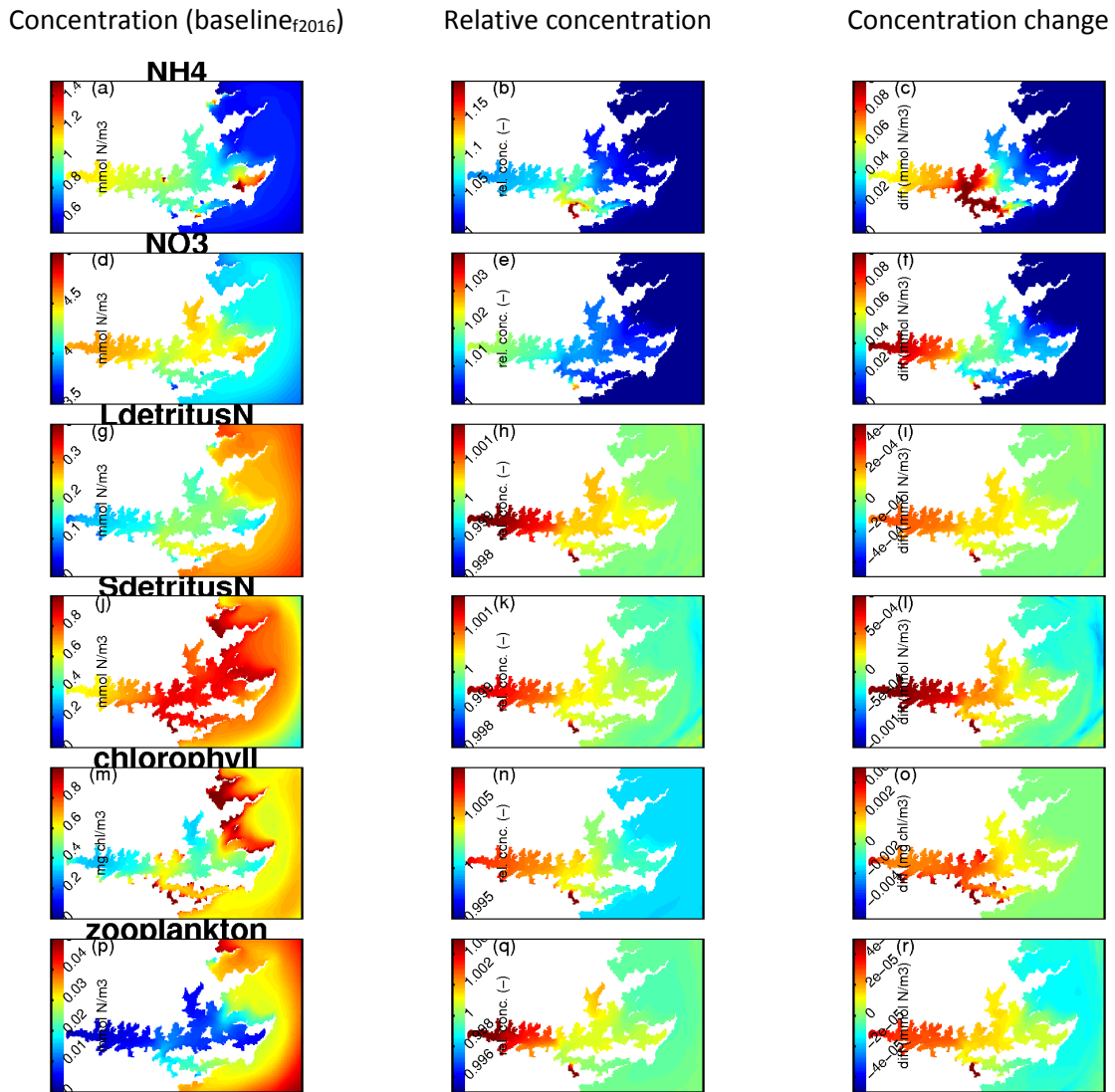


Figure 3-10: False colour maps of time-averaged, winter-time, near-surface water-quality characteristics for the AM_AF_WD and AM_AF_WD+Weka5 scenarios. Organisation of the images follows that of Figure 3-6.

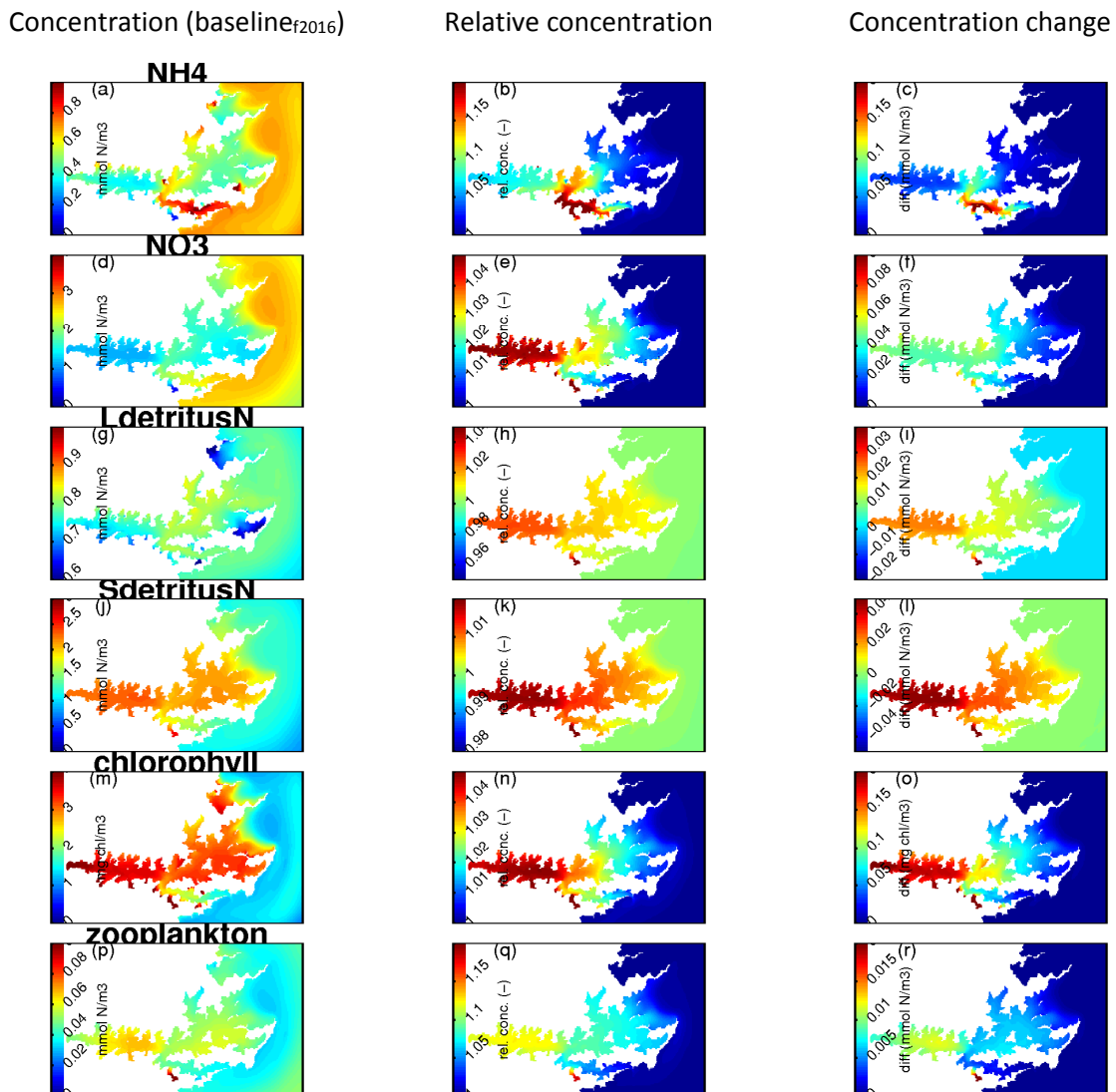


Figure 3-11: False colour maps of time-averaged, summer-time, near-surface water-quality characteristics for the AM_AF_WD and AM_AF_WD+Weka5 scenarios. Organisation of the images follows that of Figure 3-6.

3.3 Multiple-additional-farm scenarios relative to baseline_{f2016} (AM_AF_WD)

Within the sub-sections of this section, we show results from the scenarios in which two or more of the three candidate new farms are jointly introduced. Specifically, in Section 3.3.1 we show the predicted time-series of state-variable concentrations at each of the five Marlborough District Council water-quality monitoring stations (Figure 1-1) and in Section 3.3.2, we show maps of: (i) time-averaged concentration, (ii) relative concentration and (iii) concentration change associated with each scenario.

3.3.1 Time-series from the multiple-additional farms scenarios

Figure 3-12 to Figure 3-16 illustrate the simulated concentrations of each model state-variable in the upper-most layer of each water-column at each of the five Marlborough District Council water-quality sampling stations for the baseline_{f2016} scenario and three different multiple-additional-farm scenarios. We also present these multiple-additional-farm scenario results as time-series of

concentration difference (from the baseline_{f2016} scenario) in Appendix D and concentration-relative-to-baseline_{f2016} in Appendix E.

As one might expect:

- The results are qualitatively very similar to those presented for the single-farm addition scenarios. Indeed, quantitatively, the absolute and relative concentration increments arising from the multi-farm addition scenario results are approximately the sums of the component single-farm addition scenarios.
- Thus, as in the single-farm addition scenarios:
 - changes are larger in summer than in winter
 - the greatest ammonium changes are in the immediate vicinity of the farms
 - the greatest changes in seston arise further afield (Onapua Bay and Grove Arm).
- The scenario with the largest number of farms (AM_AF_WD+Tipi2+Motu5+Weka5) induces the largest changes. For chlorophyll, the time-averaged summertime increase is circa 8% in Grove Arm (Figure 3-12, Figure 3-13, Figure 3-19 and Figure 3-20). For zooplankton, it is circa 15-20%.
- At sites QCS-1 – QCS 4, the ‘swapped farms’ (AM_SF_WD+Tipi2+Motu5+Weka5) scenario tends to induce larger water-quality changes than the ‘baseline_{f2016} + two new farms’ (AM_AF_WD_+Tipi2+Weka5) scenario. This is because the former scenario implies a larger total feed load into Tory Channel and inner/central Queen Charlotte. At site QCS-5, the swapped farms scenario tends to induce smaller water-quality changes than the baseline_{f2016}+Tipi2+Weka5 scenario. This is consistent with the fact that the Otanerau farm (absent in the former scenario) is relatively close to site QCS-5 whilst the three proposed new farms are far from it.

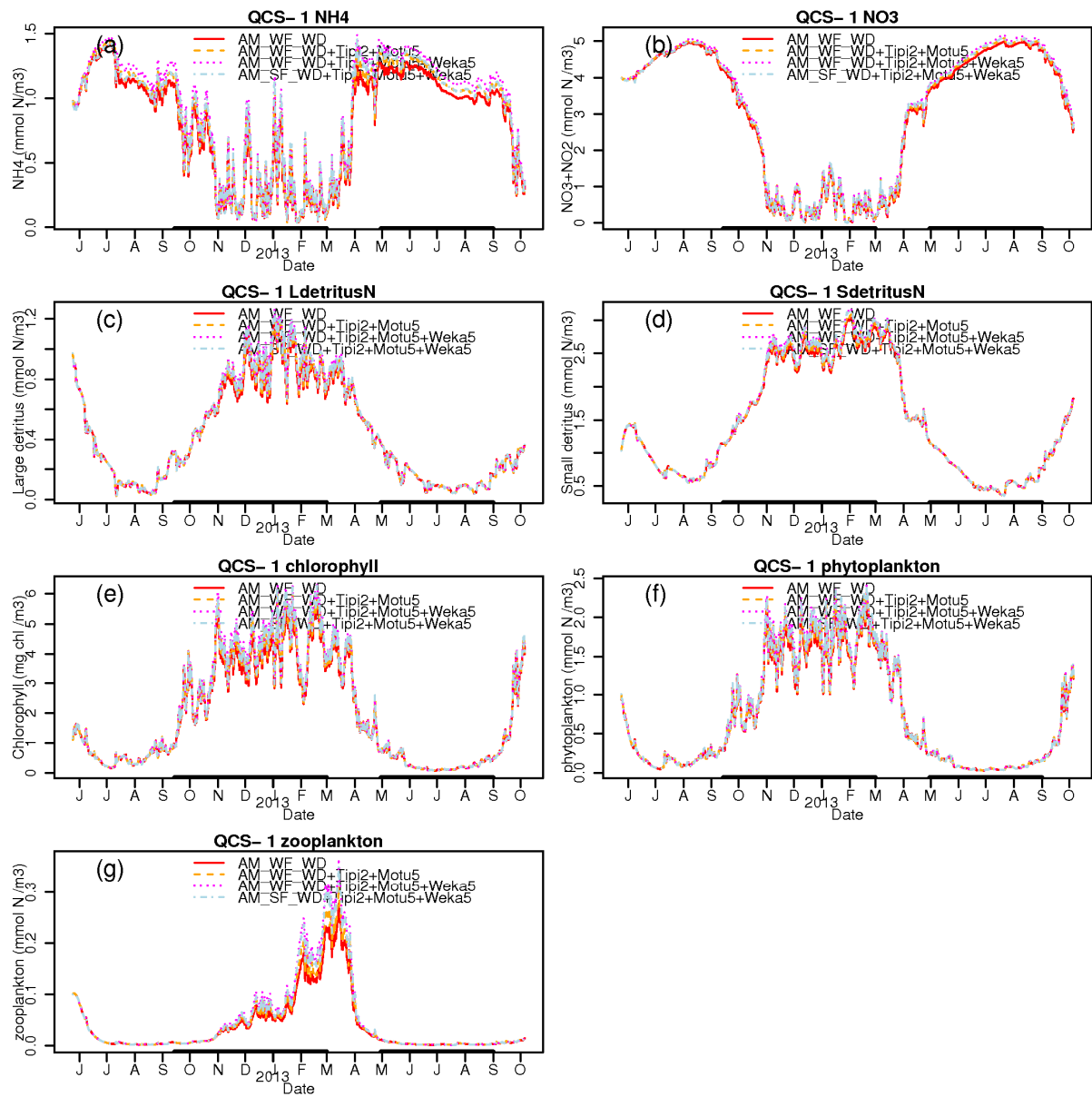


Figure 3-12: Simulated dynamics of water-quality state-variables in the uppermost layer at station QCS-1 (inner Grove Arm) under differing multiple additional fish-farm scenarios. The red line corresponds to the baseline_{f2016} scenario (AM_AF_WD). The dashed orange line corresponds to the ‘baseline_{f2016} farms plus Tipi Bay at 2000 tonne annual feed plus Motukina at 5000 tonne annual feed’ scenario. The dotted pink line corresponds to the ‘baseline_{f2016} farms plus Tipi Bay at 2000 tonne annual feed plus Motukina point at 5000 tonne annual feed plus Te Weka Bay at 5000 tonne annual feed’ scenario. The dashed-blue line corresponds to the ‘baseline_{f2016} farms (excluding Ruakaka and Otanerau) plus Tipi Bay at 2000 tonne annual feed plus Motukina point at 5000 tonne annual feed plus Te Weka Bay at 5000 tonne annual feed’ scenario.

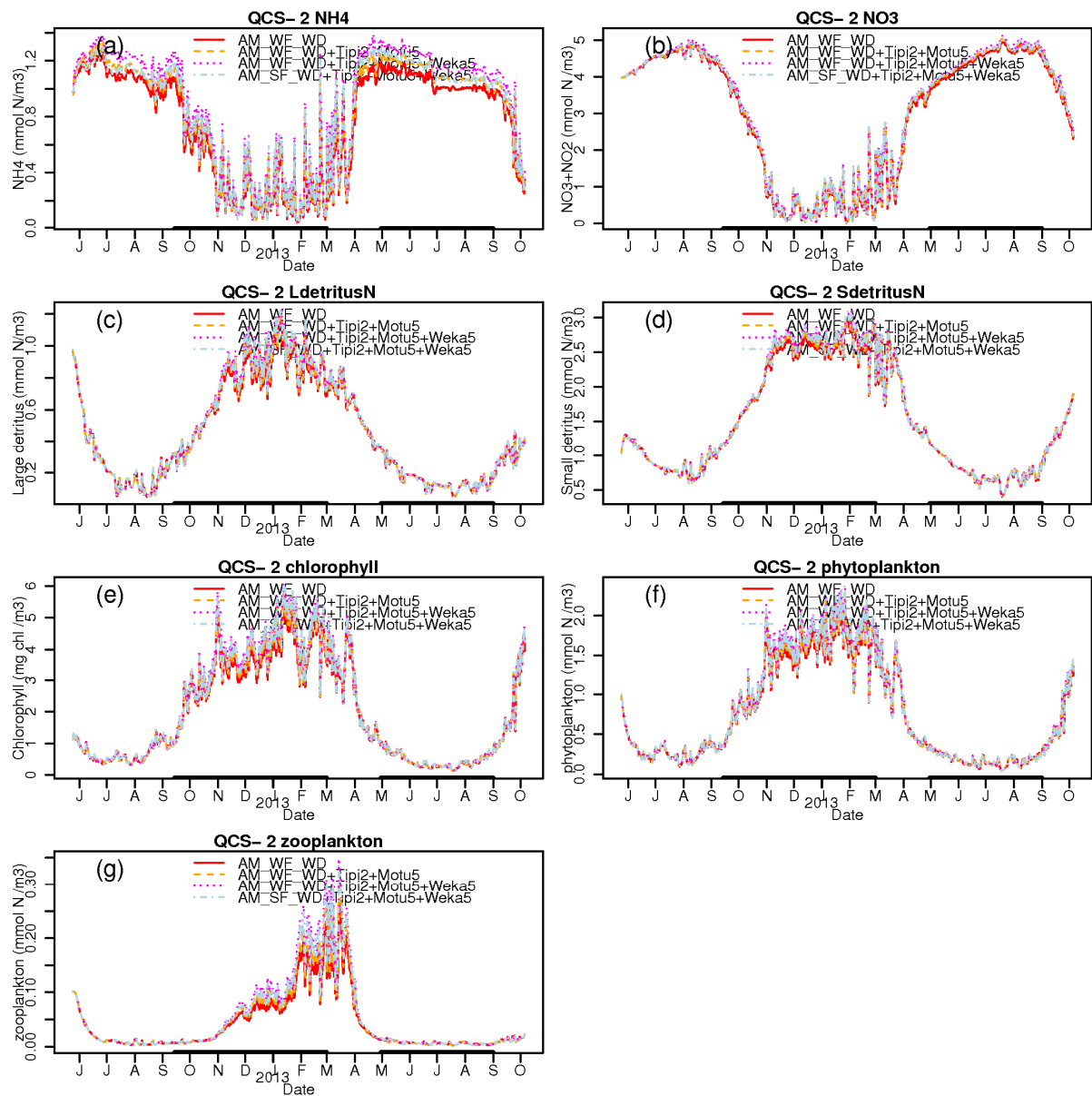


Figure 3-13: Simulated dynamics of water-quality state-variables in the uppermost layer at station QCS-2 (outer Grove Arm) under differing multiple additional fish-farm scenarios. The graph format follows Figure 3-12.

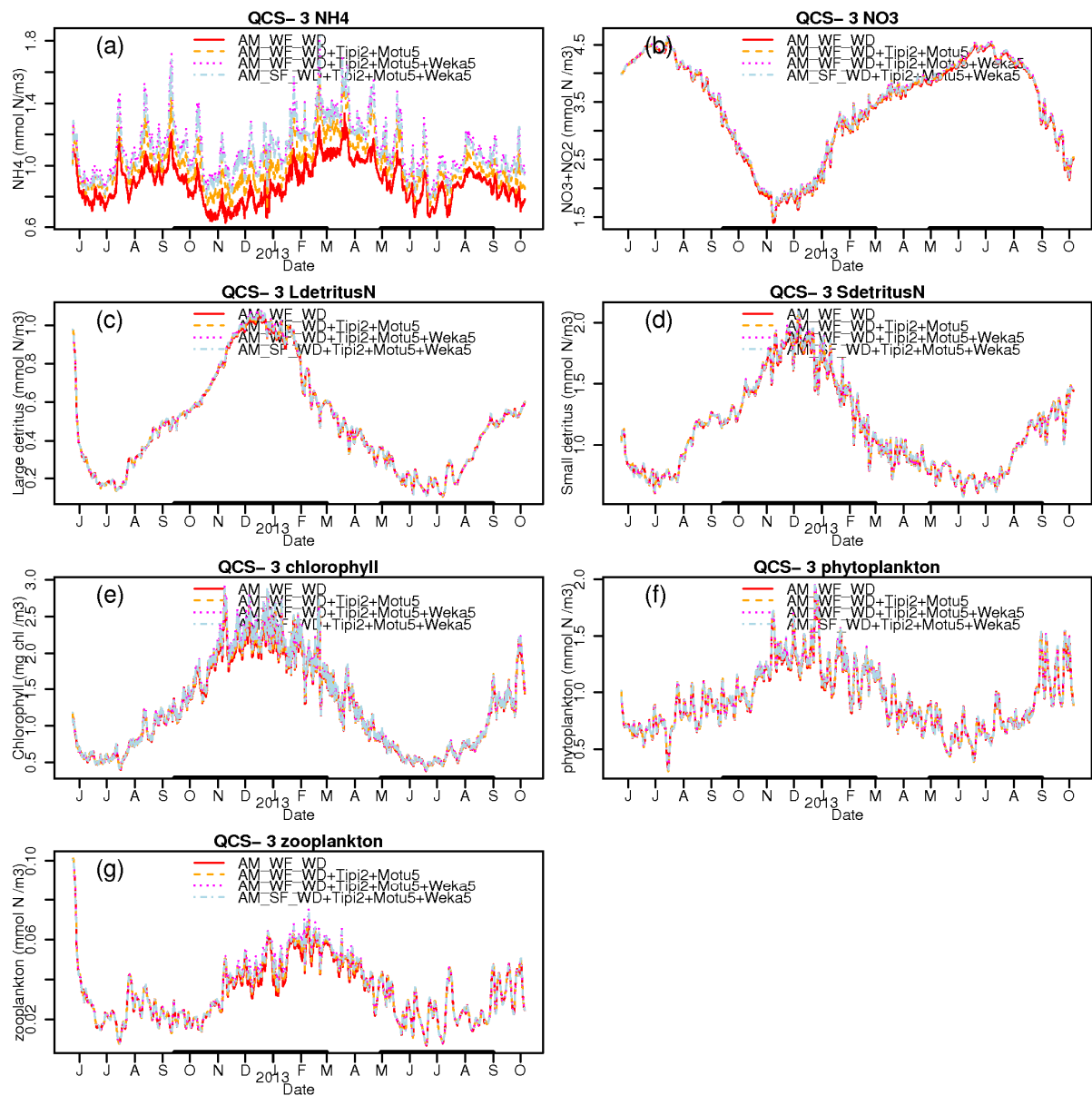


Figure 3-14: Simulated dynamics of water-quality state-variables in the uppermost layer at station QCS-3 (Tory Channel) under differing multiple additional fish-farm scenarios. The graph format follows Figure 3-12.

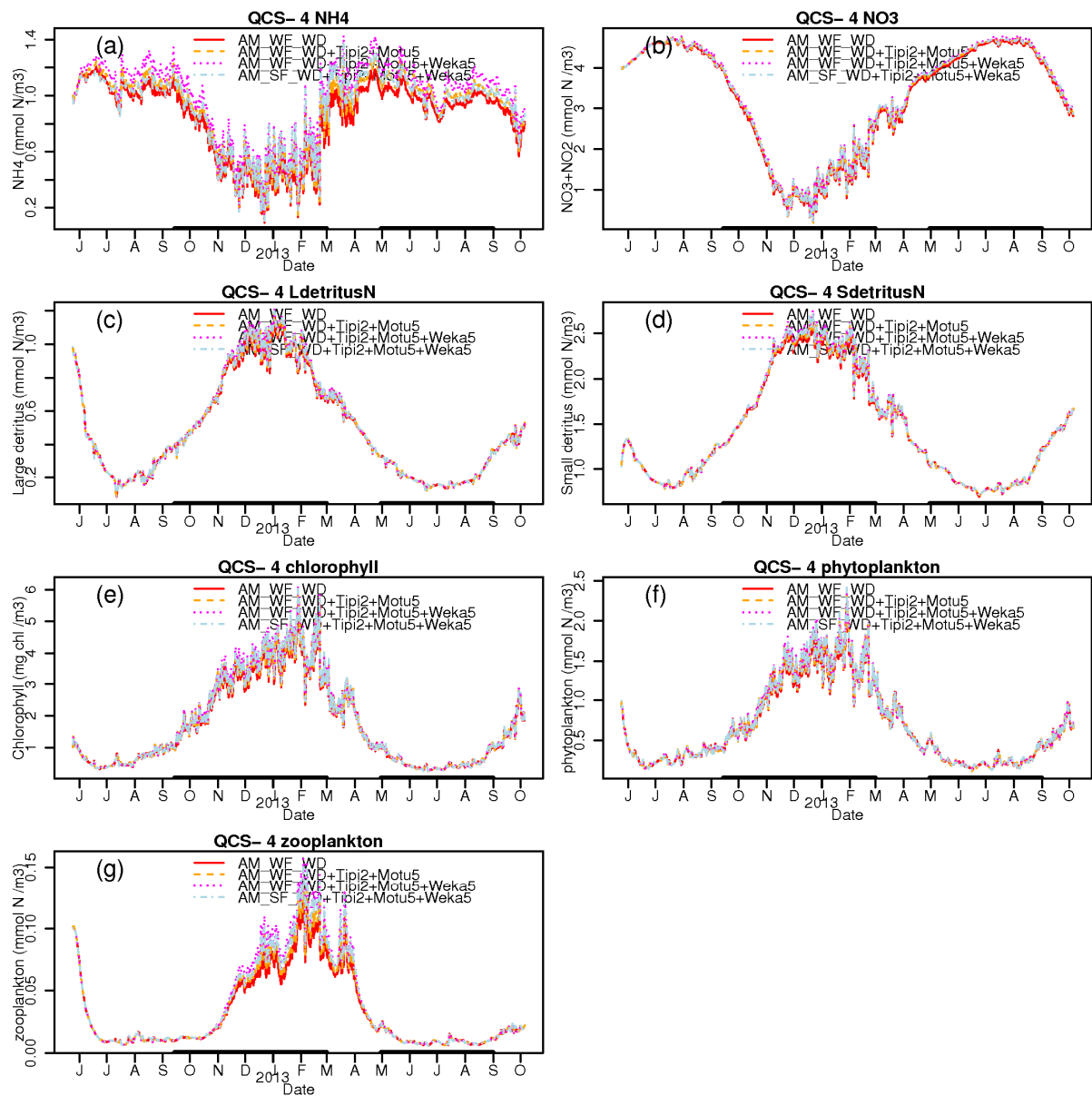


Figure 3-15: Simulated dynamics of water-quality state-variables in the uppermost layer at station QCS-4 (inner/central Queen Charlotte) under differing multiple additional fish-farm scenarios. The graph format follows Figure 3-12.

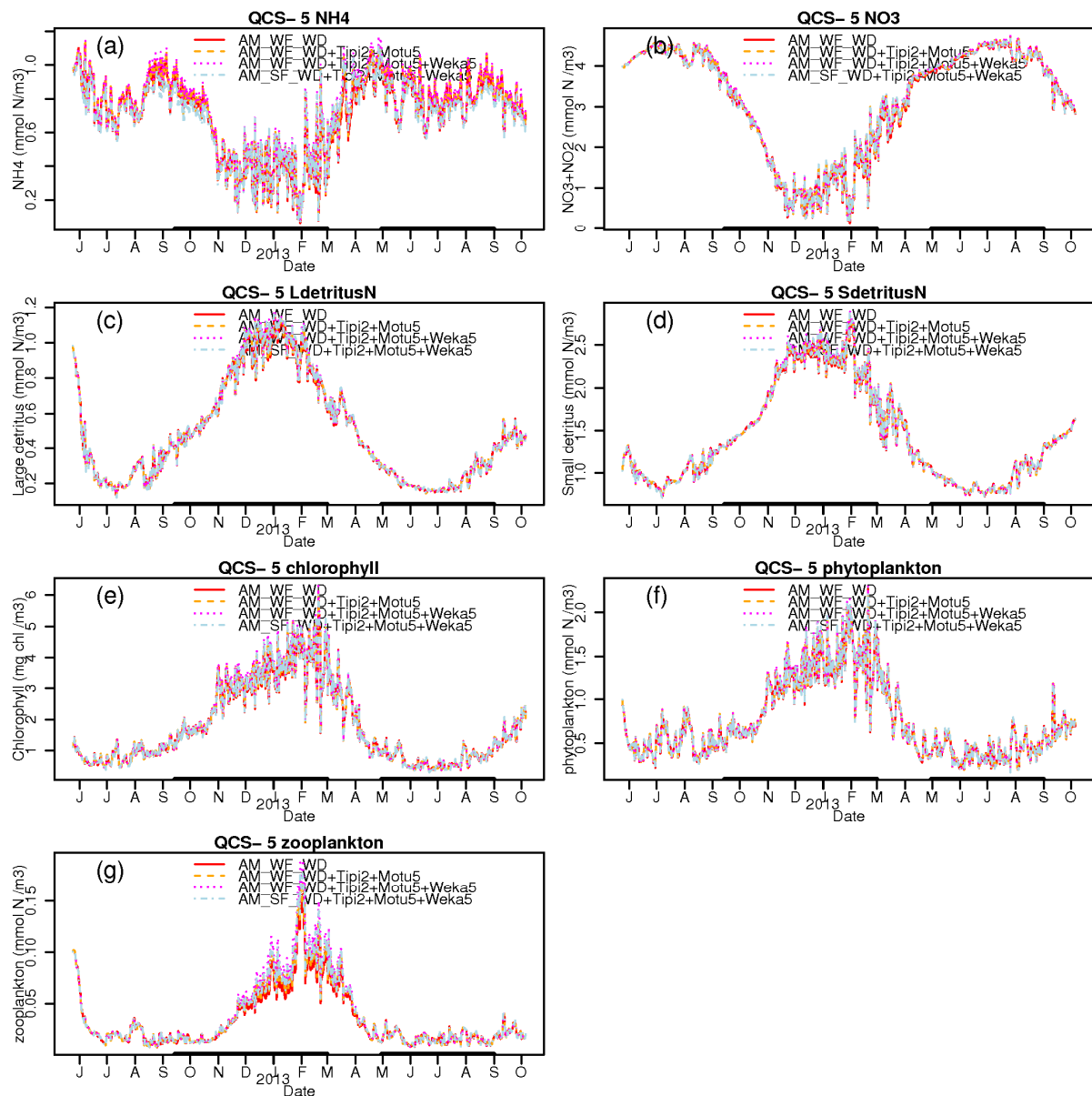


Figure 3-16: Simulated dynamics of water-quality state-variables in the uppermost layer at station QCS-5 (outer Queen Charlotte) under differing multiple additional fish-farm scenarios. The graph format follows Figure 3-12.

3.3.2 Change maps from the multiple-additional-farms scenarios

As with the time-series plots, the relative- and absolute concentration change patterns revealed by the false-colour maps (Figure 3-17 to Figure 3-22) are approximately the sum of changes induced by the individual additional farms:

- Changes in ammonium concentration are greatest in Tory Channel and central Queen Charlotte.
- Other state-variables tend to show the greatest changes in Grove Arm and in side bays of Tory Channel (especially Onapua Bay).

- Phytoplankton and chlorophyll concentrations show the greatest enhancement during the spring/summer period. This is to be expected given that nutrients tend to limit the realized rates of primary production during those periods whereas light limits production during the winter period. Enhancement is greatest in Grove Arm and Onapua Bay. In Grove Arm, enhancement amounts to 8% of the baseline_{f2016} (a concentration increase of about 0.3 mg chl m⁻³). In Onapua Bay the increase is about 10% relative to the baseline_{f2016} simulation (0.5 mg m⁻³ increase).
- During the summer, much of the additional primary production arising from the additional fish-farm-derived ammonium is predicted to pass up the food chain into the zooplankton. The relative increases in zooplankton biomass can exceed those of phytoplankton (though the zooplankton biomass remains small in comparison with phytoplankton biomass).

Change maps from the AM_AF_WD+Tipi2+Motu5 scenario

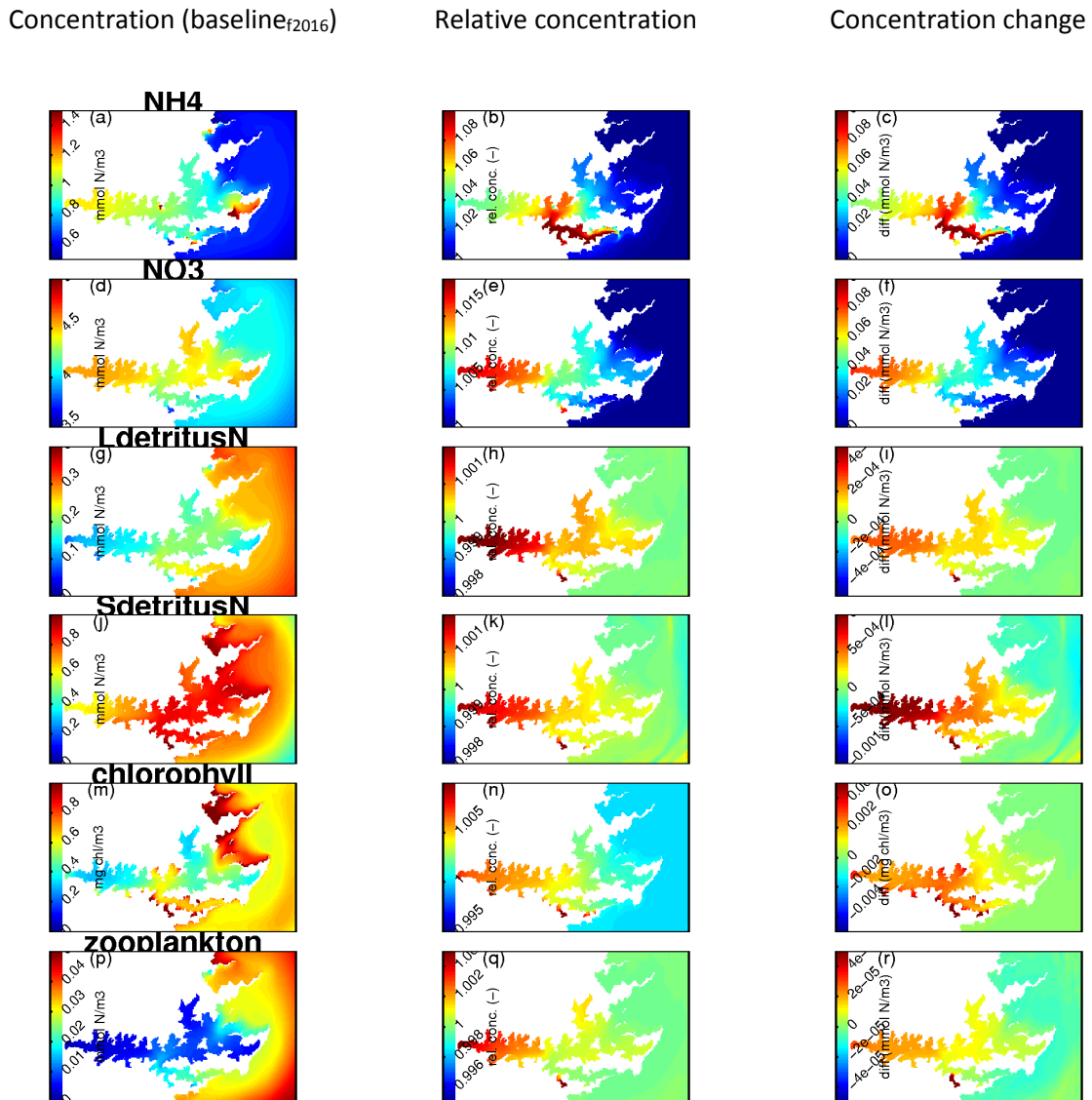


Figure 3-17: False colour maps of time-averaged, winter-time, near-surface water-quality characteristics for the AM_AF_WD and AM_AF_WD+Tipi2+Motu5 scenarios.

Concentration (baseline_{f2016})

Relative concentration

Concentration change

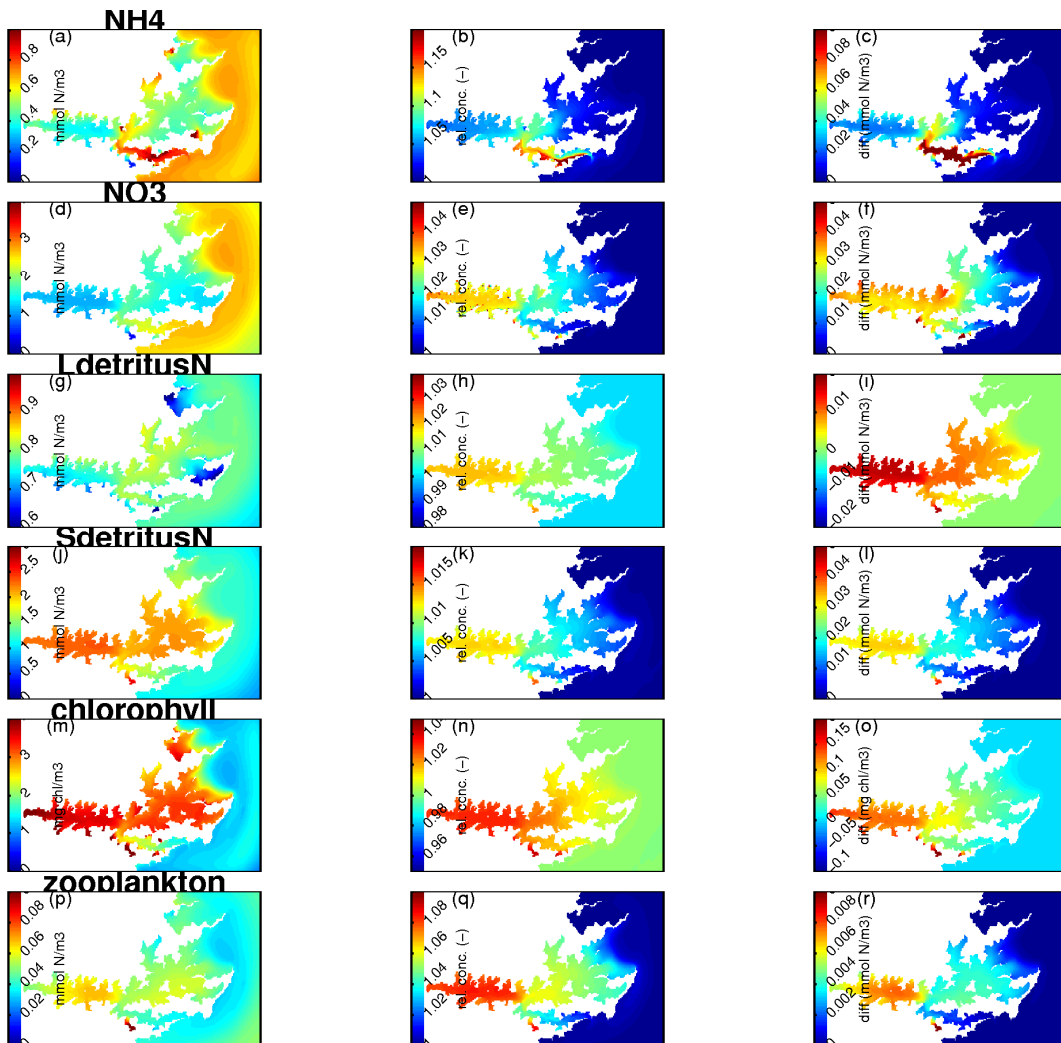


Figure 3-18: False colour maps of time-averaged, summer-time, near-surface water-quality characteristics for the AM_AF_WD and AM_AF_WD+Tipi2+Motu5 scenarios.

Change maps from the AM_AF_WD+Tipi2+Motu5+Weka5 scenario

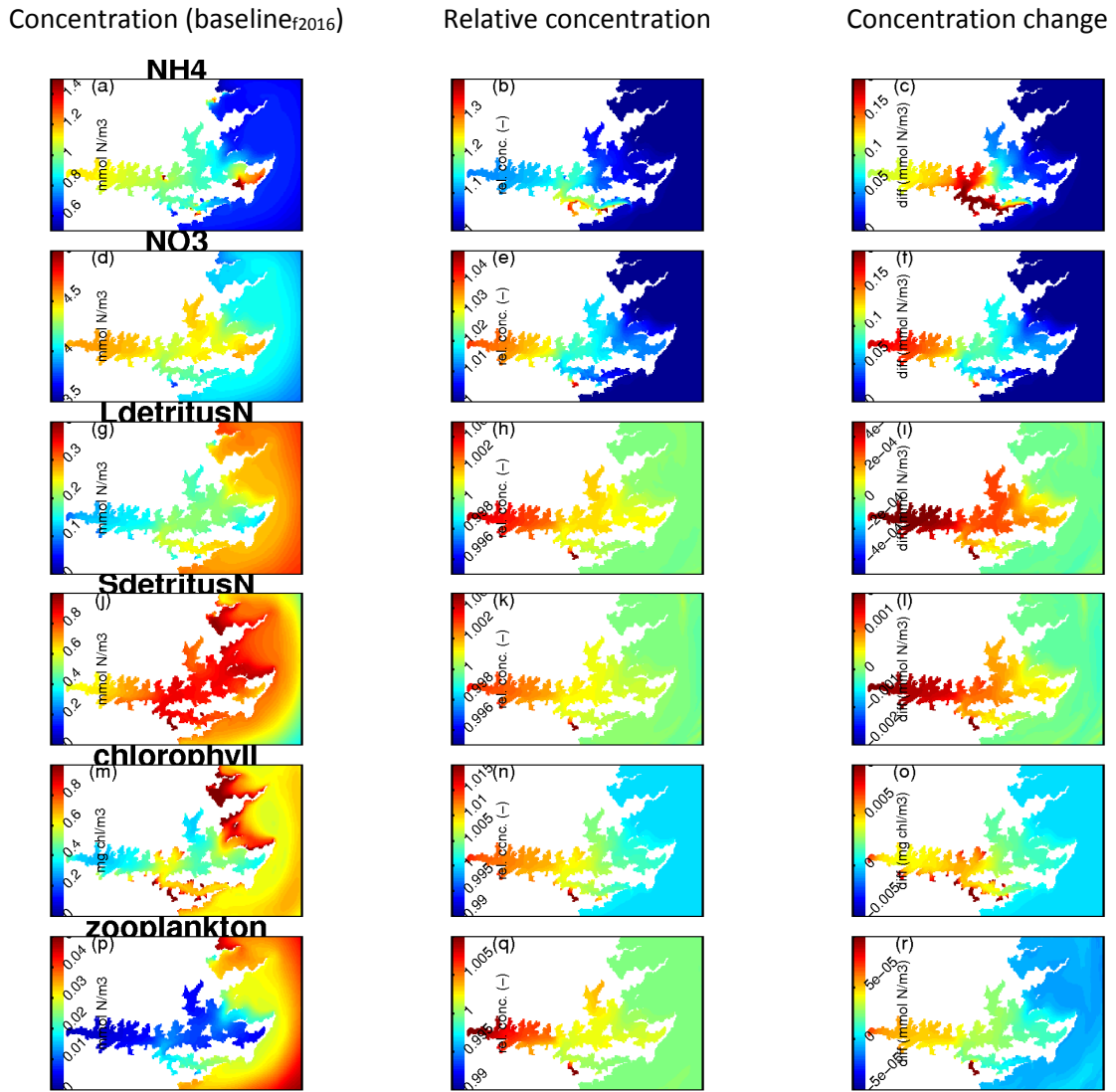


Figure 3-19: False colour maps of time-averaged, winter-time, near-surface water-quality characteristics for the AM_AF_WD and AM_AF_WD+Tipi2+Motu5+Weka5 scenarios.

Concentration (baseline_{f2016})

Relative concentration

Concentration change

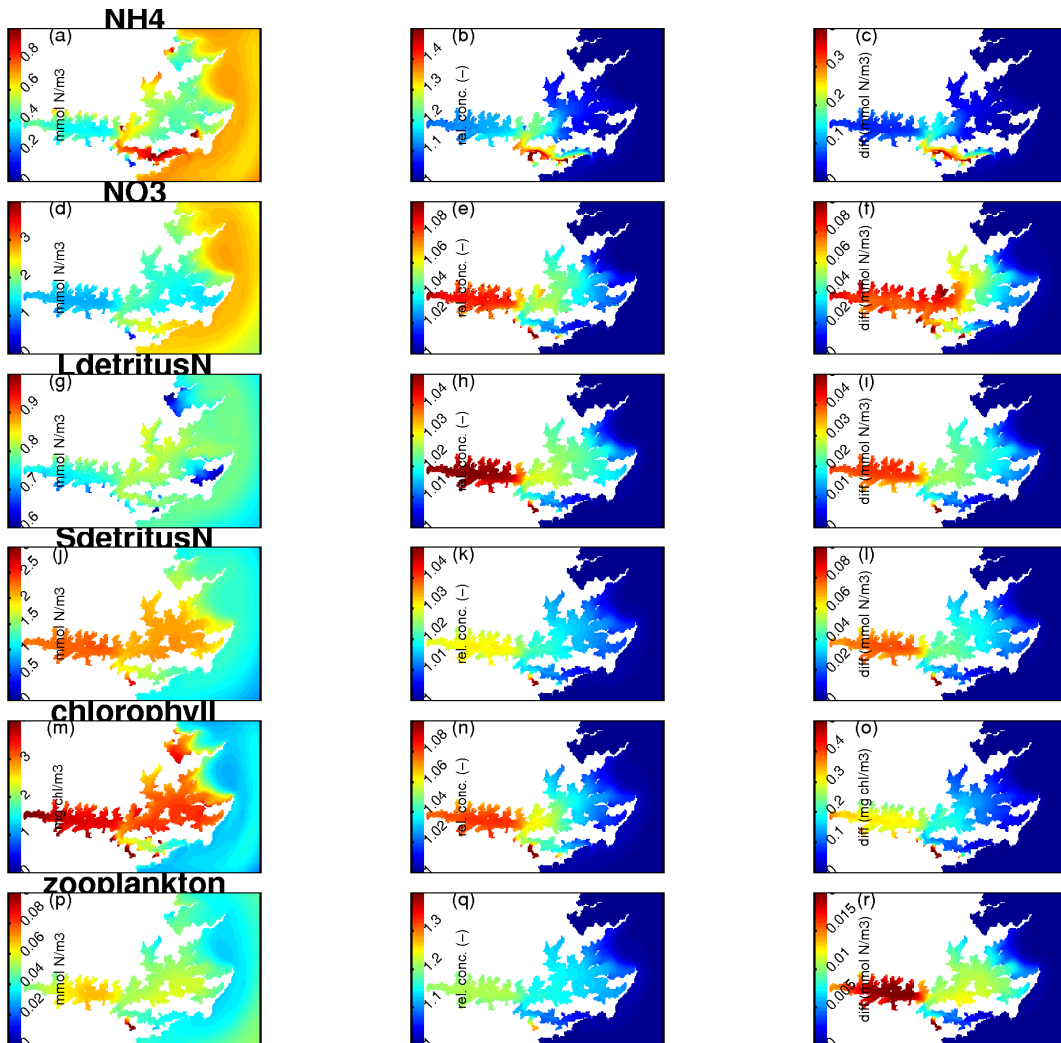


Figure 3-20: False colour maps of time-averaged, summer-time, near-surface water-quality characteristics for the AM_AF_WD and AM_AF_WD+Tipi2+Motu5+Weka5 scenarios.

Change maps from the AM_SF_WD+Tipi2+Motu5+Weka5 scenario

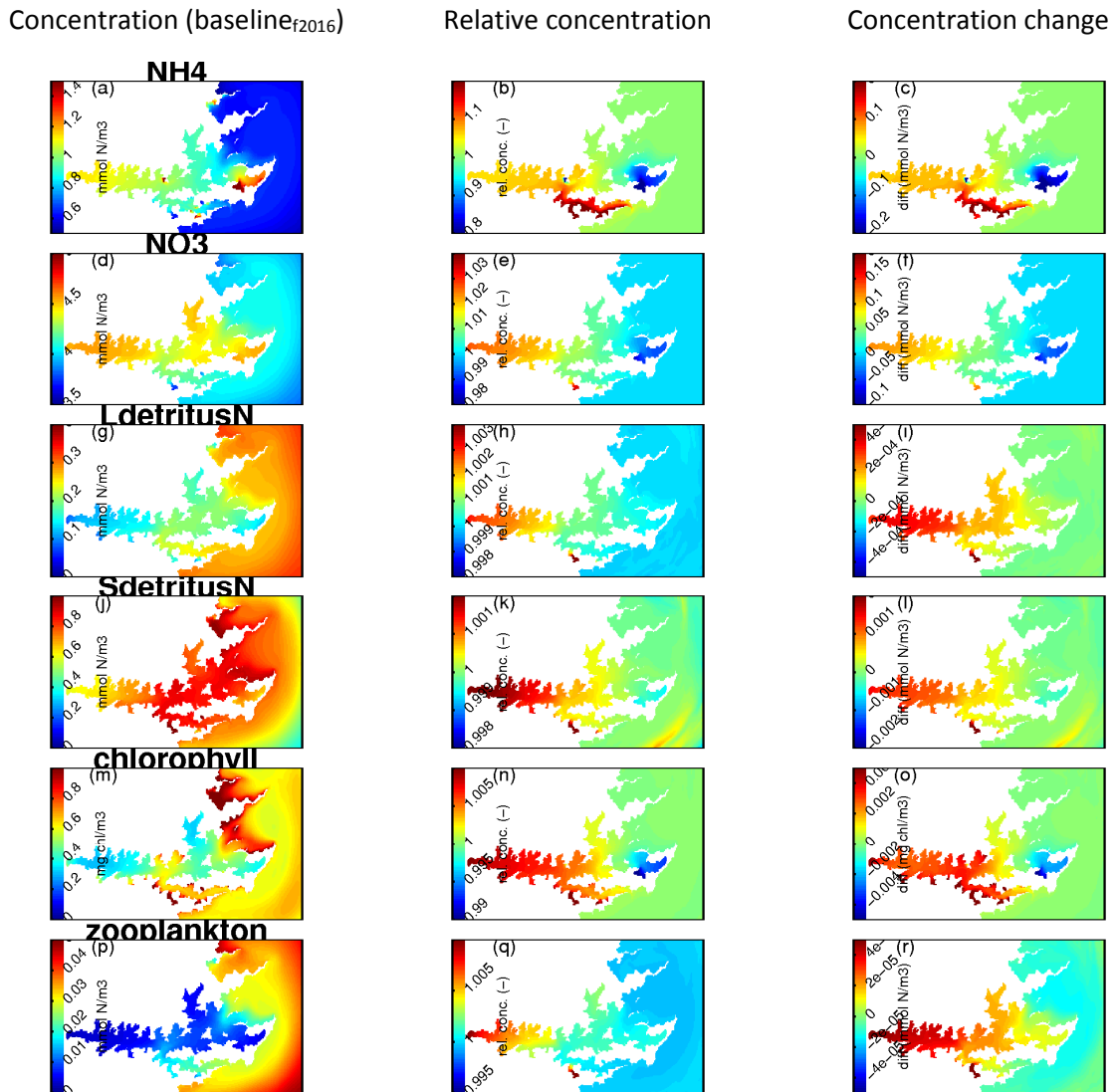


Figure 3-21: False colour maps of time-averaged, winter-time, near-surface water-quality characteristics for the AM_AF_WD and AM_SF_WD+Tipi2+Motu5+Weka5 scenario.

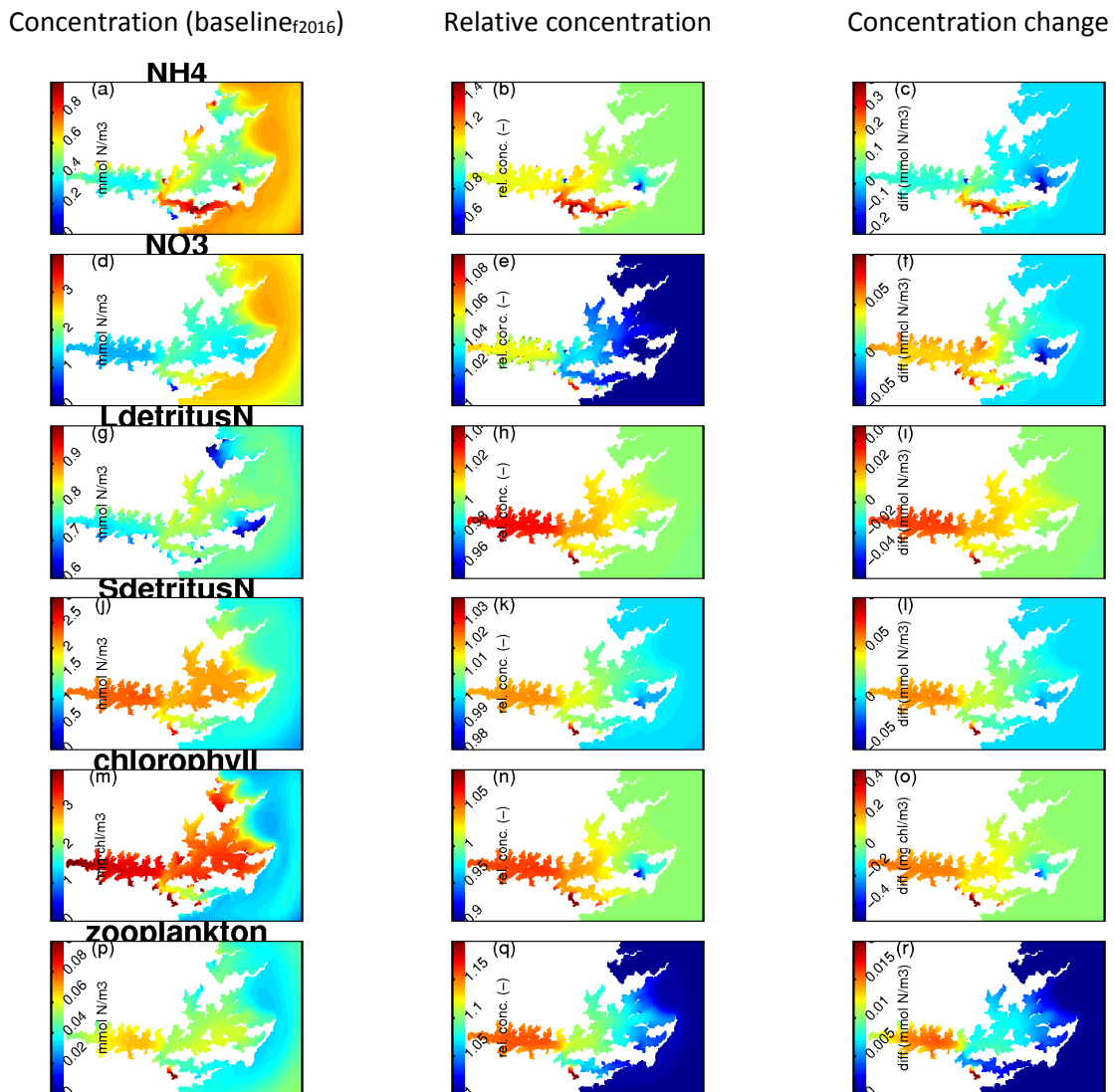


Figure 3-22: False colour maps of time-averaged, summer-time, near-surface water-quality characteristics for the AM_AF_WD and AM_SF_WD+Tipi2+Motu5+Weka5 scenario.

3.4 Baseline_{f2016}+Tipi2+Motu5+Weka5 (AM_AF_WD+Tipi2+Motu5+Weka5) in comparison with operating farms (EM_EF_WD)

The AM_AF_WD (all already-approved farms in operation) scenario has been treated as the baseline against which to assess the magnitudes of change that might arise if additional farms (beyond those already approved, rather than beyond those now in the water) are added into the system. The most recently approved fish-farm (Ngamahau) is not yet in the water. Thus, as yet, there are no field data with which to validate the quality of the baseline (AM_AF_WD) simulation results. In contrast, the existing conditions scenario (EM_EF_WD) purports to represent the farming systems that operated during the time-period that Marlborough District Council’s monitoring data stem from. In a sense, therefore, the EM_EF_WD can also be considered as a baseline (baseline_{f2012}).

3.4.1 Time-series from the baseline_{f2016}+Tipi2+Motu5+Weka5 (AM_AF_WD+Tipi2+Motu5+Weka5) scenario and operating farms scenario (EM_EF_WD)

Figure 3-23 to Figure 3-27 illustrate the time-series of simulated concentrations of each model state-variable in the upper-most layer of each water-column at each of the five Marlborough District Council water-quality sampling stations, for the EM_EF_WD and AM_AF_WD+Tipi2+Motu5+Weka5 scenarios. The same simulation results are also presented as concentration difference from the reference operating farms scenario within Appendix E.

At all stations, the qualitative simulated dynamical patterns are very similar. The general seasonal-scale variations retain the same phase and similar means and amplitudes (albeit that the AM_AF_WD+Tipi2+Motu5+Weka5 scenario tends to yield slightly higher annual means, and, perhaps, slightly larger amplitude high-frequency oscillations than the EM_EF_WD one). For particulates and NO₃, the differences between the two scenarios are trivial during the winter months and largest during the summer ones. The largest differences arise at the two inner Queen Charlotte stations (QCS-1 and QCS-2). There, the time averaged summertime chlorophyll concentration increment (difference between AM_AF_WD+Tipi2+Motu5+Weka5 and EM_EF_WD scenarios) is circa 0.5 mg chl m⁻³, whilst the largest instantaneous difference is circa 0.8 mg m⁻³ (see also Appendix E). These differences are approximately 0.1 mg m⁻³ larger than those between AM_AF_WD+Tipi2+Motu5+Weka5 and our 'approved farms' base-line (AM_AF_WD) (section 3.3).

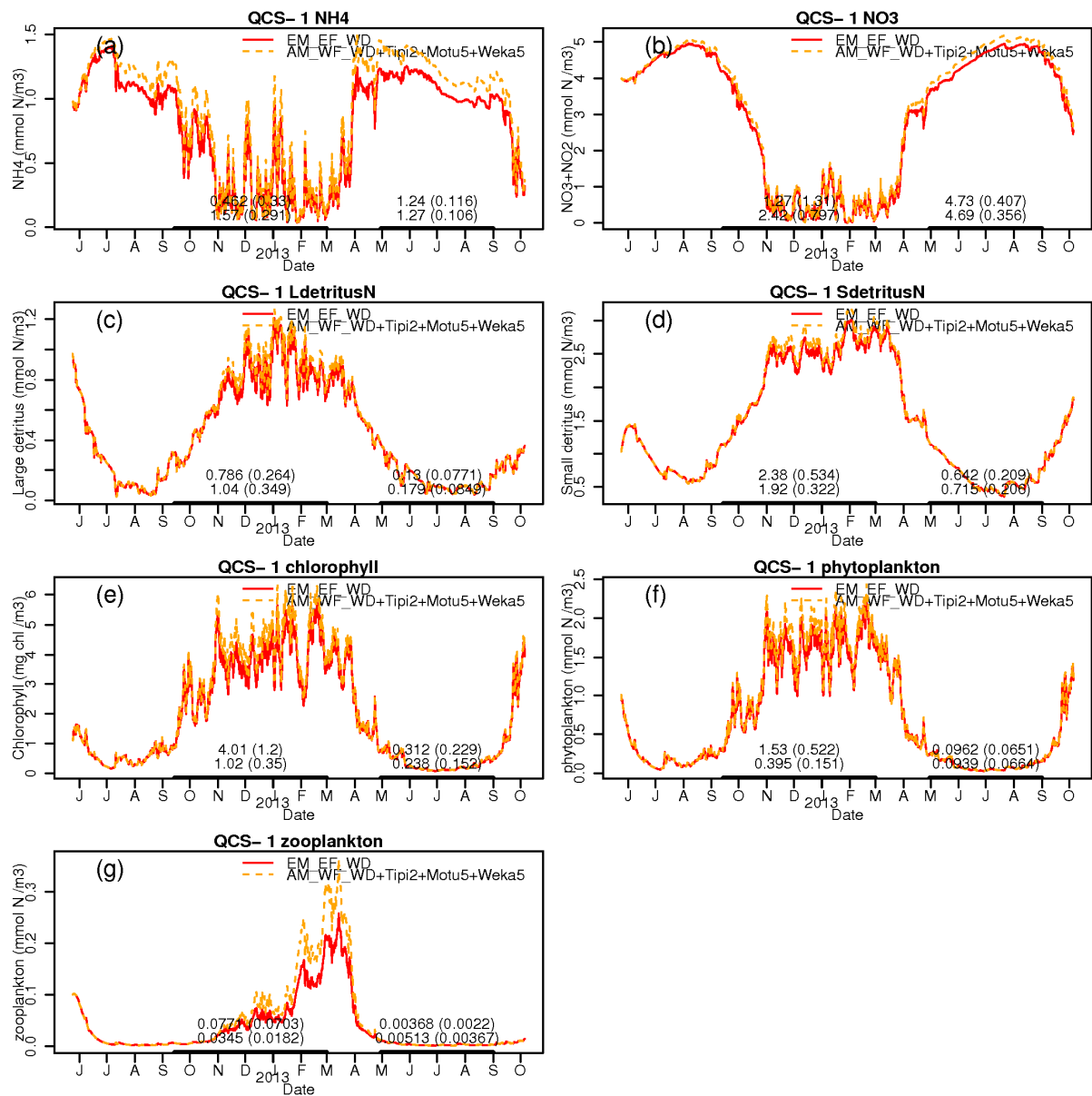


Figure 3-23: Simulated dynamics of water-quality state-variables in the uppermost layer at station QCS-1 (inner Grove Arm) in the EM_EF_WD and AM_AD_WF+Tipi2+Motu5+Weka5 scenarios. The thick black lines indicate the time-averaging periods. The numerals above them are the corresponding mean (standard deviations) for the sea-surface and sea-bed layers of the water column (upper and lower rows of text respectively) in the EM_EF_WD simulation.

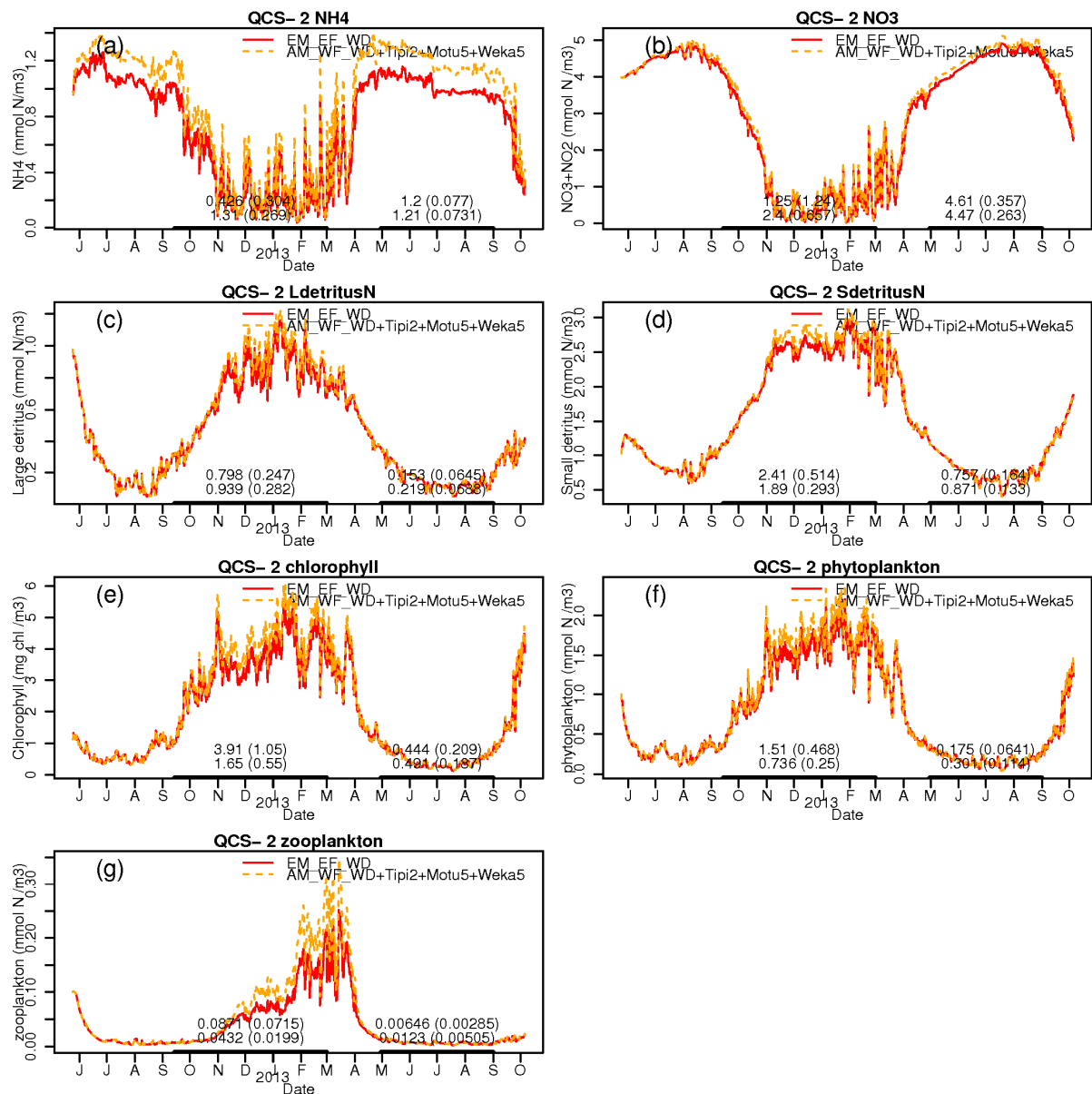


Figure 3-24: Simulated dynamics of water-quality state-variables in the uppermost layer at station QCS-2 (outer Grove Arm) in the EM_EF_WD and AM_AD_WF+Tipi2+Motu5+Weka5 scenarios. The thick black lines indicate the time-averaging periods. The numerals above them are the corresponding mean (standard deviations) for the sea-surface and sea-bed layers of the water column (upper and lower rows of text respectively) in the EM_EF_WD simulation.

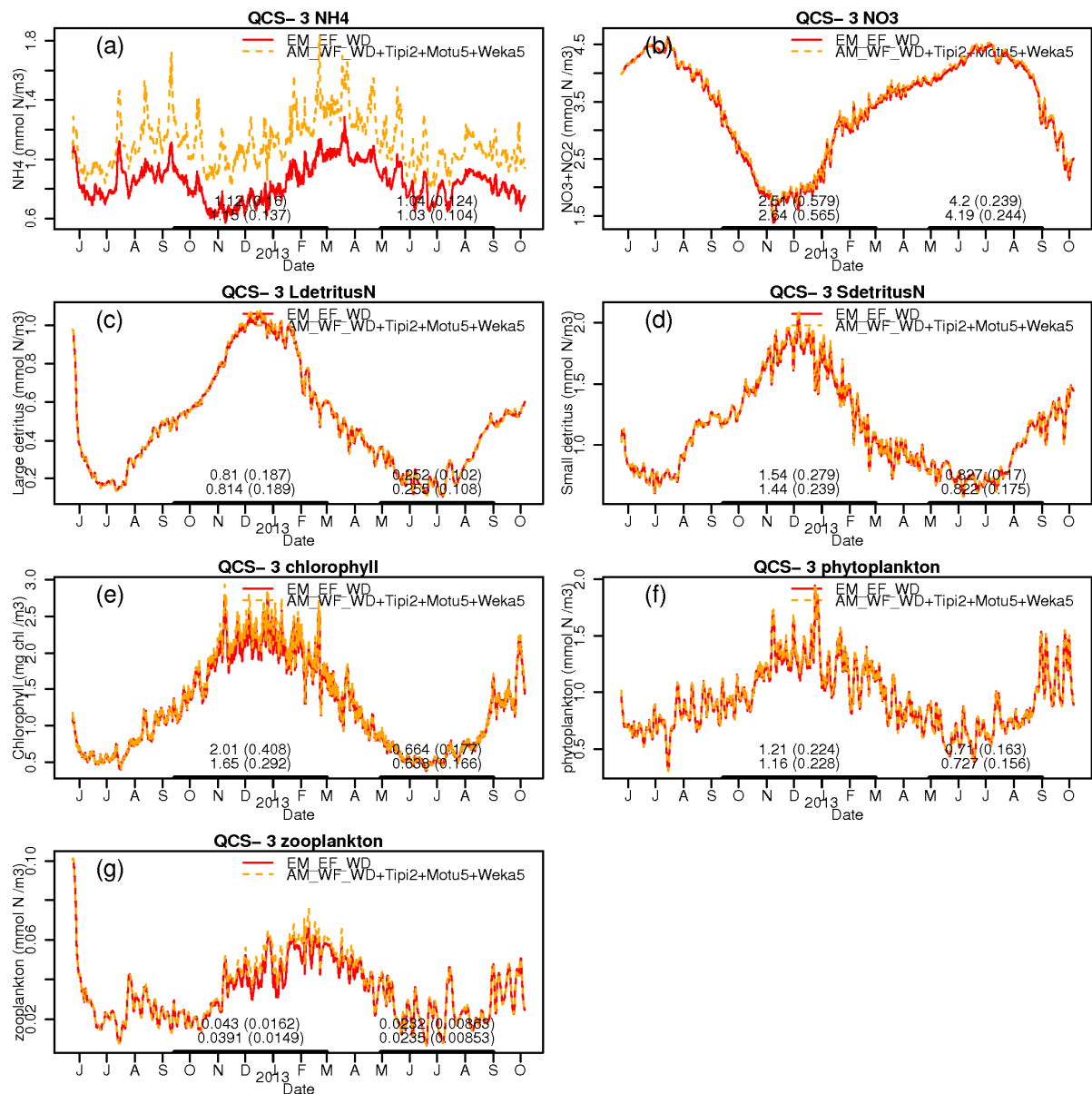


Figure 3-25: Simulated dynamics of water-quality state-variables in the uppermost layer at station QCS-3 (Tory Channel) in the EM_EF_WD and AM_AD_WF+Tipi2+Motu5+Weka5 scenarios. The thick black lines indicate the time-averaging periods. The numerals above them are the corresponding mean (standard deviations) for the sea-surface and sea-bed layers of the water column (upper and lower rows of text respectively) in the EM_EF_WD simulation.

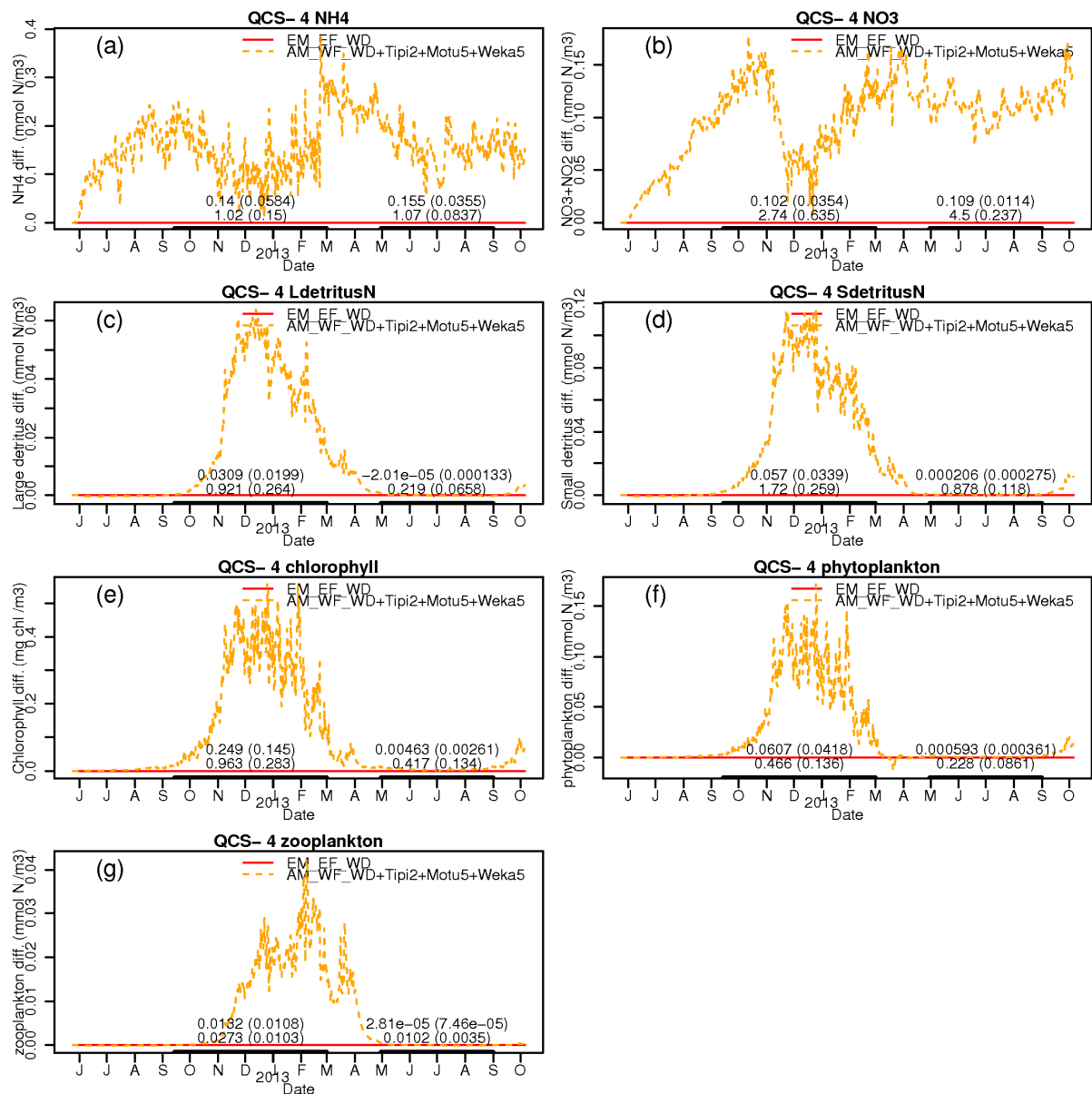


Figure 3-26: Simulated dynamics of water-quality state-variables in the uppermost layer at station QCS-4 (inner/central Queen Charlotte) in the EM_EF_WD and AM_AD_WF+Tipi2+Motu5+Weka5 scenarios. The thick black lines indicate the time-averaging periods. The numerals above them are the corresponding mean (standard deviations) for the sea-surface and sea-bed layers of the water column (upper and lower rows of text respectively) in the EM_EF_WD simulation.

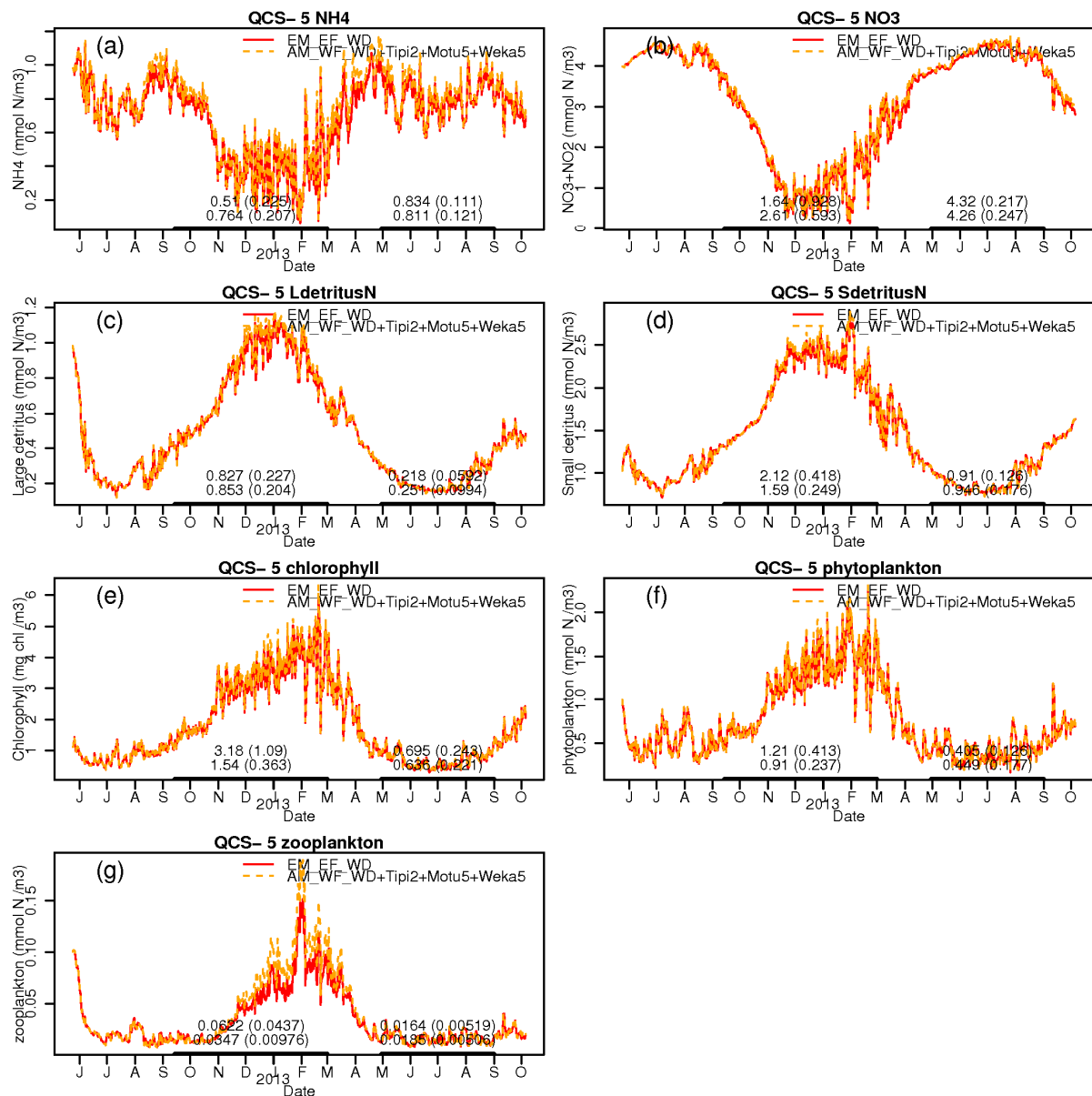


Figure 3-27: Simulated dynamics of water-quality state-variables in the uppermost layer at station QCS-5 (outer Queen Charlotte) in the EM_EF_WD and AM_AD_WF+Tipi2+Motu5+Weka5 scenarios. The thick black lines indicate the time-averaging periods. The numerals above them are the corresponding mean (standard deviations) for the sea-surface and sea-bed layers of the water column (upper and lower rows of text respectively) in the EM_EF_WD simulation.

3.4.2 Change maps for the baseline_{f2016}+Tipi2+Motu5+Weka5 (AM_AF_WD+Tipi2+Motu5+Weka5) scenario relative to operating farms (EM_EF_WD)

Figure 3-28 illustrates the change maps for the AM_AF_WD+Tipi2+Motu5+Weka5 scenario relative to the EM_EF_WD one during the winter time-averaging period. Figure 3-29 presents these maps for the spring/summer time-averaging period.

During the winter, the most evident difference between the two scenarios is the reduction of seston concentration in Otanerau/East Bay. This has nothing to do with the additional fish-farms that are present in the AM_AF_WD+Tipi2+Motu5+Weka5 scenario. Rather, it reflects the fact that the approved farms scenario (AM_AF_WD; and by implication also the AM_AF_WD+Tipi2+Motu5+Weka5 scenario) has some additional mussel farms in Otanerau/East Bay that are not present in the EM_EF_WD scenario.

In addition to the relatively large winter-time changes in Otanerau/East Bay during the winter, there are much smaller increases in seston concentration (for example, in the case of chlorophyll, $<0.01 \text{ mg chl m}^{-3}$) within inner/central Queen Charlotte and the inner parts of Tory Channel. These are likely to have been induced by the three additional fish farms rather than the additional mussel farms.

During the spring summer period, there is little/no evidence of seston depletion in Otanerau/East Bay (see Hadfield, Broekhuizen et al. (2014) for explanation) and the seston enhancement within inner/central Queen Charlotte and inner Tory Channel (esp. Onapua/Opua Bays) is larger than evident during the winter (approx. 0.5 mg m^{-3} for chlorophyll in inner/central Queen Charlotte). Again, (as implied in section 3.4.1), this is likely to be driven by the presence of the three additional farms.

Concentration (baseline_{f2016})

Relative concentration

Concentration change

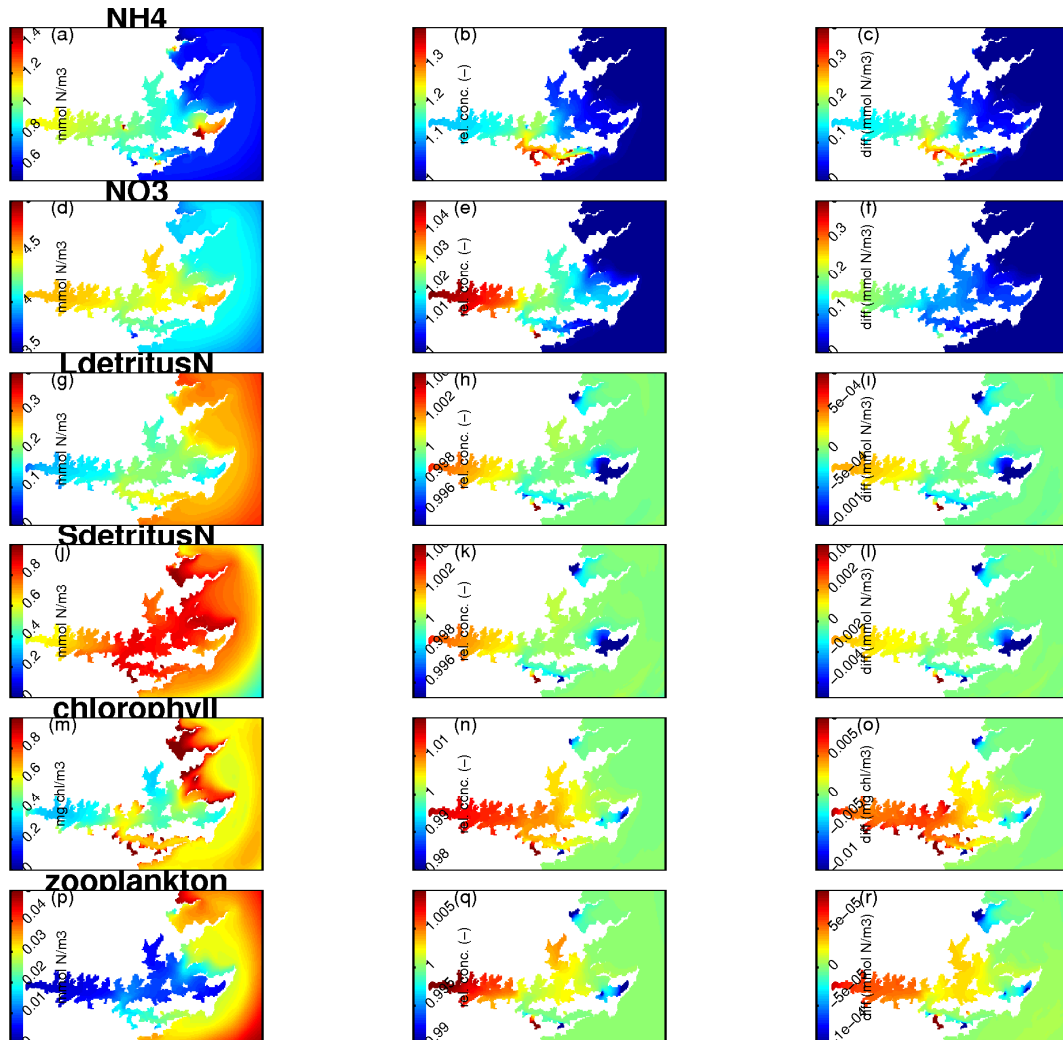


Figure 3-28: False colour maps of time-averaged, winter-time, near-surface water-quality characteristics for the EM_EF_WD and AM_AF_WD+Tipi2+Motu5+Weka5 scenarios. Left-hand images: time-average concentration in the AM_AF_WD scenario. Central images: relative concentration (AM_AF_WD+Tipi2+Motu5+Weka5 relative to EM_EF_WD). Right-hand images: concentration change (AM_AF_WD+Tipi2+Motu5+Weka5 minus EM_EF_WD).

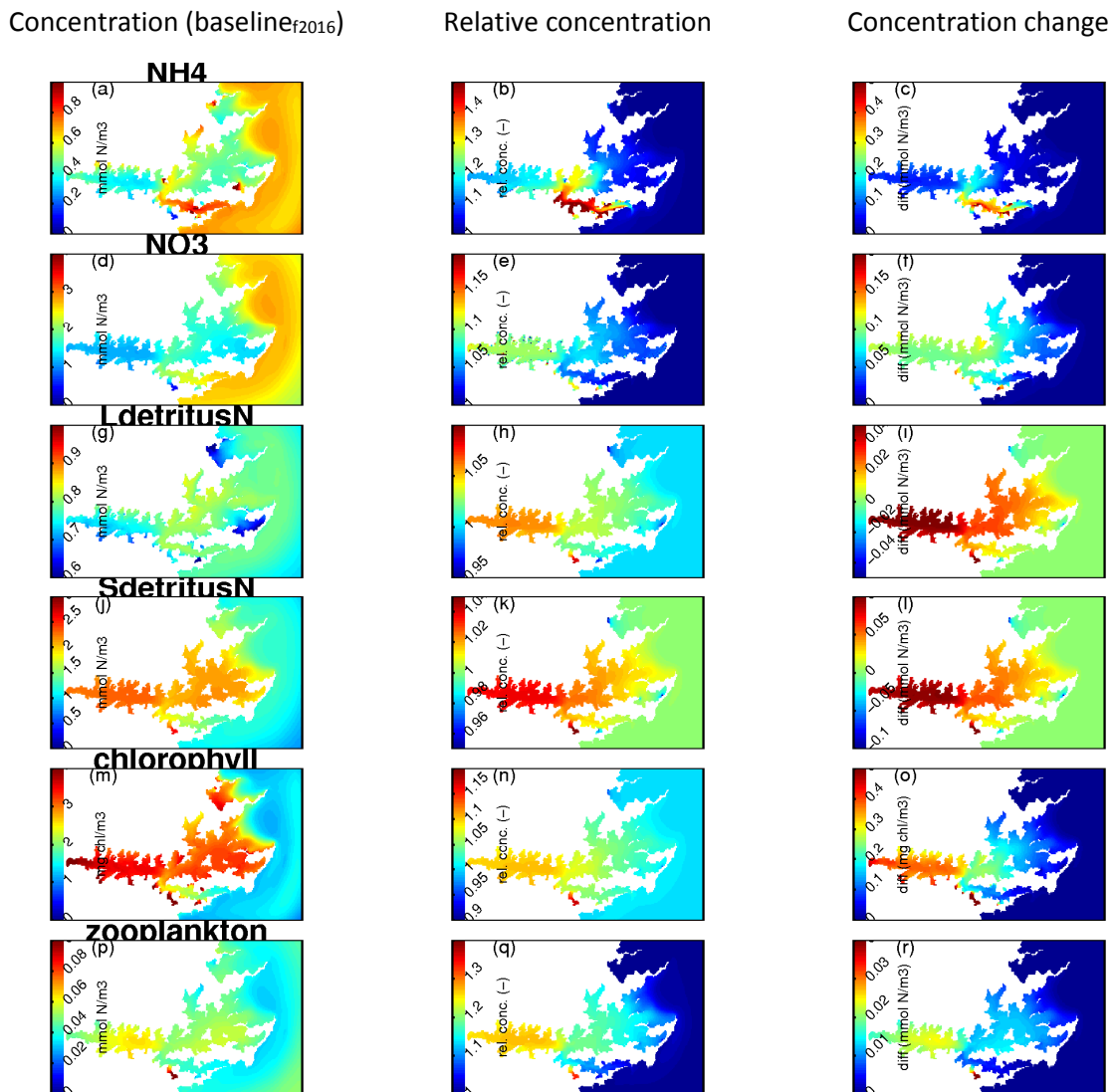


Figure 3-29: False colour maps of time-averaged, summer-time, near-surface water-quality characteristics for the EM_EF_WD and AM_AF_WD+Tipi2+Motu5+Weka5 scenarios. Left-hand images: time-average concentration in the AM_AF_WD scenario. Central images: relative concentration (AM_AF_WD+Tipi2+Motu5+Weka5 relative to EM_EF_WD). Right-hand images: concentration change (AM_AF_WD+Tipi2+Motu5+Weka5 minus EM_EF_WD).

4 Discussion & Implications

Our modelling has examined the influence which nitrogen stemming from three proposed new fish-farms may have upon the lower food-web components of the pelagic zones of the Queen Charlotte Sound and Tory Channel system. The modelling focusses upon direct trophic effects of the nitrogen. Nitrogen is a key nutrient that phytoplankton (and other plants and animals) require in order to grow. Indeed, it is often (but not invariably, see below) the factor that constrains realizable growth rates in New Zealand coastal waters.

During the winter, plant (notably phytoplankton) growth is constrained by low light inputs and low water temperatures. Nutrients that regenerate from (naturally present) rotting organic matter tend to accrue because the regeneration rate exceeds the rate at which the slowly growing plants are able to accrue nutrients. As the days lengthen, individual growth rates begin to rise. This is accelerated as the surface waters warm (causing stratification that 'traps' the phytoplankton in the light-rich surface layers). As phytoplankton growth rates (esp. those in the surface layer) rise and their population biomass expands, the total rate of nutrient uptake comes to exceed the rate of regeneration from rotting material. Thus, the pool of readily available inorganic nutrient becomes depleted (esp. in the surface layers). Once the initial pool of nutrient is depleted, further plant growth becomes nutrient-limited and can proceed only as rapidly as additional inorganic nutrient is imported into the location (by means of: slow regeneration from local organic matter, vertical import from the light-poor deeper layers and by horizontal import of nutrient nitrogen from elsewhere (if such nutrient nitrogen is actually available)).

Once incorporated into particulate matter, nitrogen can influence the attenuation of light – hence potential phytoplankton growth rates. Of necessity, significant quantities of nitrogen can only be incorporated into particulate matter when light is plentiful. Thus, during the light-limited winter period, farm-derived nutrient cannot readily be incorporated into plant biomass and there can be little effect upon light attenuation. During the summer, phytoplankton can assimilate the nutrient and any biomass increase will influence light attenuation. Whilst this may not materially influence (suppress) depth-integrated primary production, it can lead to suppression of production in deeper water in favour of production in shallower parts.

For farm-derived nitrogen to have a material influence upon the food-web at any given location:

- a) The local system must be sensitive/responsive to the additional nitrogen. As noted above, this implies that the system will be more responsive during spring/summer than during late autumn/winter.
- b) The farm-derived nitrogen must reach the location/region in question.
- c) The farm-derived nutrient must be a significant component of the local system's nutrient budget.
- d) The farm-derived nitrogen must remain 'resident' within the region for sufficiently long for the system to be able to respond to it.

There is a tension between (b) and (d). Transport tends to be dominated by currents. Flows into a region are rapidly balanced by outflows. Thus, processes which transport nutrient into a region also tend to induce nutrient export. Where import is rapid, the local system may show little trophic response to the imported nutrient – because the nutrient (and any plankton which have grown in response to the nutrient) will be rapidly exported to elsewhere. Where import is very slow, too little

nutrient will enter the system over relevant time-scales (days – months) for it to represent a significant component of the local system's budget.

In the simulations, Tory Channel shows moderately large ammonium increases – because it is the direct recipient of the farm-derived ammonium. On the other hand, even during summer, it shows only small changes in seston – because the ammonium is exported from Tory Channel (some, out into Cook Strait, some to Queen Charlotte) before the phytoplankton have sufficient time to incorporate much of the ammonium. Some of the ammonium which enters Queen Charlotte from Tory Channel moves seaward (out toward Long Island and beyond). During the summer, it does engender a phytoplankton (hence, detrital and zooplankton response) – but this is muted by dilution with 'unmodified' Cook Strait water entering the seaward end of Queen Charlotte on each tide (i.e., the farm nutrient is not an overwhelming component of the nitrogen budget for that region). In contrast, ammonium which enters Grove Arm tends to remain there for sufficient time to enable phytoplankton to respond to it. Furthermore, the farm nutrient represents a non-trivial additional component of that sub-region's nitrogen budget. A similar story holds for some side-bays (such as Onapua).

4.1 Modelling limitations

Biogeochemical models (like that used here) typically produce relatively crude representations of the complex bio-geophysical systems under study. Some components of reality are entirely excluded (whether explicitly, or implicitly). Other aspects of reality are included, but only in simplified form. A model will not reproduce all details of reality accurately. Nevertheless, such models remain one of the few -- but imperfect -- ways for us to produce integrated pictures of spatially and temporally diverse real world systems.

Our model considers the effects that fish-farms may have upon the lower food-web – but it only considers the role that feed-derived nitrogen may play. It does not consider other nutrients. The Marlborough District Council data indicate that nitrogen is invariably the most limiting element within Grove Arm, and often the most limiting one in Tory Channel and central/outer Queen Charlotte (though silicon has sometimes been more limiting in these regions).

Much of our discussion has focussed upon chlorophyll. This is primarily because chlorophyll is one of the few variables for which a water-quality threshold has been set with respect to fish farming in the Sounds. Chlorophyll is a molecule that is found within all plants (incl. phytoplankton). This is the pigment which is responsible for most photosynthetic production. Thus, chlorophyll is important in its own right. In practice, however, it is also routinely measured as a means of assessing phytoplankton abundance – because chlorophyll is easy/cheap to measure in comparison with counting and measuring phytoplankton cells! In reality, phytoplankton abundance is determined by much more than mere nitrogen input rates (or even nitrogen concentrations). To varying degrees, the concentrations of other nutrients, the instantaneous (and historical) light intensities (and spectral composition), water temperature, strength of vertical mixing, taxonomic composition of the initial phytoplankton community, time-course of grazing pressure etc., can all influence the evolution of total phytoplankton biomass. Similar complexities apply within all the other components of the real-world food-web. The model represents only some of these factors, and even those are only represented in simplified form. In the model (as in the real world), it is the rate coefficients (specific mortality rate, specific ingestion rates, maximal photosynthetic rates, mineralization rates etc.,) which will help to determine where (geographically, and within the foodweb) farm-derived nitrogen will tend to accrue. Unfortunately, many of these important coefficients are poorly known. In part

this is because most are not fundamental physical constants (such that they may vary across taxa and across space and time within taxa). The dynamics that any model produces are influenced by the chosen coefficient values (as well as the functional forms/equations chosen to represent each process). We have not investigated the model's sensitivity to any coefficient values or to any changes in the equations that are used within the model to approximate the structure and function of the real-world food-web.

The model does not consider oxygen. Fish farming will increase the system's demand for oxygen. The fish themselves require oxygen. Furthermore oxygen will be consumed by the biogeochemical processes that convert fish-derived ammonium to nitrate, mineralizing organic matter stemming from the farms (faeces, uneaten food). Similarly, should the fish-farm-derived nutrients stimulate a net increase in organic matter production, then this additional organic matter will create a new oxygen demand when (and where) it decays – perhaps at some distance away from the farms. Marlborough District Council hold about two years' worth of monthly dissolved oxygen data from the Queen Charlotte system, but those data indicate that oxygen concentrations remain high (>85% saturation) throughout most of the water column and throughout the year. The only exceptions have occurred within Grove Arm - where near-bed concentrations have dropped to 60-70% saturation during some summer months. Those concentrations are above the sub-lethal effects threshold of the vast majority of marine taxa that have been studied (Vaquer-Sunyer and Duarte 2008). Unpublished measurements of dissolved oxygen within the fish-pens of Queen Charlotte Sound/Tory Channel indicate that oxygen concentrations tend to be a little lower inside the pens than further afield. Clearly, it would not be in the fish-farmers' interest to run their farms at stocking rates which would induce local (to the farm) hypoxia. Such direct self-interest does not entirely preclude the possibility that fish-farming might induce far-field hypoxia, but the need to maintain adequate near-field dissolved oxygen may make it less likely that far-field hypoxia will arise.

The model does not consider the effects that the biofouling community (encrusting macro-algae and invertebrates) associated with the farm may have. Fish farm nets are cleaned regularly, and, at the regional-scale, they are likely to represent only a small proportion of the already-available hard-surface onto which encrusting organisms could settle.

The model does not consider the effects that farm structures will have upon patterns of flow. They certainly do influence flow, but this occurs mostly at the local/bay-scale. Plew (2011) reports results from a simulation model of Pelorus Sound currents that included the effects of the (approximately 600) mussel farms within that system upon flow. He focussed upon Waihinu Bay and Port Ligar (where mussel farms occupy about 10% of each bay). He reported that, farms within each bay may have caused bay-scale average current speeds to drop by circa 7-8% in Port Ligar and circa 3% in Waihinu. At finer scales, changes were larger: the model suggested that current speeds would often drop several tens of percent within individual farms. Conversely, addition of the farms yielded higher (approximately doubled) current speeds immediately outside some of the added farms. For Port Ligar, inclusion of the effects of all the farms within Pelorus (as well as those of the bay itself) reduced current speeds by a further 3%. The location of farms was important with regard to effects on currents with greater bay scale (and beyond) reductions in flows caused by farms located in regions of faster currents. Many of the farms in Pelorus are located in side bays where flows are less than in the main channel. We anticipate that the effect on current speeds over Pelorus as a whole is likely to be around 5% (D. Plew, NIWA, pers. comm.). In total, the pens of the proposed three new farms within Tory Channel would occupy approximately 4 ha. Tory Channel has a surface area of approximately 1800 ha. Thus, the proposed new fish farms would occupy <1% of the area of Tory Channel. Despite the fact that the new farms will be exposed to relatively high current speeds, we

surmise that their incremental effect upon large-scale flow in Tory Channel will be very small (<1% reduction) [D. Plew, NIWA, pers. comm].

The three additional farms that we have been asked to consider were all in Tory Channel and two of the three are very close to one another. Strong tidal currents ensure that Tory Channel (and the immediately adjacent part of Queen Charlotte) is vigorously mixed and flushed relatively rapidly. The individual 'pelagic-zone footprints' of each farm quickly coalesce. The far-field footprints of each individual farm occupy similar parts of Queen Charlotte and the multiple farm footprints are very similar to those which would be inferred from simple addition of the corresponding footprints from individual-farm simulations. This near-additivity indicates that the model predictions (with respect to fish-farming at the scales that we have considered) are not sensitive to any of the non-linear interactions present within the model's mathematical structure.

As noted in Hadfield, Broekhuizen et al. (2014) and Broekhuizen, Hadfield et al. (2015), benthic denitrification rates can become suppressed when organic loadings to the seabed become too high. If this occurs over a sufficiently large fraction of the region, this can induce a positive feed-back loop that exacerbates the progression towards eutrophy. Hadfield, Broekhuizen et al. (2014) examined an (implausibly) worst-case scenario – in which denitrification did not operate anywhere in the model domain. A more plausible, scenario would be to assume that denitrification might cease in the immediate environs of the farms. We have not examined that scenario. We note that New Zealand King Salmon Ltd. and Marlborough District Council have recently agreed upon a set of best practice management protocols aimed at precluding the most extreme adverse benthic effects that can be associated with fish farming. If these protocols work as intended, they should limit the extent to which denitrification under the existing fish-farms can become suppressed. In the same way, the water-quality monitoring & response protocols (Morrisey, Anderson et al. 2015, see also next sub-section) that have been agreed between NZKS and Marlborough District Council should preclude serious enrichment of the Sounds by the existing farms [but note, that if the proposed new farms were not operated by NZKS, these protocols would not automatically apply to those new farms].

Given the approximations that are introduced in these biogeochemical models, and the uncertainties concerning many of the model's coefficients, it is conceivable that, in reality, the farms will induce larger (or smaller) phytoplankton (chlorophyll) changes than those suggested by the model. We are inclined to believe that the real world changes will be smaller. The fact that the 'operating farms' scenario variant of the model over-predicts summertime phytoplankton concentrations (whilst getting other explicit components of the model foodweb 'about right'¹⁴) suggests that the model may have a tendency to 'capture' too much farm-derived nitrogen within an explicit phytoplankton population during the summer. This excess capture must be at the expense of a deficit of capture of a real-world component that is implicitly (or explicitly) either: (a) present within the model system or, (b) absent from the model system. Since the model gets the dynamics of the other explicit foodweb components 'about right' (Hadfield, Broekhuizen & Plew, 2014), it seems probable that the implicit deficit (that we believe must be occurring somewhere) arises in some real-world component that is absent from the model. In reality, benthic detritus, organic solutes (open-water and pore-water) and pore-water inorganic solutes all represent significant nitrogen stores that are absent from this model. In this model, farm-derived nitrogen which 'should' accrue into those pools is falsely forced to accrue within one of the model's explicit components (in our case, seemingly, in the phytoplankton). Unfortunately, there have been comparatively few measurements of benthic

¹⁴ Though, at some stations, there is a tendency for deep water nitrate concentrations to remain 'low' for too long during the mid/late summer period and for ammonium concentrations to be toward the lower end of the observed range.

nutrient dynamics in Queen Charlotte and Pelorus – making it difficult to reliably gauge the spatial and temporal variability in the sizes of the various benthic nutrient pools.

4.2 Water-quality thresholds

A formal review of water-quality standards relating to aquaculture (or anything else) is outside the scope of our contract. Nonetheless, we offer a brief commentary to provide context that will help with interpretation of our simulation results.

If the proposed new farms were to be granted, they would undoubtedly be governed by consent conditions. Those may well include water-quality limits. As an example, the consent conditions governing the three recently consented NZKS salmon farms (two in Pelorus Sound, one in Tory Channel) include both seabed health and water-quality standards. Amongst other things, the water-quality conditions stipulate that the farms should not cause chlorophyll concentrations to exceed 5 mg chl m^{-3} ^{15, 16}. They also stipulate that they should not cause the system to move towards eutrophy. To achieve those ends, the conditions required that provisional water-quality standards and management response protocols be nominated and agreed upon by an independent review panel. A suite of provisional standards have been negotiated and approved by the review panel (Morrisey, Anderson et al. 2015)¹⁷. The standards and protocols will be reviewed periodically (and may change as a result). The present versions include provision for assessment and possible intervention should monitoring reveal chlorophyll concentrations (as measured on a GF-C filter¹⁸) in excess of 3.5 mg m^{-3} in three successive months (at any one station, or across several stations). Note however, that whilst each exceedance of 3.5 mg m^{-3} triggers a process aimed at determining whether the exceedance was driven by farms, further interventions aimed at reducing farm-effects will only be required in the event that the farms are deemed to be the cause of the exceedance. The reader is referred to Morrisey, Anderson et al. (2015) for a more detailed description of the protocols.

In MDC's water-quality sampling in Queen Charlotte Sound (monthly at five stations since July 2011 up to and including March 2015), 5 mg chl m^{-3} (measured using a GF-C filter) has been exceeded in four water samples. All were near-surface (rather than near bed) samples. Two stemmed from station QCS-1 (April 2013, August 2013) and two from station QCS-2 (May 2013, August 2013). Both stations are within inner Queen Charlotte. In total, there have been more than 90 near-surface water samples collected at stations QCS-1 and QCS-2. Thus, 5 mg m^{-3} has been exceeded in about 5%

¹⁵ Different phytoplankton species are of differing sizes. The smallest taxa have cell sizes $< 1 \mu\text{m}$. The largest are $> 100 \mu\text{m}$. The term microplankton is often used to refer to phytoplankton $> 20 \mu\text{m}$. Those in the $2 - 20 \mu\text{m}$ range are often referred to as nanoplankton. Those $< 2 \mu\text{m}$ are referred to as picoplankton.

¹⁶ The consent conditions state only that chlorophyll should not exceed 5 mg m^{-3} without commenting upon what time-scales and space-scales (how many samples) should be considered when calculating the concentration or upon how chlorophyll should be measured.

¹⁷ In a separate process, NZKS and MDC have negotiated a set of protocols to manage seabed health around the NZKS farms Keeley, N., Gillard, M., Broekhuizen, N., Ford, R., Schuckard, R., Ulrich, S. (2015) Best Management Practice guidelines for salmon farms in the Marlborough Sounds: Benthic environmental quality standards and monitoring protocol (Version 1.0 January 2015). *MPI Technical Paper*. Ministry of Primary Industries, Wellington: 47. <http://www.mpi.govt.nz/news-and-resources/publications/>.

¹⁸ GF-C filters have a nominal pore-size of approx. $1.2 \mu\text{m}$. GF-C or, more commonly, GF-F ($0.7 \mu\text{m}$) are commonly used to measure phytoplankton Moran 1999. In practice, both capture very similar quantities of phytoplankton, and both fail to capture very small cells Moran, X.A.G., Gasol, J.M., Arin, L., Estrada, M. (1999) A comparison between glass fiber and membrane filters for the estimation of phytoplankton POC and DOC production. *Marine Ecology - Progress Series*, 187: 31-41. Knefelkamp, B., Carstens, K., Wiltshire, K.H. (2007) Comparison of different filter types on chlorophyll-a retention and nutrient measurements. *Journal of Experimental Marine Biology and Ecology [J. EXP. MAR. BIOL. ECOL.]*, 345: 61-70. The consent conditions do not discuss what size-fractions of phytoplankton should be considered when calculating chlorophyll abundance but we note that Marlborough District Council data stem from GF-C filters. The majority of NIWA's own data from the region (Pelorus Sound) stem from GF-C filters and we believe that the majority of other data-sets (e.g., those of the Cawthron Institute) will also have used GF-C or, perhaps, GF-F filters.

of the near-surface sampling records from inner Queen Charlotte. The vast majority (79 of 90 records) of near-surface measurements from inner Queen Charlotte have been below 3 mg chl m⁻³.

By way of comparison, the NOAA Assessment of Estuarine Trophic Status (ASSETS) is a USA-derived protocol for evaluating eutrophication based on the National Estuarine Eutrophication Assessment (NEEA) database (Bricker, Ferreira et al. 2003). Bricker et al. conclude that chlorophyll concentrations that are in excess of 5 mg chl m⁻³ during the 'annual bloom period' are considered indicative of at least a moderate impact¹⁹. Systems in which chlorophyll concentrations do not exceed 5 mg Chl m⁻³ during the annual bloom period are deemed to be unimpacted.

4.3 Assessment relative to water-quality standards

We acknowledge the fact that the model suggests that (even in the baseline_{f2016}) the 5 mg m⁻³ threshold will be broken from time to time, but we re-iterate that: (a) this is already happening (infrequently) in reality but we do not believe that it is indicative that the system is in imminent danger of 'collapse', (b) there is evidence to suggest that the model is over-estimating time-averaged chlorophyll concentration under the 'existing operating conditions' (EM_EF_WD, baseline_{f2012}) scenario. If, (i) the model were generating more realistic summertime chlorophyll concentrations in the 'existing operating conditions' (EM_EF_WD) scenario, and (ii) the predicted chlorophyll increments arising from the various alternative (increased) farming scenarios remain of the same magnitude (same excursion size, but over-and-above the true present-day time-average), the 5 mg chl m⁻³ threshold is unlikely to be come to be broken on a frequent basis. Elaborating further: since, (i) the vast majority of historical chlorophyll measurements in the surface waters of inner Queen Charlotte have been less than 3 mg m⁻³, and (ii) the maximum simulated time-averaged total chlorophyll increase in the inner Sound is circa 0.5-0.7 mg m⁻³ (relative to the existing operating conditions scenario), (iii) the maximum instantaneous increment is predicted to be circa 0.8 mg m⁻³, we consider it unlikely that values >5 mg m⁻³ (GF-C chlorophyll) will become a frequent occurrence (i.e., we suspect that the system is unlikely to shift from Bricker's 'unimpacted' category into the 'moderately impacted one'). Nonetheless, values in excess of 5 mg Chl m⁻³ may become a little more common. Similarly, breaches of the precautionary 3.5 mg Chl m⁻³ threshold that has been agreed for the three new NZKS fish farms: Ngamahau (Tory Channel), Waitata and Richmond (Pelorus Sound) may come to be exceeded more frequently than it has been in the recent past.

The difference between the simulated chlorophyll concentrations in the baseline_{f2016}+Tipi2+Motu5+Weka5 and existing operating farms (EM_EF_WD) scenarios suggests that time-averaged summertime-concentrations of total chlorophyll may increase by circa 0.5-0.7 mg m⁻³ in inner/central Queen Charlotte and Tory Channel relative to present day conditions. If we assume that all of that additional chlorophyll accrues into cells that are large enough to be captured on a GF-C filter, we can calculate an upper bound upon the extent to which GF-C filterable chlorophyll concentration will increase.

The average (standard deviation) of GF-C filtered spring summertime chlorophyll from the two Marlborough District Council stations that are within inner Queen Charlotte (QCS-1 & 2) is 1.24 (0.66) mg chl m⁻³ (Table 3-1). Adding 0.5 to 1.24, we infer that summertime average GF-C filterable chlorophyll concentration may rise to a maximum of approximately 1.7 - 1.8 mg chl m⁻³ (an increase

¹⁹ We discuss Bricker et al. analysis and the 5 mg m⁻³ threshold because it is broadly consistent with the mandated consent conditions for the three recently approved NZKS farms in the Sounds. The reader should not infer that we are advocating in favour (or against) applying the NOAA classification scheme to the Marlborough Sounds within this report. The NOAA scheme is but one of several in the literature. Unfortunately, whilst most offer chlorophyll thresholds, many are vague in important details (e.g., degree of spatial-temporal averaging to apply to field data before comparing measurements with thresholds, size-fraction of the phytoplankton community to consider etc.).

of approximately 37-45%). Those magnitudes of change are similar to coefficient of variation (standard deviation/mean = 0.66/1.24 = 0.53). This implies that the change is not especially extreme relative to the variation in summertime measurements. Nonetheless, as a persistent (chronic), summertime change it does feel large enough to be note-worthy (indicative that some other aspects of system function/behaviour may change). It is not clear what (if any) additional changes may occur in response to the increased phytoplankton (and zooplankton) or how large they would be but we suspect that they would be subtle. We note that mussel yields in Beatrix Bay varied by approximately 25% over the 1995-2005 period seemingly driven by a (approximately) three-fold (300%) variation in particulate nitrogen concentrations (Zeldis, Howard-Williams et al. 2008). On that basis, we speculate that a 45% change in phytoplankton/chlorophyll is unlikely to drive major changes through direct trophic linkages.

In the preceding paragraph, we suggest that the direct trophic consequences of any phytoplankton increase will be small, but it is important to note that there may be other (perhaps, larger) effects. The increased detrital concentrations will exert an additional oxygen demand as it decays. This may increase the extent to which the seawater becomes under-saturated with oxygen. The oxygen data from the Marlborough District Council monitoring are scarce (< two years' worth) in comparison with the data on nutrients etc., but dissolved oxygen levels have usually exceeded 7.5 mg O₂ L⁻¹ (roughly 85-90% saturation) throughout the water-column. The lowest oxygen concentrations have been recorded in the near-bed waters at sites QCS-1 and QCS-2 (around 6-6.5 mg L⁻¹ (60-70% saturation) during the summers of 2013/14 and 2014/15). 6 mg O₂ m⁻³ is well above the lethal concentrations for the majority of taxa that are most sensitive to hypoxia (such as fish and crustacean). Indeed, 6 mg O₂ m⁻³ is also well above the median concentrations for sub-lethal effects for members of these taxa (approx. 4 mg O₂ m⁻³, Vaquer-Sunyer and Duarte 2008). Whilst the ROMS/Fennel model does offer dissolved oxygen as an optional state-variable, we have not yet turned this variable on. Thus, we can make no quantitative statements about changes in oxygen levels in response to additional fish-farm inputs.

Comparison of the concentrations of dissolved reactive phosphorus and dissolved inorganic nitrogen in Queen Charlotte Sound with the so-called Redfield ratio²⁰ suggest that nitrogen (N) is more limiting than phosphorus (P), but comparison of dissolved reactive silicon and dissolved inorganic nitrogen concentrations with the so-called extended Redfield ratio²¹ suggest that the diatom community may sometimes be silicon (Si) (rather than nitrogen) limited within Queen Charlotte (notably in Tory Channel and the central/outer parts of Queen Charlotte²²). Fish feed contains N and P, but little or no Si. Thus, the nutrient-stream emanating from a fish-farm will tend to increase the N:Si nutrient ratio in the water. All phytoplankton require nitrogen, but only some (notably, diatoms) require silicon. During periods of Si-limitation, nitrogen inputs (such as those from fish farms) may be disproportionately incorporated into taxa that do not require silicon in order to grow (e.g., dinoflagellates and many small flagellates etc.). Loosely speaking, larger forms (such as dinoflagellates and diatoms) are believed to be more likely to be grazed by larger grazers (copepods etc.) and hence pass upward through the foodweb into fish and the like. In contrast, smaller forms are believed to be more likely to be consumed by protozoal grazers. Their energy and biomass may

²⁰ An empirical ratio summarising the elemental composition of seston in the deep ocean: 106:16:1 (C:N:P by atoms). Redfield, A.C. (1934) On the proportions of organic derivatives in sea water and their relation to the composition of plankton. *James Johnstone Memorial Volume*. Liverpool University Press, Liverpool.

²¹ An extension of the original Redfield ratio to include other elements – notably silicon: 106:16:15:1 (C:N:Si:P, by atoms) Brzezinski, M.A. (1985) The Si:C:N ratio of marine diatoms: interspecific variability and the effect of some environmental variables. *Journal of Phycology*, 21: 347-357.

²² The model does not carry any representation of Si, or Si-limitation. The consequent absence of intermittent Si-limitation may partially explain the model's tendency to over-estimate summertime phytoplankton concentrations.

not pass up into higher parts of the foodweb (Richardson 1997). There is some evidence that the different phytoplankton taxa are of differing nutritional value to grazer populations (Cloern 2001). It is therefore conceivable that some grazers may benefit (and others may be disadvantaged) if farm-derived nitrogen inputs were to be large enough to substantially reduce the probability (in space and/or time) that the system will be N-limited. Since our model lacks silicon as a state-variable and makes no distinctions between differing algal or grazer taxa. We cannot make any quantitative statements about how individual taxa might change.

4.4 Onapua Bay

Onapua Bay has developed harmful algal blooms in the past, particularly blooms of the toxic dinoflagellate *Alexandrium catenella* (a Paralytic-Shellfish-Poisoning species) (MacKenzie, Harwood et al. 2013). The conditions that enabled those blooms are not well understood. Our model does not explicitly represent toxic algae as independent component(s) of the phytoplankton community. Rather, it has only one phytoplankton class, representing total phytoplankton. Thus, we cannot use our model to make any quantitative statements about how the magnitude or frequency of toxic algal blooms would change in response to additional farms. Nonetheless, in all of our additional farms scenarios, we note that the addition of farms led to increased concentrations of ammonium and phytoplankton within Onapua Bay. Indeed, during summer, that inlet generally showed the largest magnitude increases in phytoplankton concentration. It is reasonable to assume that the magnitude of response exhibited within Onapua Bay will be positively correlated with farm proximity to the bay and farm size (feed load). Since Te Weka Point is the closest farm to Onapua and one of the two largest farms (5000 tonne annual feed cf 2000 tonne at Tipi Bay), it is not surprising that this farm is predicted to induce the largest changes in Onapua. Conversely, the Tipi Bay farm (which is the most distant and the smallest) induces the smallest changes. We have not sought to determine whether the (simulated) high phytoplankton populations which accrue within Onapua Bay sometimes become transported elsewhere (i.e., whether Onapua Bay can act as a 'seed area' for blooms which spread elsewhere). Whilst the farms are unlikely to influence the probability of physical conditions that favour export, they clearly influence the probability of a bloom developing within Onapua bay. If (a) Onapua bay does occasionally act as a seed area from which blooms spread, and (b) the abundance of the 'bloom population' at the time that it exits from Onapua Bay influences the subsequent size and/or life-time of the exported bloom, then it seems reasonable to infer that Te Weka farm is the one that is most likely to influence the characteristics of any exported blooms.

5 Conclusions

The key findings from this work are:

- Farms in Tory Channel placed close to the Cook Strait entrance (Tipi Bay, and to a lesser extent Motukina) will induce smaller changes in the water-quality of Tory Channel and Queen Charlotte Sounds than farms close to the junction with Queen Charlotte (Te Weka and, to a lesser extent, Motukina). There are two reasons for this. Firstly, the farm which is closest to Cook Strait (Tipi Bay) is the smallest of the three proposed (2000 tonne annual feed versus 5000 tonne for the other two). Secondly, on the ebb tide, water flows out of Tory Channel into Cook Strait and little of this water returns on the subsequent incoming tide. A farm close to the Cook Strait end of Tory Channel exports a larger fraction of its nitrogen waste into Cook Strait.
- For ammonium, the largest farm-effects arise in the immediate farm vicinities. For nitrate and seston, the largest effects arise in Grove Arm and side bays of Tory Channel (especially Onapua Bay). Again, the explanation is straight-forward. Fish farms are net sources of ammonium (directly excreted by the fish), and of particulate organic nitrogen (faeces and waste feed) – which degrades into ammonium. It takes some time for the phytoplankton to fully incorporate the farm-derived ammonium into new biomass. During that time, the water (containing the additional ammonium and seed phytoplankton population) has been transported away from the source farm and subject to dispersive mixing. A similar argument holds with respect to conversion of ammonium into nitrate by bacterial activity. The combination of dispersive mixing and gradual uptake by phytoplankton and bacteria implies that ammonium concentration increases must decline with increasing distance from the farm. Conversely, population increases by phytoplankton etc., take time to develop, so phytoplankton and seston concentration increases tend to be greatest at some distance (travel time) away from the farms.
- The farms are predicted to have little effect upon phytoplankton, zooplankton and detritus during the winter-months. During those months, algal growth is limited by light rather than nutrients. Thus, the additional nitrogen can only be slowly incorporated into additional biomass. Much of it is exported from the system before it can be utilized.
- Regardless of which farms are added, the largest summertime changes in phytoplankton abundance tend to arise in Onapua Bay and Grove Arm. The changes in Onapua Bay tend to exceed those in Grove Arm.
- During the summer (nutrient limited) period, phytoplankton and detritus concentrations are predicted to increase by circa 1–6% (relative to the summertime baseline_{f2016}) in the single-farm addition scenarios. The Te Weka farm tends to induce the largest changes. The Tipi Bay farm tends to induce the smallest.
- The smallest (by total annual feed load) ‘multiple farms scenario’ (AM_AF_WD+Tipi2+Motu5) yields summertime chlorophyll and detritus concentration increases of circa 3-5% within Grove Arm and Onapua Bay (smaller elsewhere).

- The intermediate (by total annual feed load) ‘multiple farms scenario’ (namely the ‘swapped farms’ scenario, AM_SF_WD+Tipi2+Motu5+Weka5) yields summertime chlorophyll and detritus increases of circa 5-6% in Grove Arm and Onapua Bay (smaller elsewhere).
- In the largest multiple-farms scenario (AM_AF_WD+Tipi2+Motu5+Weka5), the summertime chlorophyll and detritus increases in Grove Arm and Onapua Bay are predicted to be 8–10% of the baseline_{f2016} concentration (increases of circa 0.3-0.5 mg chl m⁻³). Relative to the simulated existing operating conditions scenario, the increases amount to 0.5-0.7 mg m⁻³ (10-15%).
- Threshold chlorophyll concentrations of 3.5 mg m⁻³ and 5 mg m⁻³ are both relevant in the context of the existing NZKS farms in Queen Charlotte/Tory Channel. The addition of new fish-farms, instantaneous chlorophyll concentrations will, perhaps, exceed 5 mg m⁻³ more often than they have over the past four years’ of monitoring, but we believe that such events will remain rare and short-lived. Indeed, we believe they will usually remain below 3.5 mg m⁻³ (even in the three-additional-farms scenario).

We have been asked to make recommendations *for/against farm placement/relocation sites with respect to simulated water-quality impacts*. A subsequent report {Broekhuizen, 2016 #2665} considers further combinations of farms within Tory Channel, and we address this ‘recommendations-question’ within the Discussion section of that report (taking into account the results from the scenarios considered in this first report and that subsequent one).

6 Acknowledgements

We thank Mark Gillard (Aquaculture Direct Ltd) for his help in determining how to allocate fish and fish feed across the three potential new farms. We thank New Zealand King Salmon Ltd. for making their historical feed data available to us for this project. We thank Marlborough District Council for making their monitoring data publicly available.

7 References

- Bricker, S.B., Ferreira, J.G., Simas, T. (2003) An integrated methodology for assessment of estuarine trophic status. *Ecological Modelling*, 169: 39-60.
- Broekhuizen, N., Hadfield, M., Plew, D. (2015) *A biophysical model for the Marlborough Sounds part 2: Pelorus Sound*: 163.
- Brzezinski, M.A. (1985) The Si:C:N ratio of marine diatoms: interspecific variability and the effect of some environmental variables. *Journal of Phycology*, 21: 347-357.
- Cloern, J.E. (2001) Our evolving conceptual model of the coastal eutrophication problem. *Marine Ecology Progress Series*, 210: 223-253.
file:///H:/was_p/pdf_reprints/cloern2001_m210p223.pdf
- Fennel, K., Wilkin, J., Levin, J., Moisan, J., O'Reilly, J., Haidvogel, D. (2006) Nitrogen cycling in the Middle Atlantic Bight: results from a three-dimensional model and implications for the North Atlantic nitrogen budget. *Global Biogeochemical Cycles*, 20: GB3007.
10.1029/2005GB002456
- Hadfield, M., Broekhuizen, N., Plew, D. (2014) A biophysical model of the Marlborough Sounds: part 1: Queen Charlotte & Tory Channel. *NIWA Client Report (for Marlborough District Council)*: 183.
<http://www.marlborough.govt.nz/Environment/Coastal/Hydrodynamic-Models-of-the-Sounds.aspx>
- Keeley, N., Gillard, M., Broekhuizen, N., Ford, R., Schuckard, R., Urlich, S. (2015) Best Management Practice guidelines for salmon farms in the Marlborough Sounds: Benthic environmental quality standards and monitoring protocol (Version 1.0 January 2015). *MPI Technical Paper*. Ministry of Primary Industries, Wellington: 47.
<http://www.mpi.govt.nz/news-and-resources/publications/>
- Knefelkamp, B., Carstens, K., Wiltshire, K.H. (2007) Comparison of different filter types on chlorophyll-a retention and nutrient measurements. *Journal of Experimental Marine Biology and Ecology [J. EXP. MAR. BIOL. ECOL.]*, 345: 61-70.
- MacKenzie, L., Harwood, T., Tonks, A., Robinson, J., Knight, B. (2013) Seafood safety risks from paralytic shellfish poisoning dinoflagellate blooms in New Zealand: 2012-2013, *Cawthron Report*, 2346: 38. <http://www.foodsafety.govt.nz/elibrary/industry/seafood-risks-paralytic-shellfish-blooms.pdf>
- Moran, X.A.G., Gasol, J.M., Arin, L., Estrada, M. (1999) A comparison between glass fiber and membrane filters for the estimation of phytoplankton POC and DOC production. *Marine Ecology - Progress Series*, 187: 31-41.
- Morrisey, D., Anderson, T., Broekhuizen, N., Stenton-Dozey, J., Brown, S., Plew, D. (2015) *Baseline monitoring report for new salmon farms, Marlborough Sounds*, NEL1014-020 (NIWA Project NZK13401): 252.

- Plew, D.R. (2011) Shellfish farm-induced changes to tidal circulation in an embayment, and implications for seston depletion. *Aquaculture Environment Interactions*, 1: 201-214. 10.3354/aei00020
- Redfield, A.C. (1934) On the proportions of organic derivatives in sea water and their relation to the composition of plankton. James Johnstone Memorial Volume. Liverpool University Press, Liverpool.
- Richardson, K. (1997) Harmful or exceptional phytoplankton blooms in the marine ecosystem. *Advance in Marine Biology*, 31: 301-385.
- Safi, K., Gibbs, M.M. (2003) Importance of different size classes of phytoplankton in Beatrix Bay, Marlborough Sounds, New Zealand, and the potential implications for the aquaculture mussel *Perna canaliculus*. *New Zealand Journal of Marine and Freshwater Research*, 37(2): 267-272.
- Vaquer-Sunyer, R., Duarte, C.M. (2008) Thresholds of hypoxia for marine biodiversity. *Proceedings of the National Academy of Science of the United States of America*, 105(40): 15452-15457. doi:10.1073/pnas.0803833105
- Zeldis, J.R., Howard-Williams, C., Carter, C.M., Schiel, D.R. (2008) ENSO and riverine control of nutrient loading, phytoplankton biomass and mussel aquaculture yield in Pelorus Sound, New Zealand. *Marine Ecology - Progress Series*, 371(131-142). <http://www.int-res.com/articles/meps2008/371/m371p131.pdf>

Appendix A Time-series from the single additional farm scenarios (concentration difference)

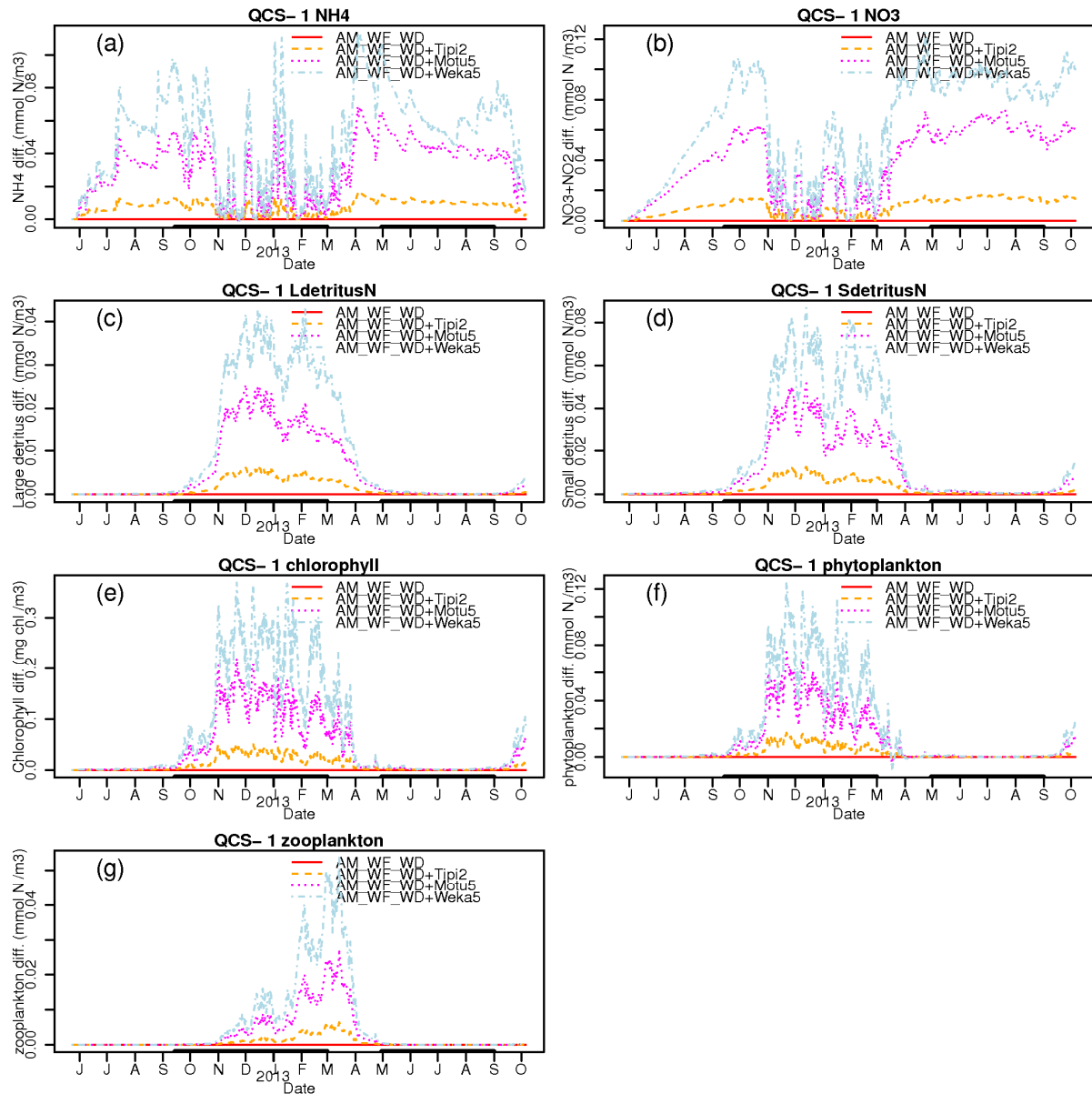


Figure A-1: Simulated dynamics of water-quality state-variables in the uppermost layer at station QCS-1 under differing single additional fish-farm scenarios. Dynamics are expressed as concentration change from the baseline_{f2016}, AM_AF_WD scenario. A value greater than 0.0 indicates that the concentration stemming from the alternative scenario exceeds that in the baseline_{f2016} scenario.

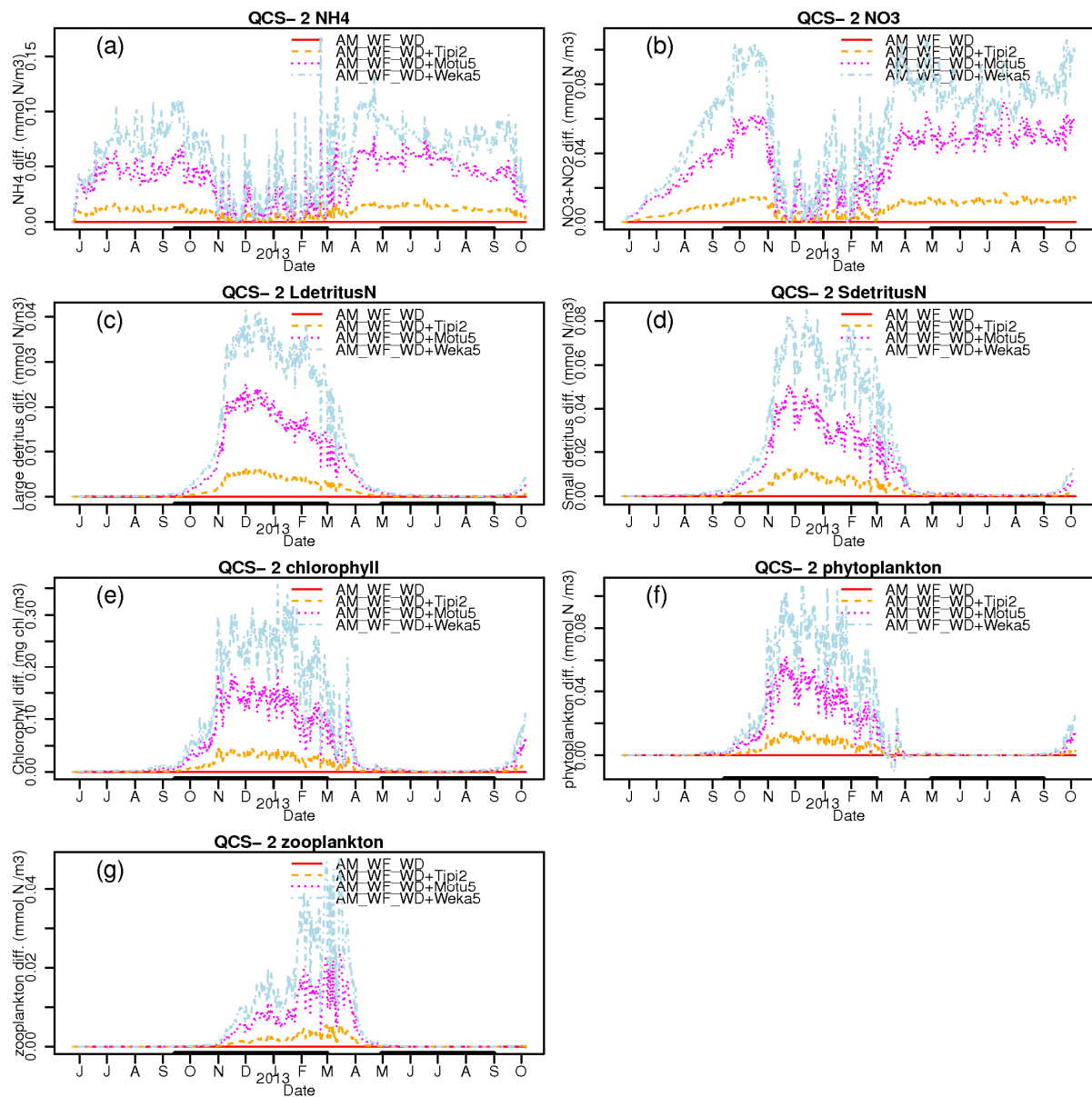


Figure A-2: Simulated dynamics of water-quality state-variables in the uppermost layer at station QCS-2 under differing single additional fish-farm scenarios. Dynamics are expressed as concentration change from the baseline_{f2016}, AM_AF_WD scenario. A value greater than 0.0 indicates that the concentration stemming from the alternative scenario exceeds that in the baseline_{f2016} scenario.

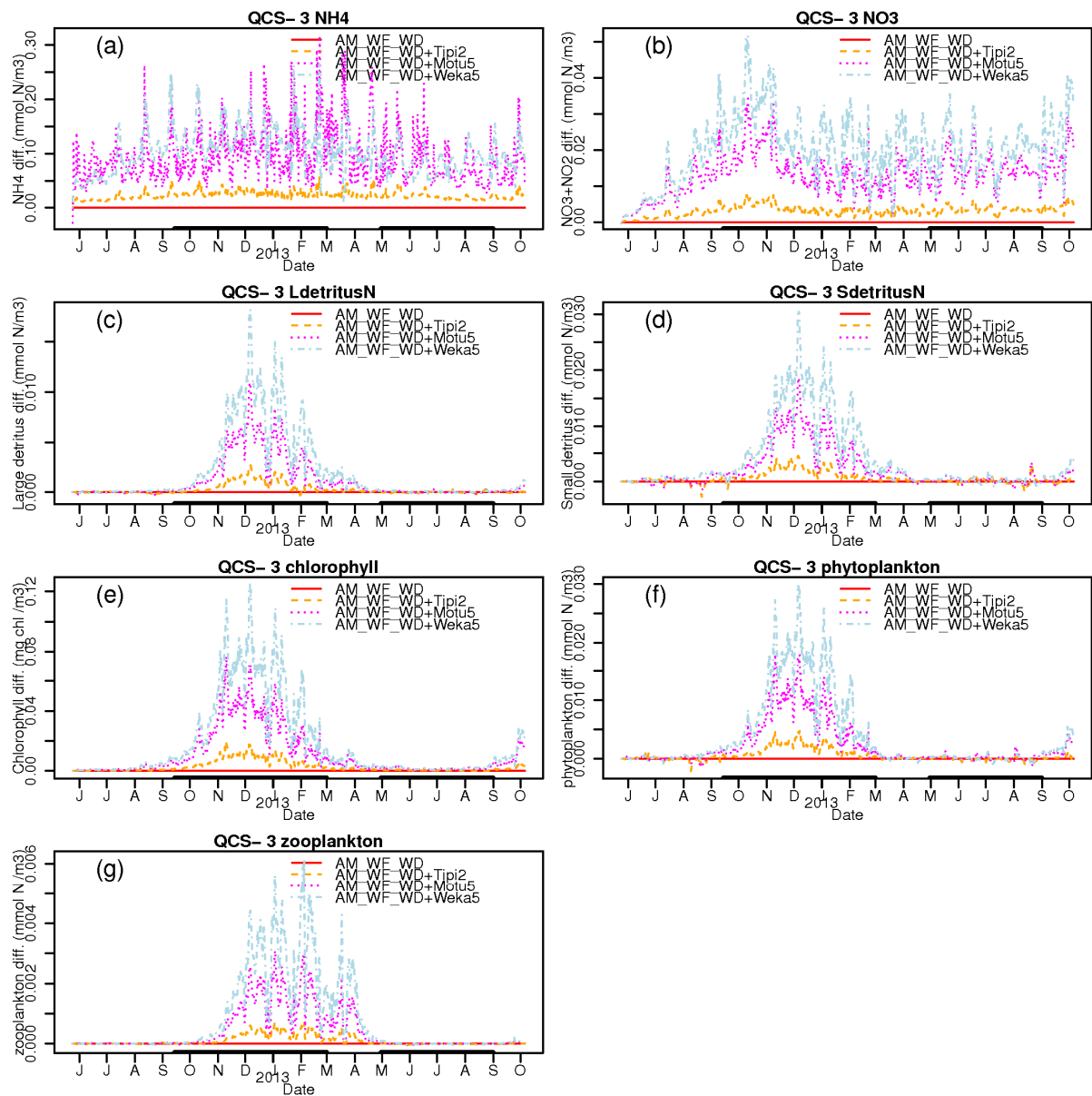


Figure A-3: Simulated dynamics of water-quality state-variables in the uppermost layer at station QCS-3 under differing single additional fish-farm scenarios. Dynamics are expressed as concentration change from the baseline_{f2016}, AM_AF_WD scenario. A value greater than 0.0 indicates that the concentration stemming from the alternative scenario exceeds that in the baseline_{f2016} scenario.

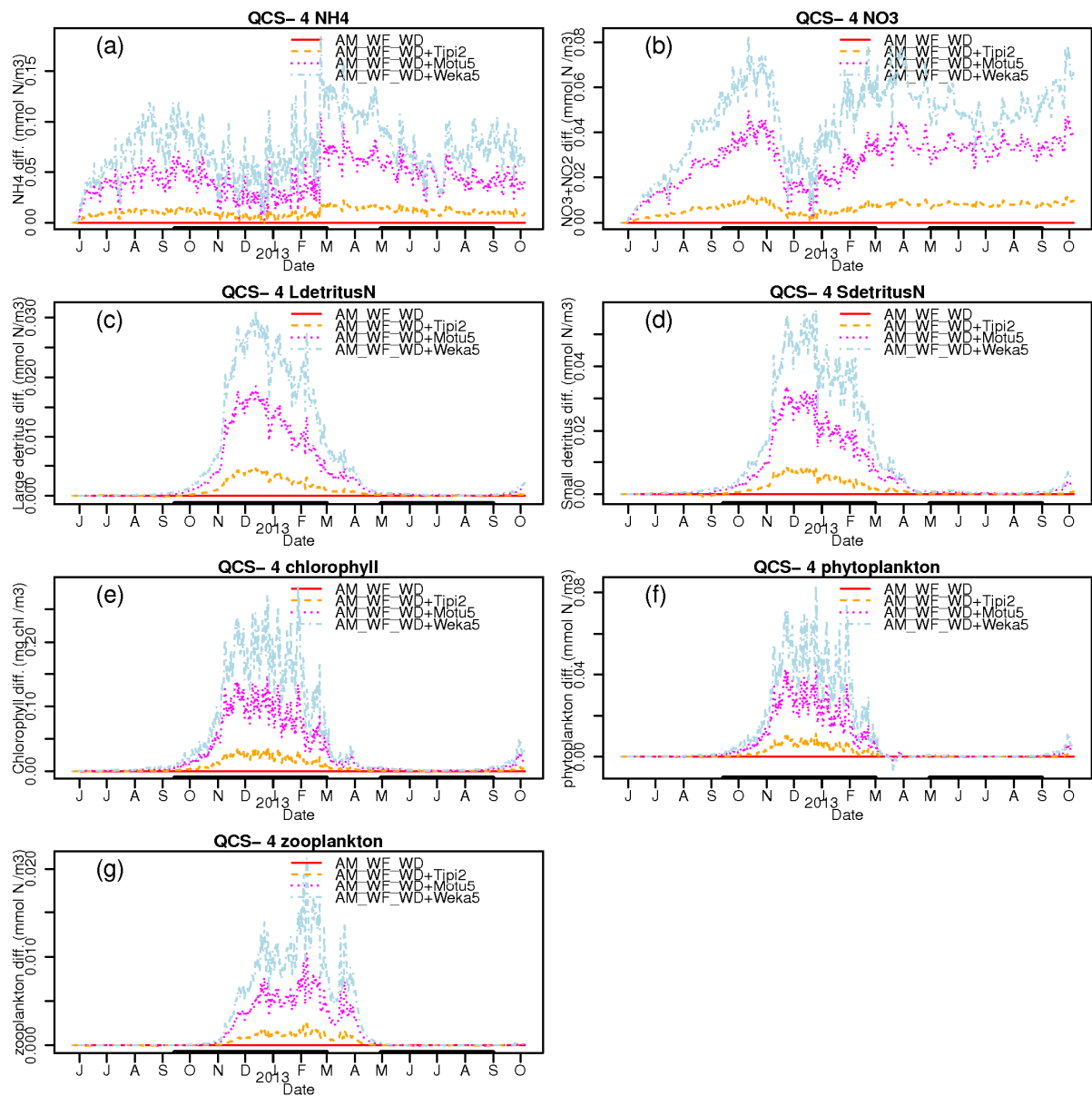


Figure A-4: Simulated dynamics of water-quality state-variables in the uppermost layer at station QCS-4 under differing single additional fish-farm scenarios. Dynamics are expressed as concentration change from the baseline_{f2016}, AM_AF_WD scenario. A value greater than 0.0 indicates that the concentration stemming from the alternative scenario exceeds that in the baseline_{f2016} scenario.

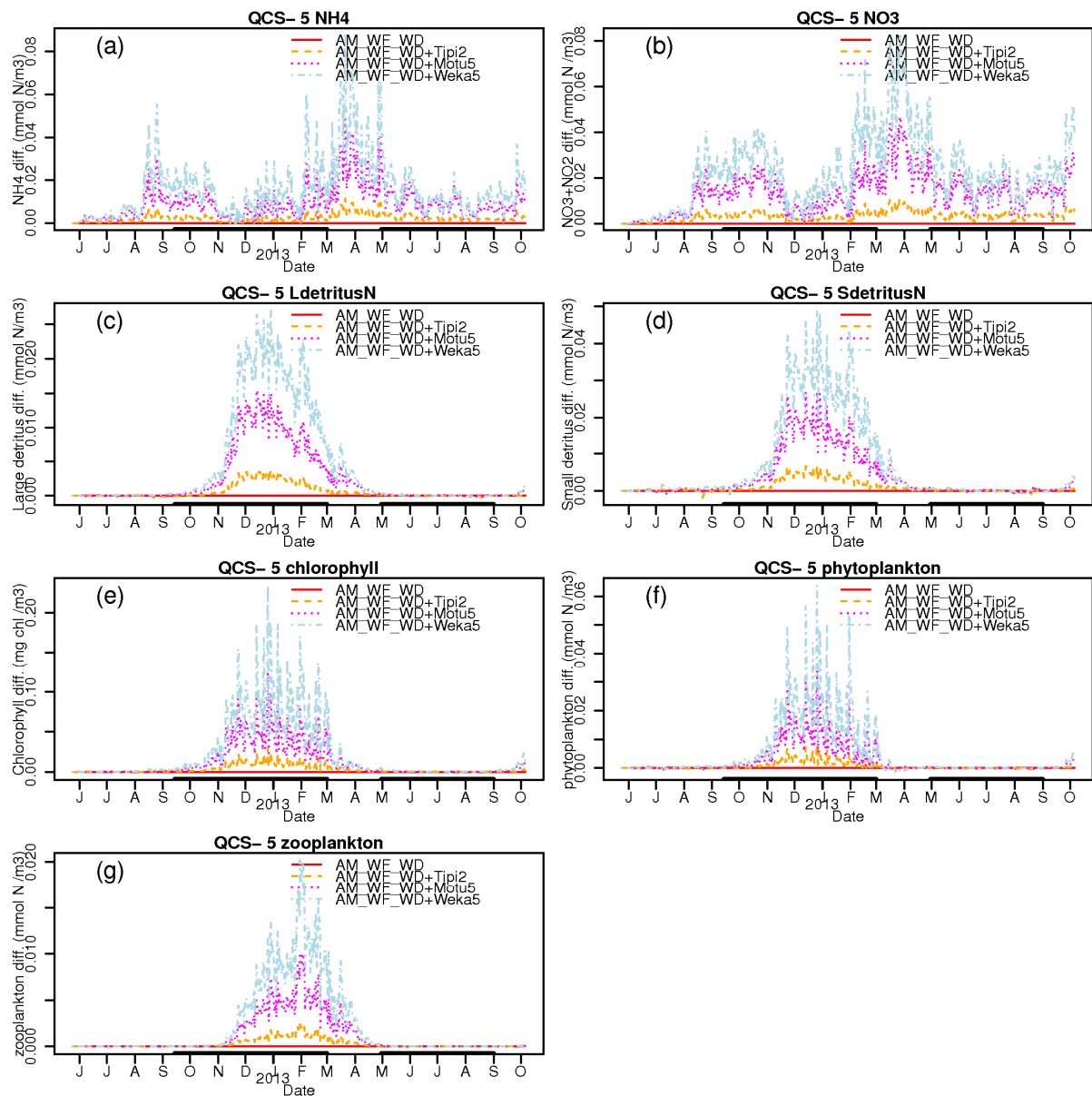


Figure A-5: Simulated dynamics of water-quality state-variables in the uppermost layer at station QCS-5 under differing single additional fish-farm scenarios. Dynamics are expressed as concentration change from the baseline_{f2016}, AM_AF_WD scenario. A value greater than 0.0 indicates that the concentration stemming from the alternative scenario exceeds that in the baseline_{f2016} scenario.

Appendix B Time-series from the single additional farm scenarios (relative concentration)

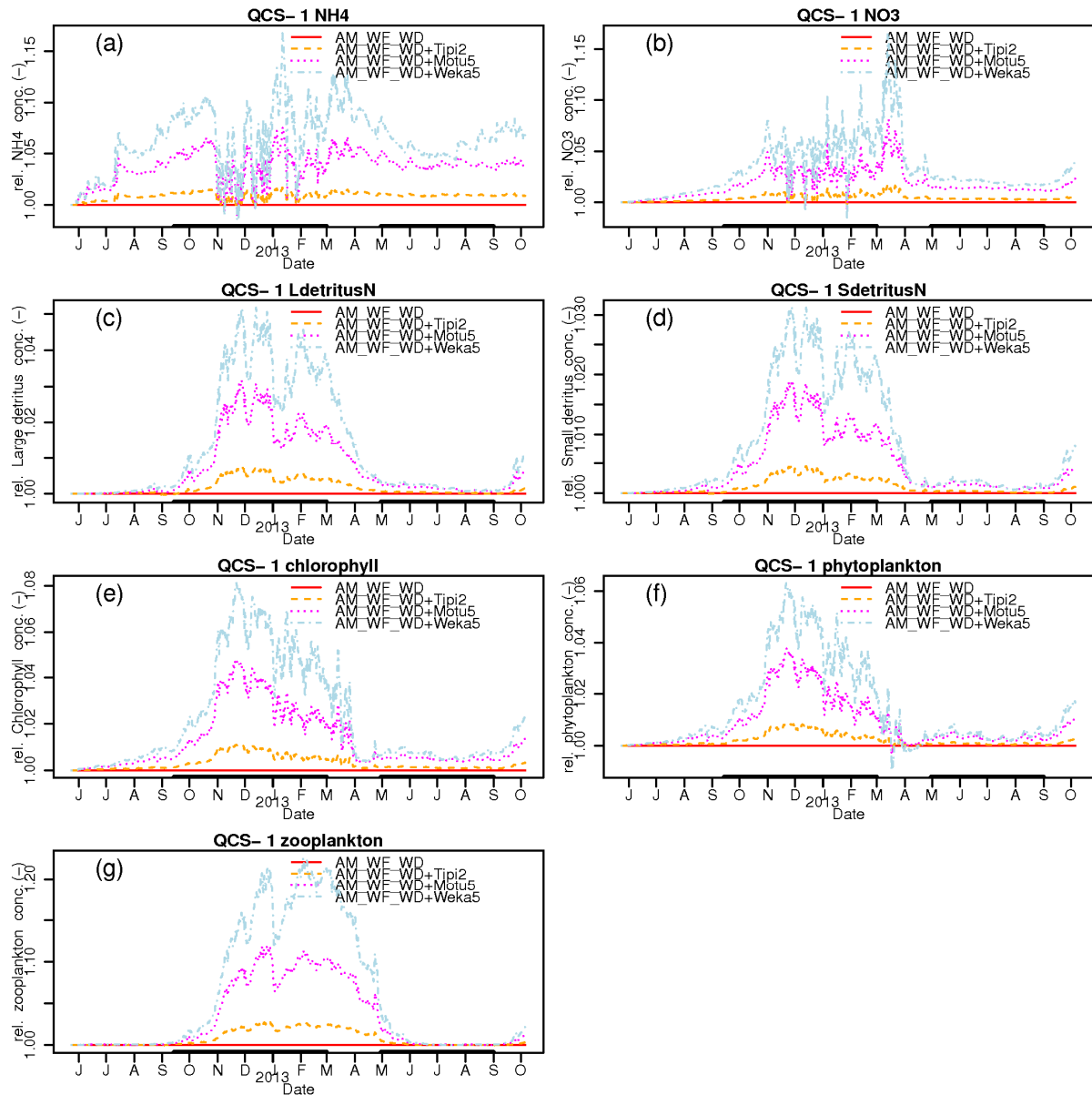


Figure B-1: Simulated dynamics of water-quality state-variables in the uppermost layer at station QCS-1 under differing single additional fish-farm scenarios. Dynamics are expressed as concentration relative to the baseline_{f2016}, AM_AF_WD scenario. A value greater than 1.0 indicates that the concentration stemming from the alternative scenario exceeds that in the baseline_{f2016} scenario.

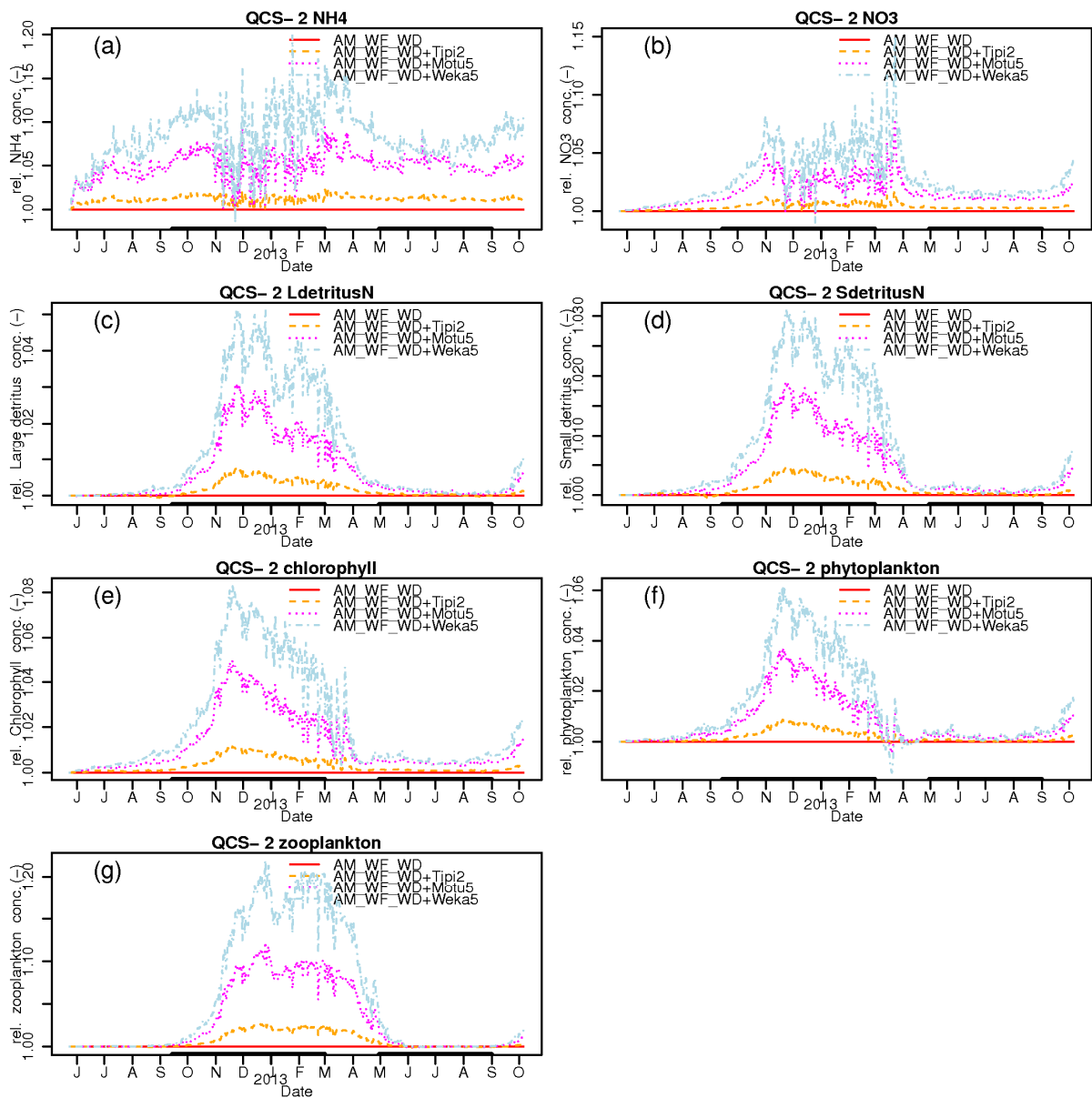


Figure B-2: Simulated dynamics of water-quality state-variables in the uppermost layer at station QCS-2 under differing single additional fish-farm scenarios. Dynamics are expressed as concentration relative to the baseline_{f2016}, AM_AF_WD scenario. A value greater than 1.0 indicates that the concentration stemming from the alternative scenario exceeds that in the baseline_{f2016} scenario.

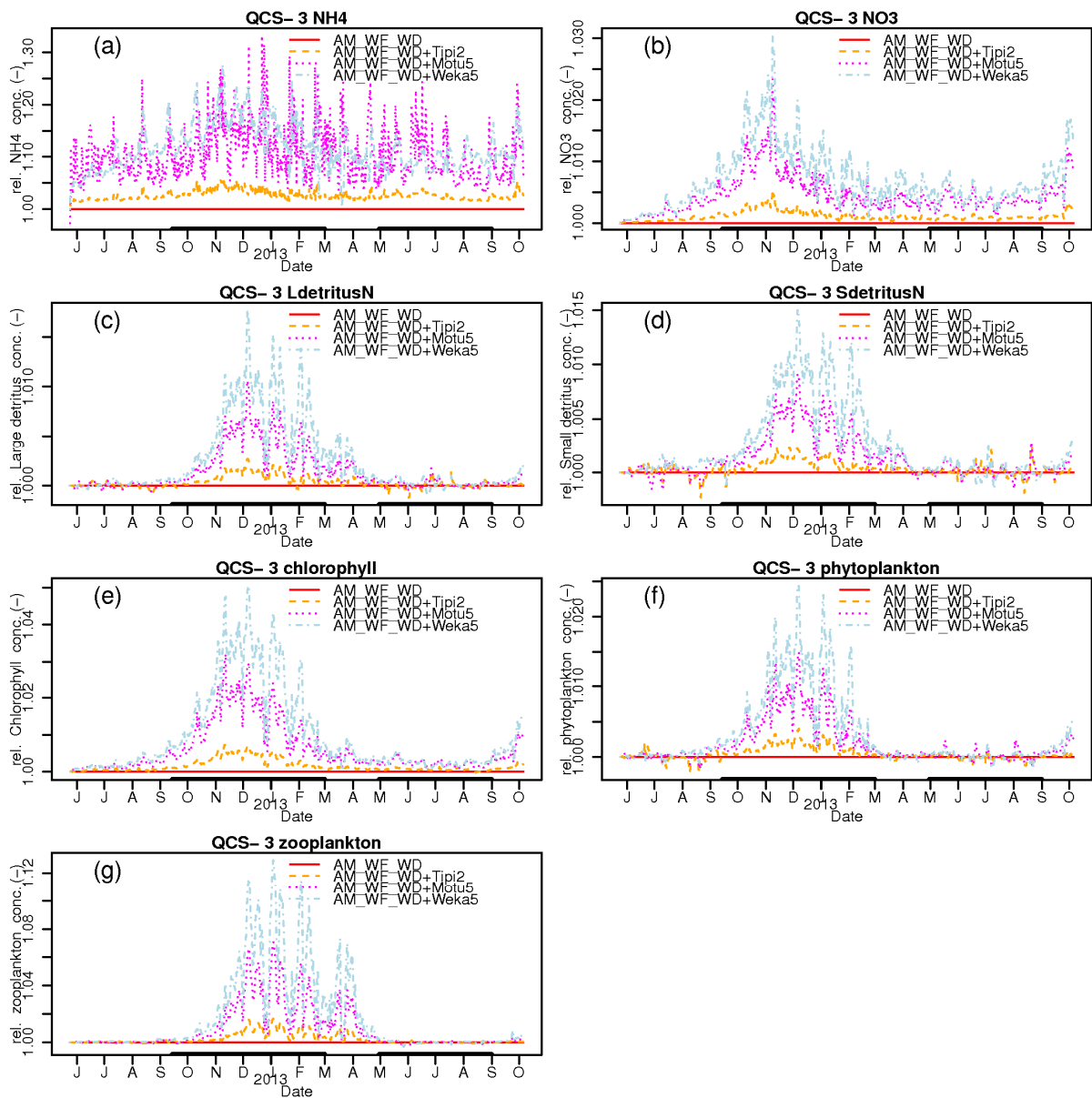


Figure B-3: Simulated dynamics of water-quality state-variables in the uppermost layer at station QCS-3 under differing single additional fish-farm scenarios. Dynamics are expressed as concentration relative to the baseline_{f2016}, AM_AF_WD scenario. A value greater than 1.0 indicates that the concentration stemming from the alternative scenario exceeds that in the baseline_{f2016} scenario.

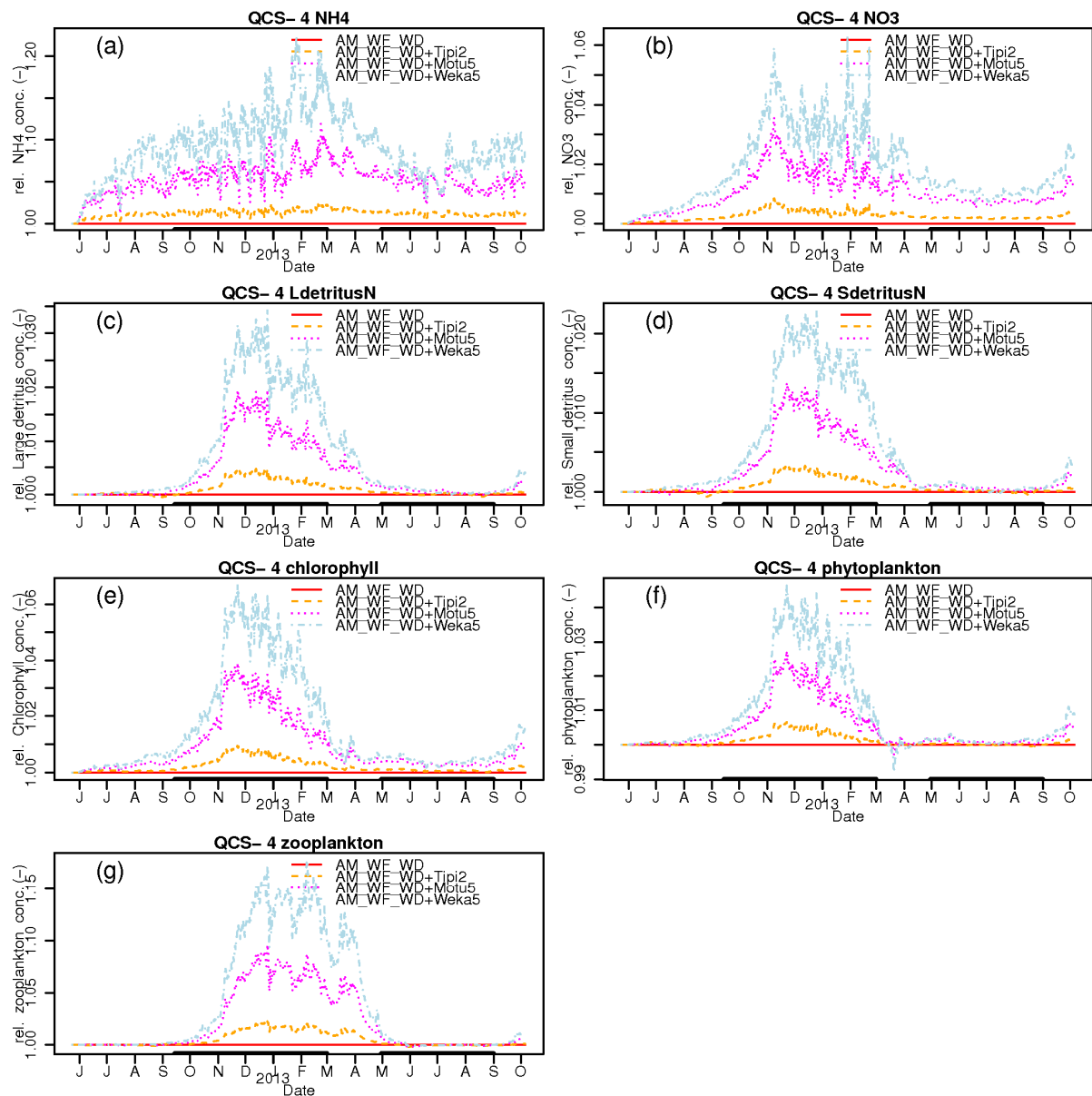


Figure B-4: Simulated dynamics of water-quality state-variables in the uppermost layer at station QCS-4 under differing single additional fish-farm scenarios. Dynamics are expressed as concentration relative to the baseline_{f2016}, AM_AF_WD scenario. A value greater than 1.0 indicates that the concentration stemming from the alternative scenario exceeds that in the baseline_{f2016} scenario.

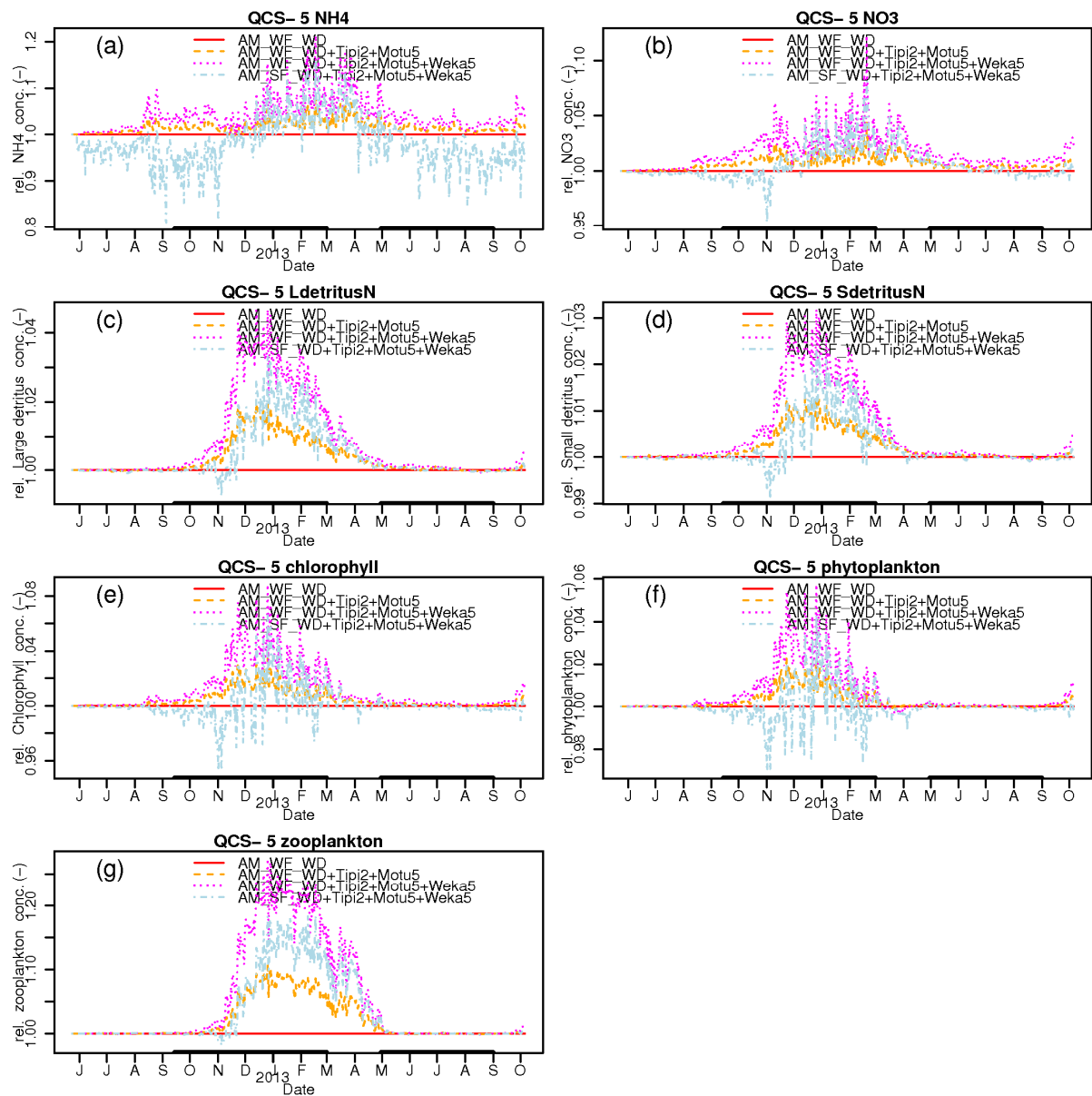


Figure B-5: Simulated dynamics of water-quality state-variables in the uppermost layer at station QCS-5 under differing single additional fish-farm scenarios. Dynamics are expressed as concentration relative to the baseline_{f2016}, AM_AF_WD scenario. A value greater than 1.0 indicates that the concentration stemming from the alternative scenario exceeds that in the baseline_{f2016} scenario.

Appendix C Time-series from the multiple additional farm scenarios (concentration change)

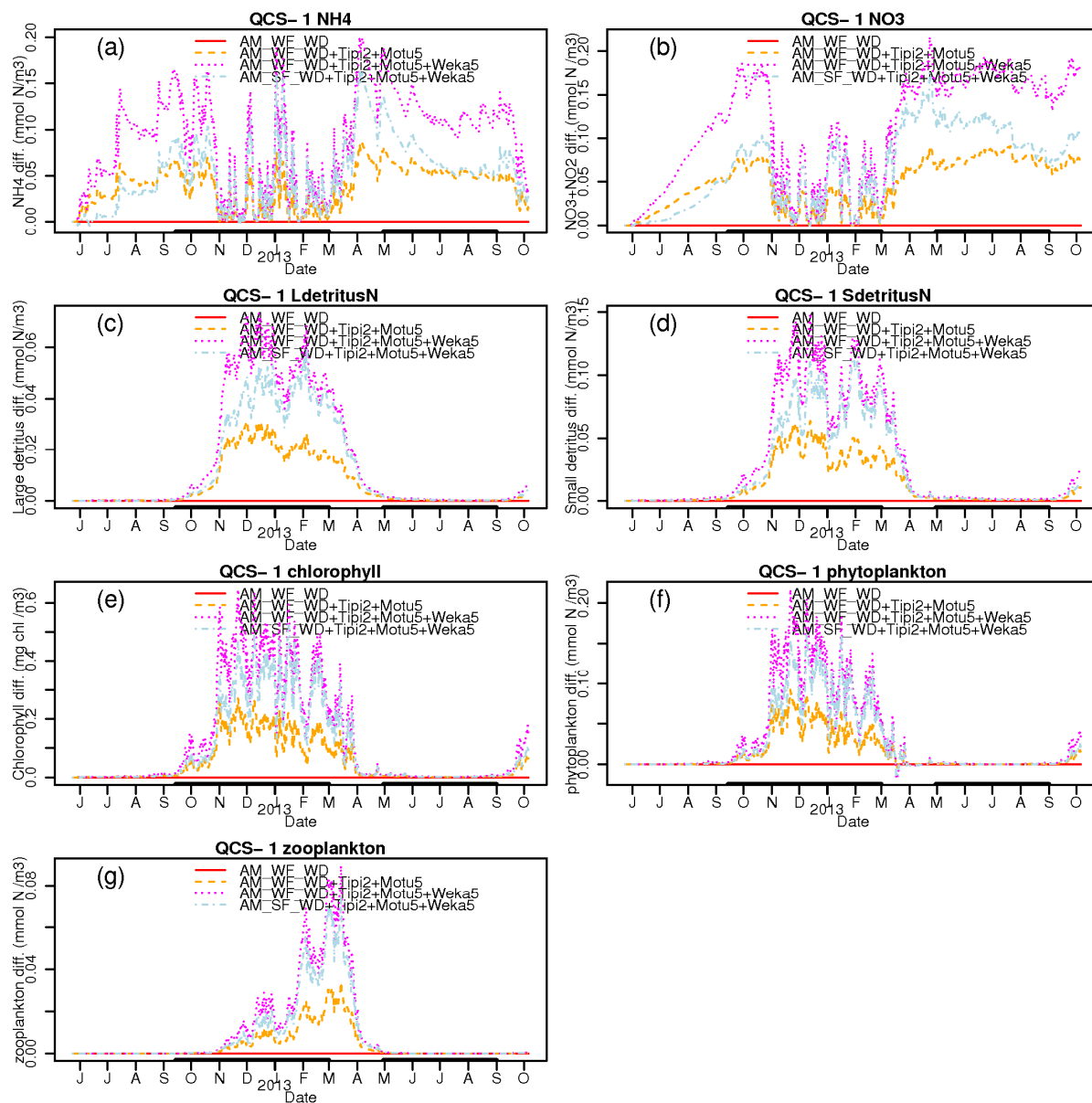


Figure C-1: Simulated dynamics of water-quality state-variables in the uppermost layer at station QCS-1 under differing single additional fish-farm scenarios. Dynamics are expressed as concentration change from the baseline_{f2016}, AM_AF_WD scenario. A value greater than 0.0 indicates that the concentration stemming from the alternative scenario exceeds that in the baseline_{f2016} scenario.

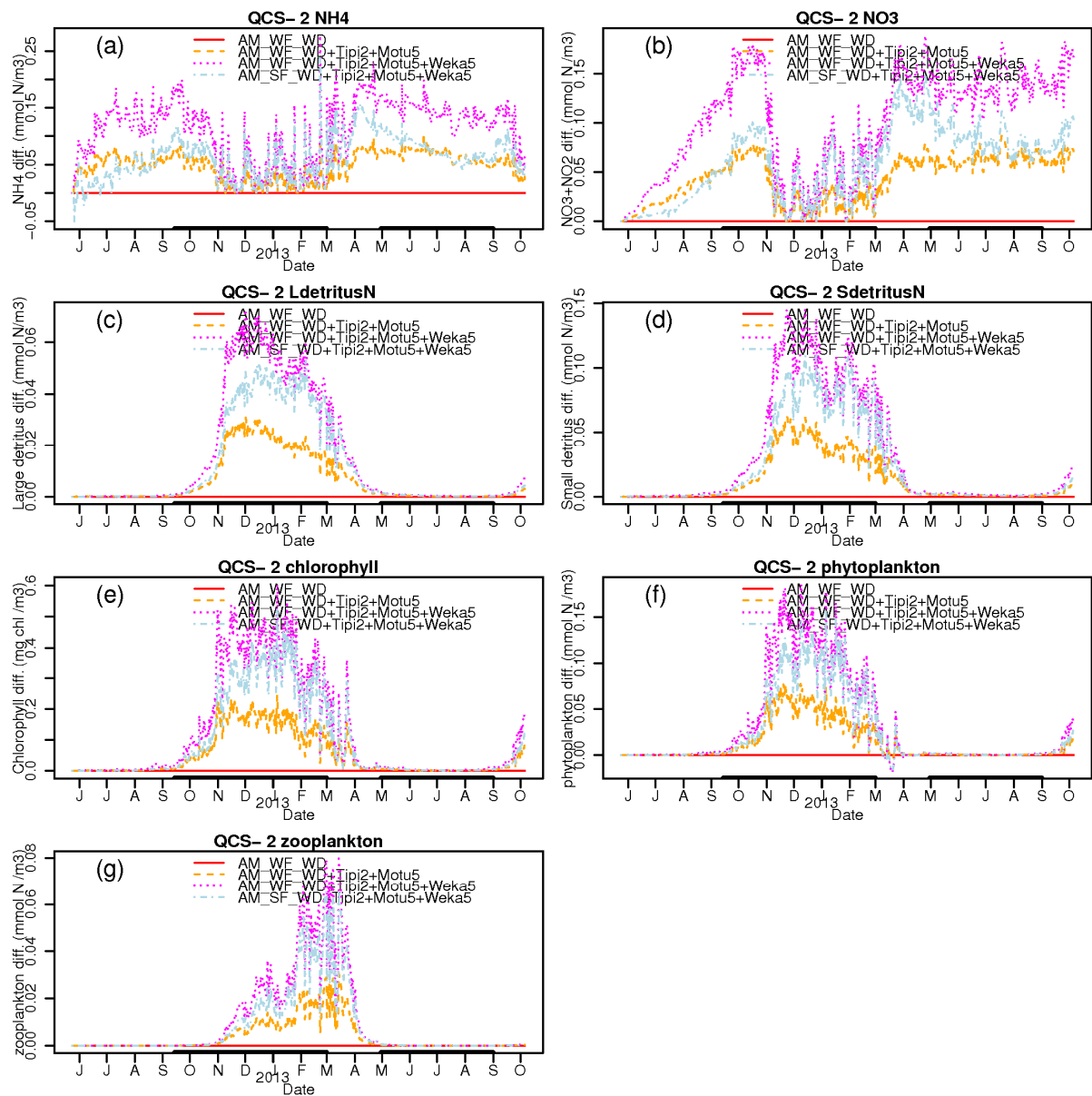


Figure C-2: Simulated dynamics of water-quality state-variables in the uppermost layer at station QCS-2 under differing single additional fish-farm scenarios. Dynamics are expressed as concentration change from the baseline_{f2016}, AM_AF_WD scenario. A value greater than 0.0 indicates that the concentration stemming from the alternative scenario exceeds that in the baseline_{f2016} scenario.

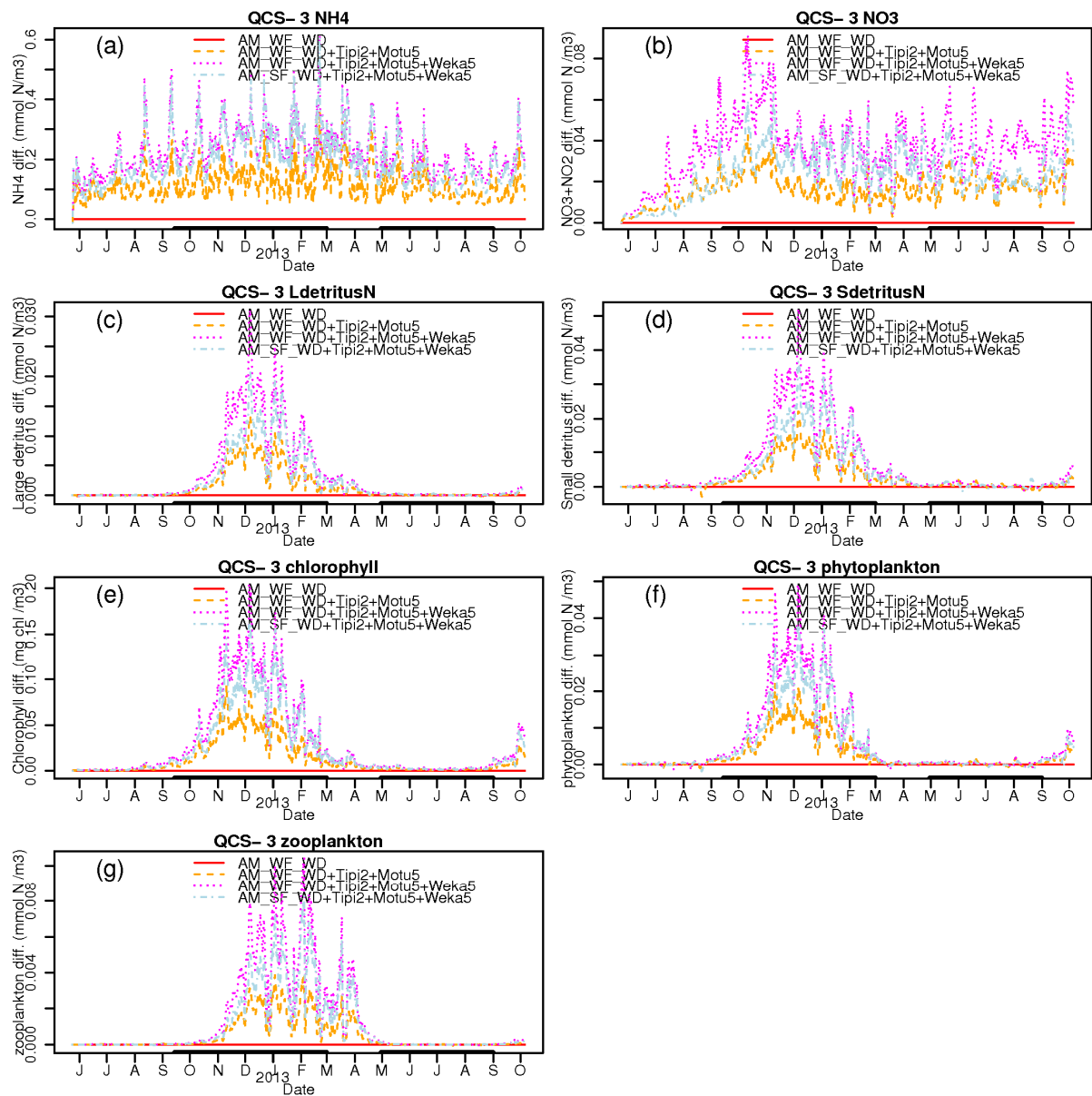


Figure C-3: Simulated dynamics of water-quality state-variables in the uppermost layer at station QCS-3 under differing single additional fish-farm scenarios. Dynamics are expressed as concentration change from the baseline_{f2016}, AM_AF_WD scenario. A value greater than 0.0 indicates that the concentration stemming from the alternative scenario exceeds that in the baseline_{f2016} scenario.

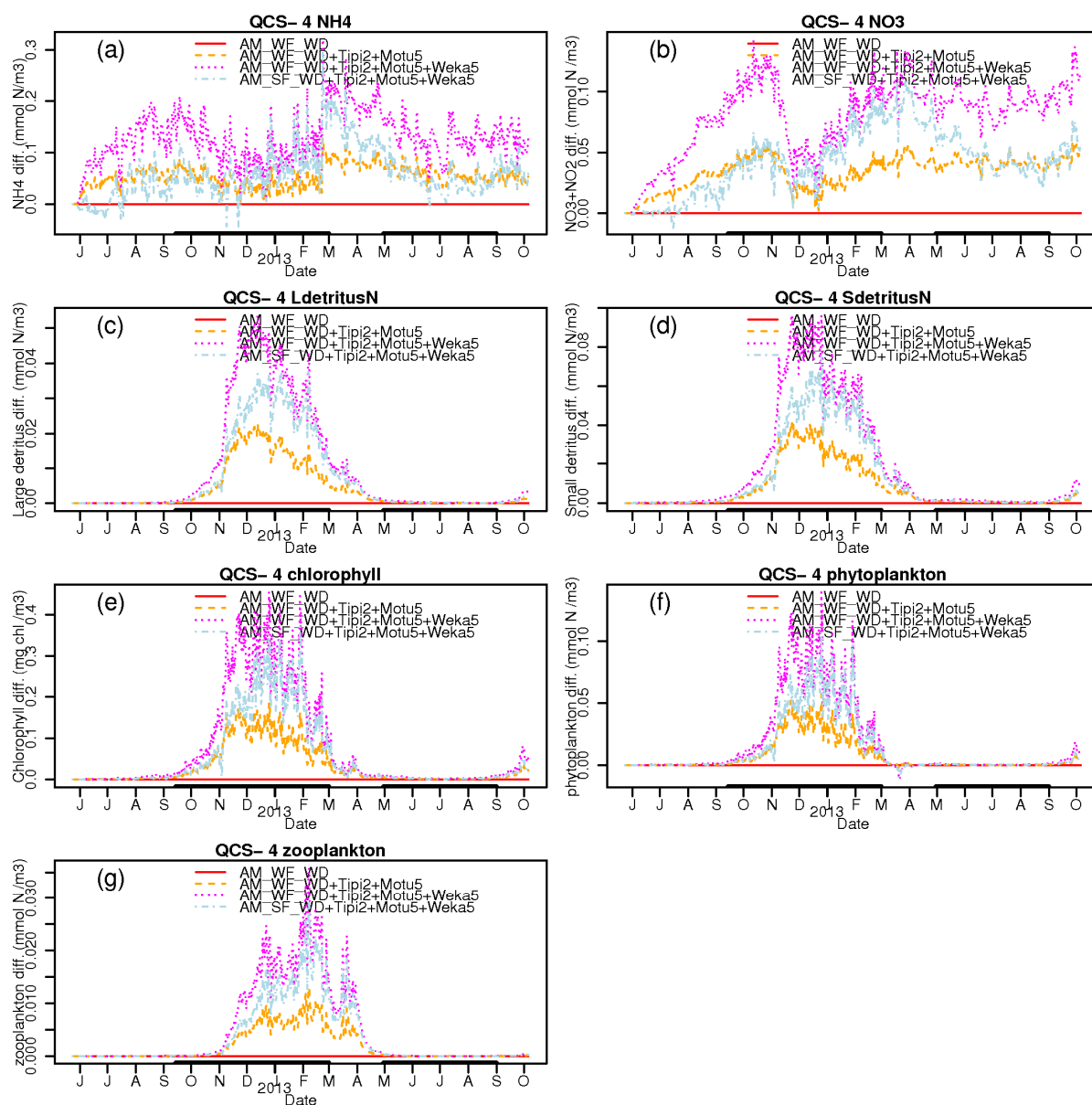


Figure C-4: Simulated dynamics of water-quality state-variables in the uppermost layer at station QCS-4 under differing single additional fish-farm scenarios. Dynamics are expressed as concentration change from the baseline_{f2016}, AM_AF_WD scenario. A value greater than 0.0 indicates that the concentration stemming from the alternative scenario exceeds that in the baseline_{f2016} scenario.

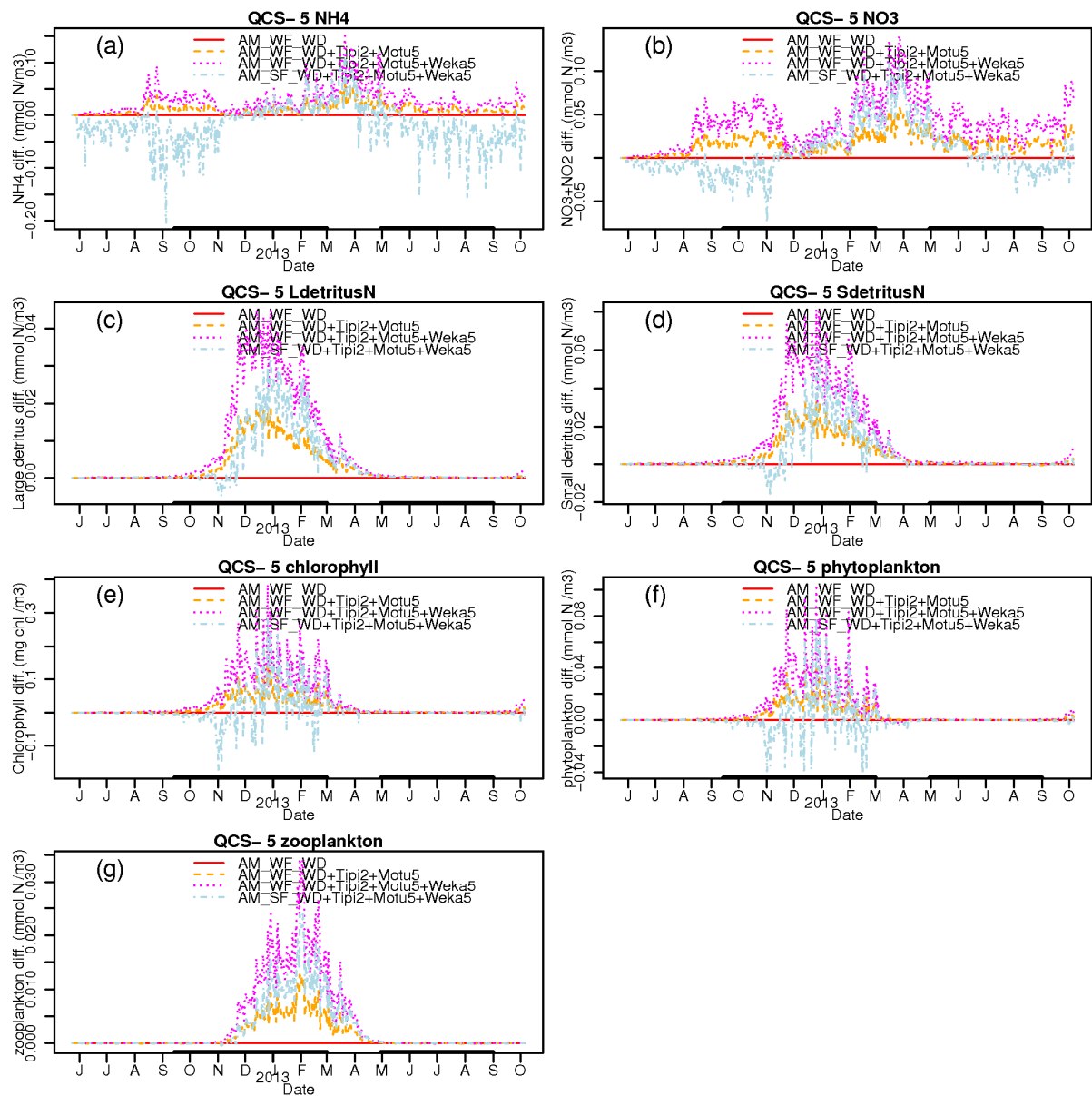


Figure C-5: Simulated dynamics of water-quality state-variables in the uppermost layer at station QCS-5 under differing single additional fish-farm scenarios. Dynamics are expressed as concentration change from the baseline_{f2016}, AM_AF_WD scenario. A value greater than 0.0 indicates that the concentration stemming from the alternative scenario exceeds that in the baseline_{f2016} scenario.

Appendix D Time-series from the multiple additional farm scenarios (relative concentration)

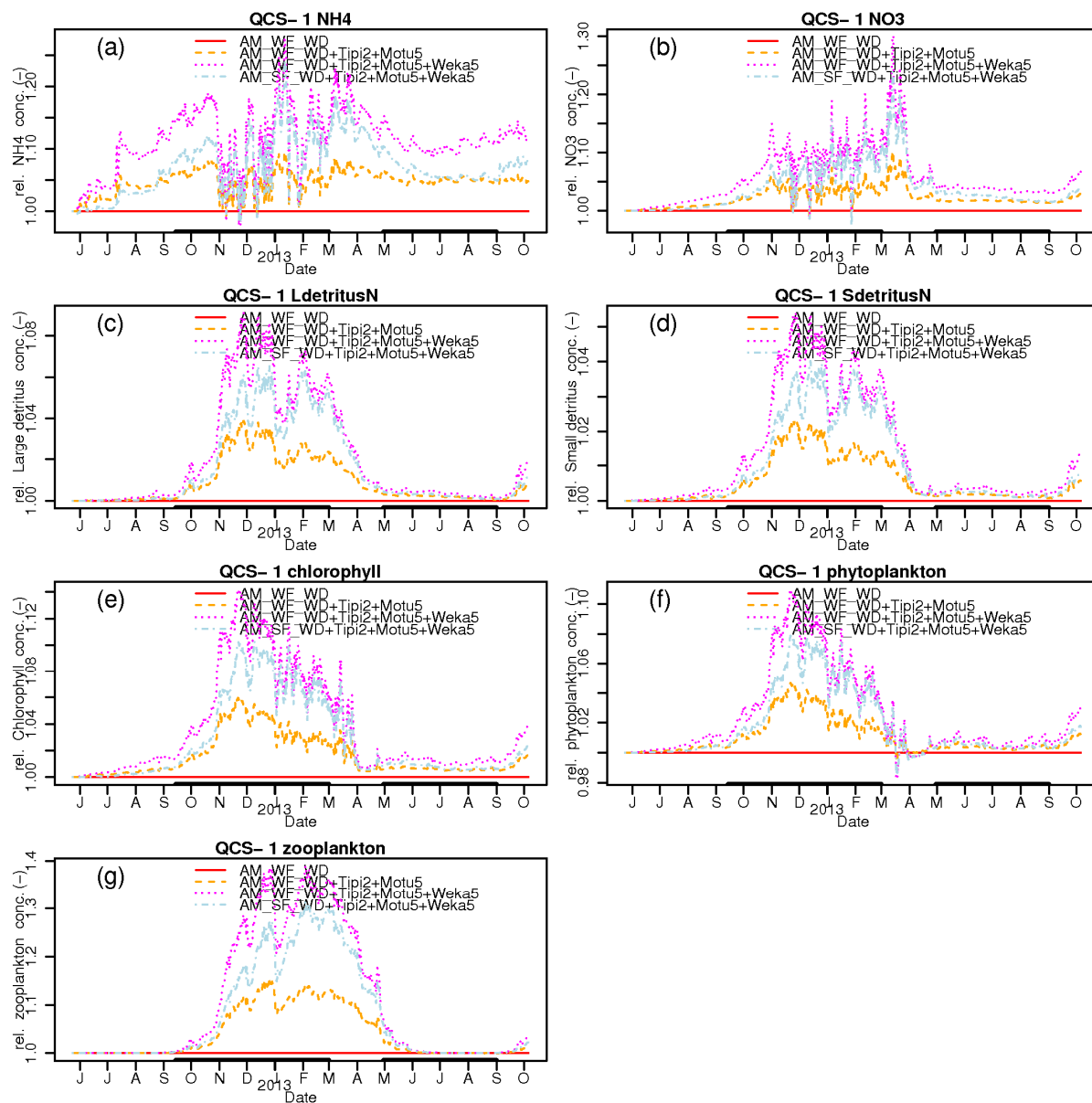


Figure D-1: Simulated dynamics of water-quality state-variables in the uppermost layer at station QCS-1 under differing multiple-additional fish-farm scenarios. Dynamics are expressed as concentration relative to the baseline_{f2016}, AM_AF_WD scenario. A value greater than 1.0 indicates that the concentration stemming from the alternative scenario exceeds that in the baseline_{f2016} scenario.

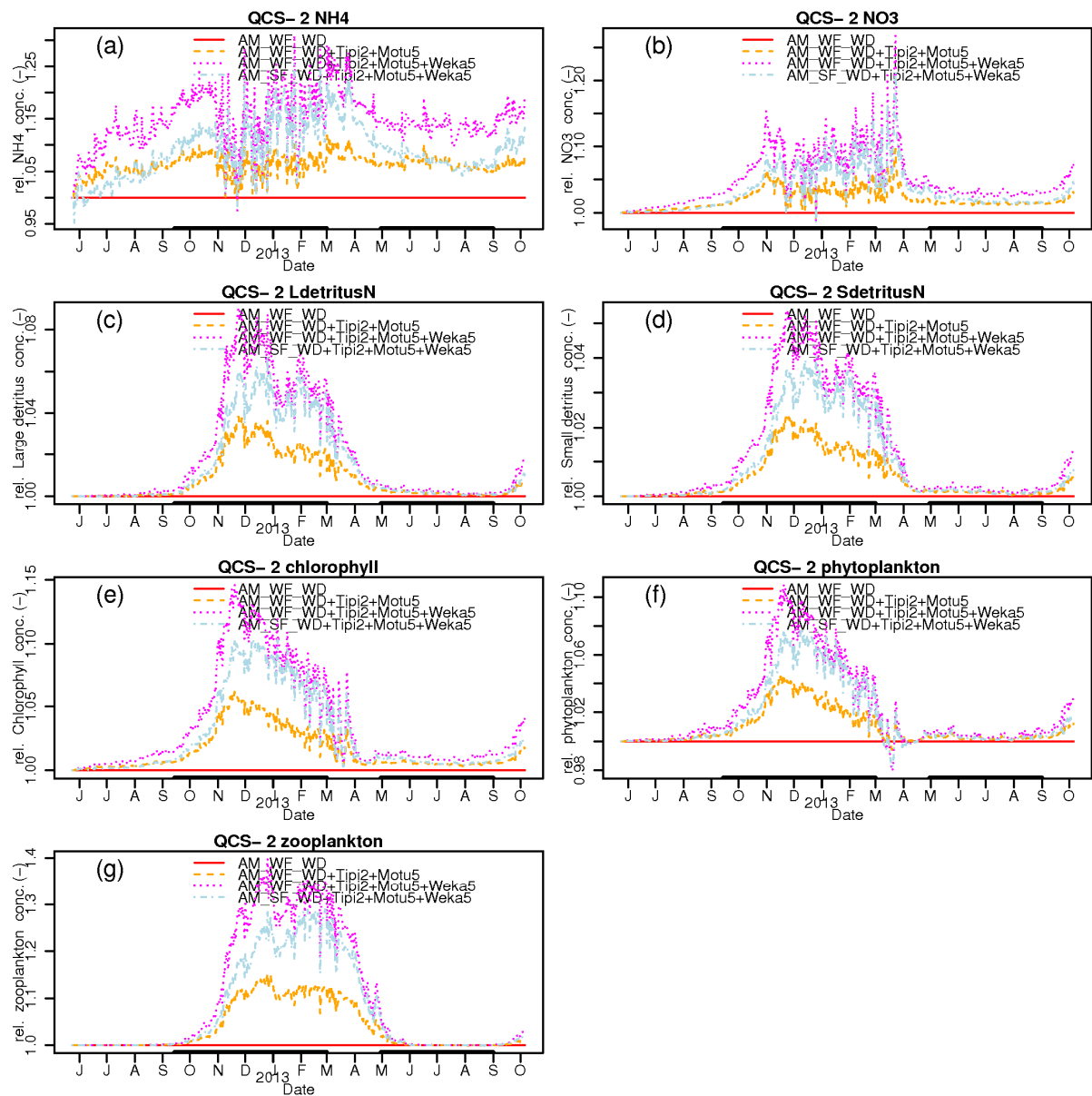


Figure D-2: Simulated dynamics of water-quality state-variables in the uppermost layer at station QCS-2 under differing multiple-additional fish-farm scenarios. Dynamics are expressed as concentration relative to the baseline_{f2016}, AM_AF_WD scenario. A value greater than 1.0 indicates that the concentration stemming from the alternative scenario exceeds that in the baseline_{f2016} scenario.

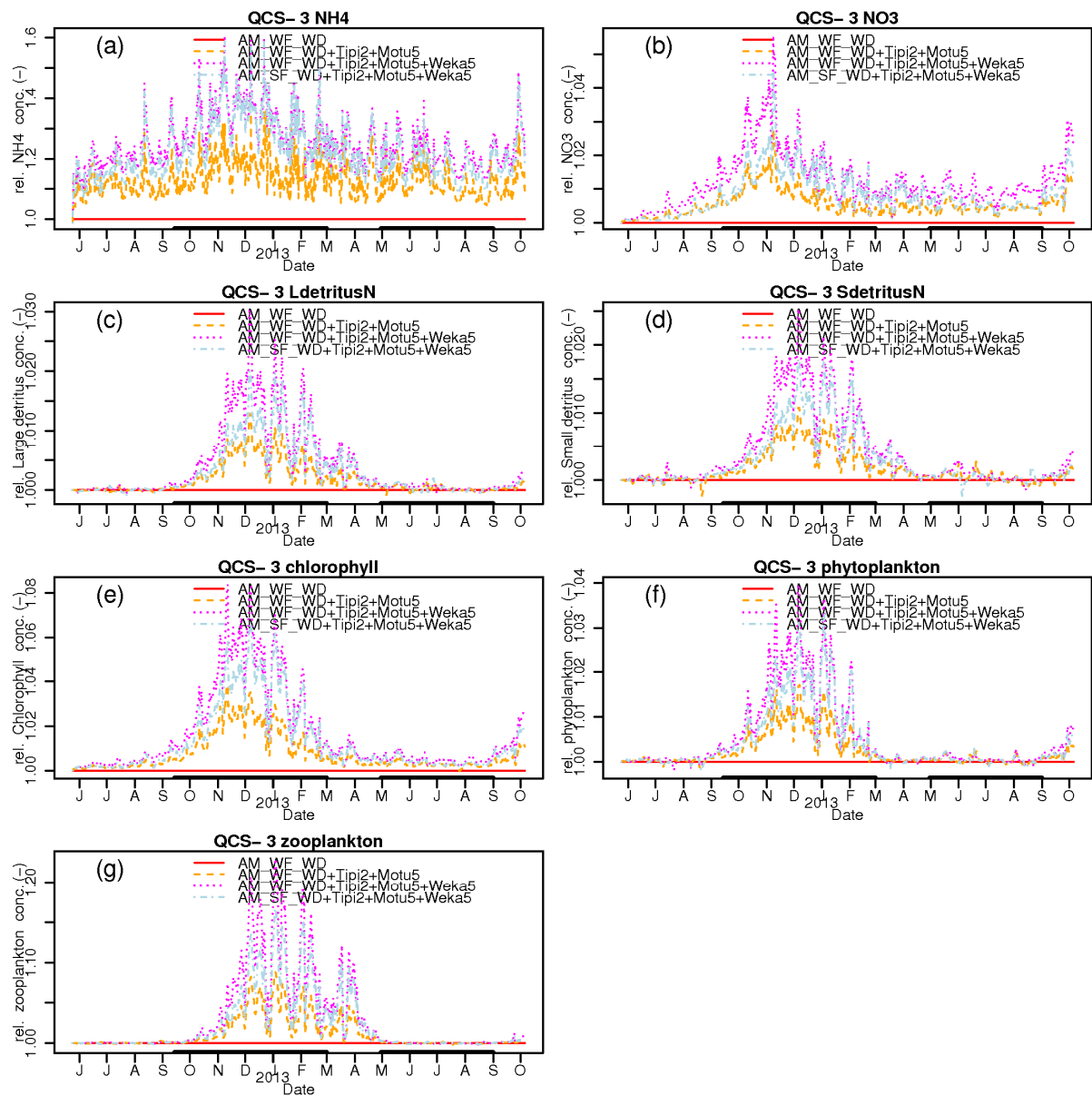


Figure D-3: Simulated dynamics of water-quality state-variables in the uppermost layer at station QCS-3 under differing multiple-additional fish-farm scenarios. Dynamics are expressed as concentration relative to the baseline_{f2016}, AM_AF_WD scenario. A value greater than 1.0 indicates that the concentration stemming from the alternative scenario exceeds that in the baseline_{f2016} scenario.

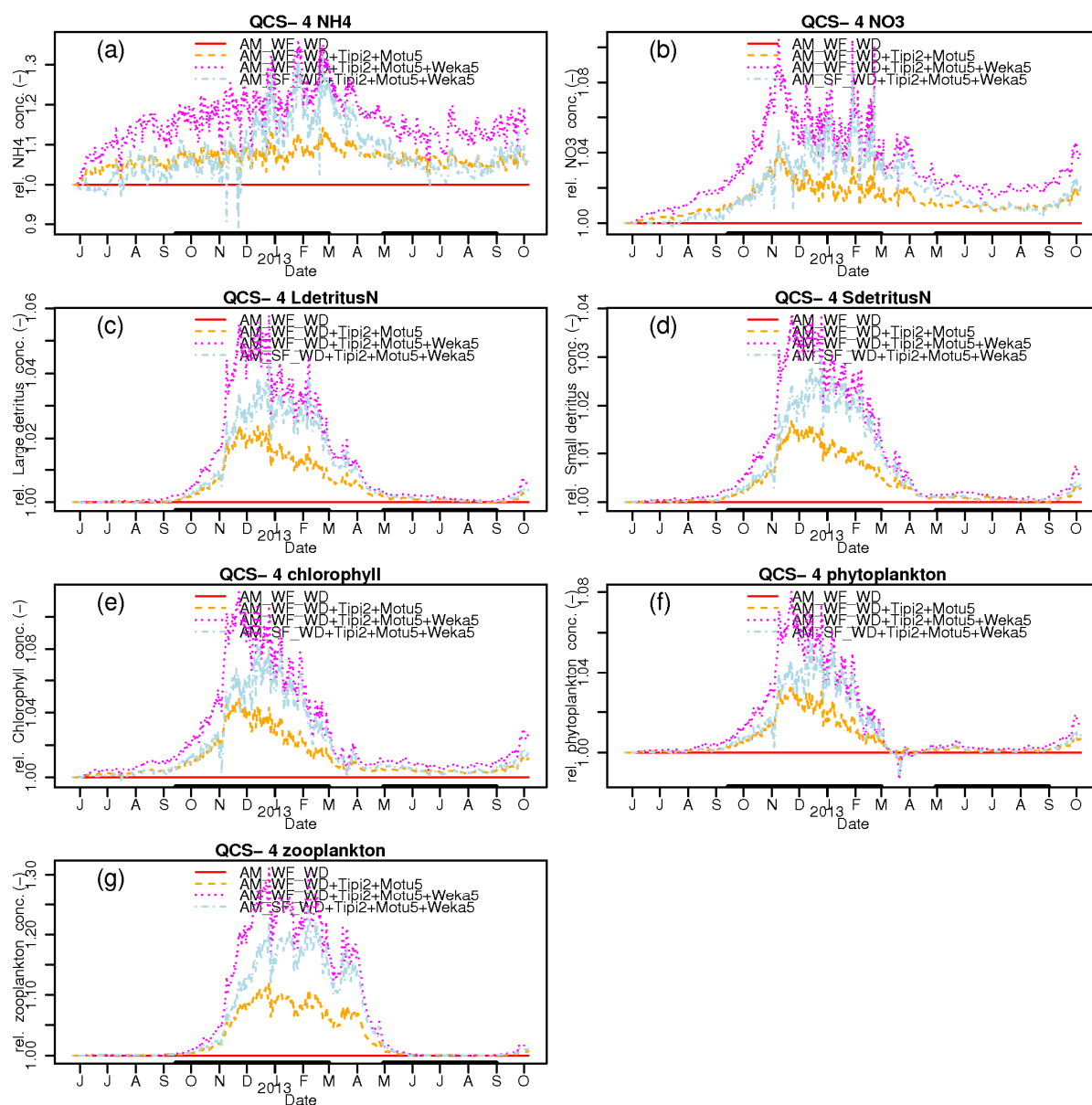


Figure D-4: Simulated dynamics of water-quality state-variables in the uppermost layer at station QCS-4 under differing multiple-additional fish-farm scenarios. Dynamics are expressed as concentration relative to the baseline_{f2016}, AM_AF_WD scenario. A value greater than 1.0 indicates that the concentration stemming from the alternative scenario exceeds that in the baseline_{f2016} scenario.

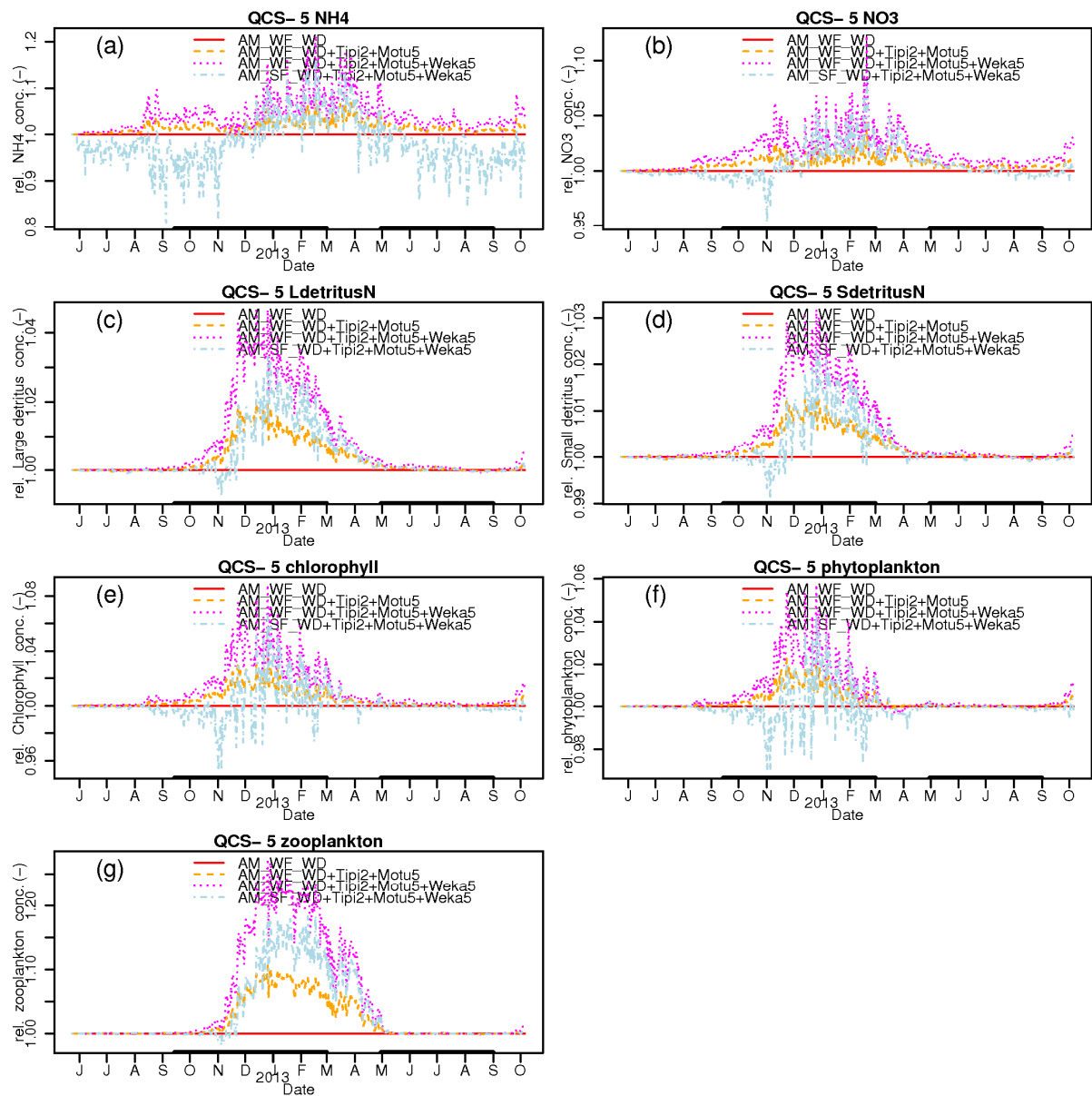


Figure D-5: Simulated dynamics of water-quality state-variables in the uppermost layer at station QCS-5 under differing multiple-additional fish-farm scenarios. Dynamics are expressed as concentration relative to the baseline_{f2016}, AM_AF_WD scenario. A value greater than 1.0 indicates that the concentration stemming from the alternative scenario exceeds that in the baseline_{f2016} scenario.

Appendix E Time-series of concentration difference between the baseline_{f2016}+Tipi2+Motu5+Weka5 (AM_AF_WD+Tipi2+Motu5+Weka5) and operating farms (EM_EF_WD) scenarios

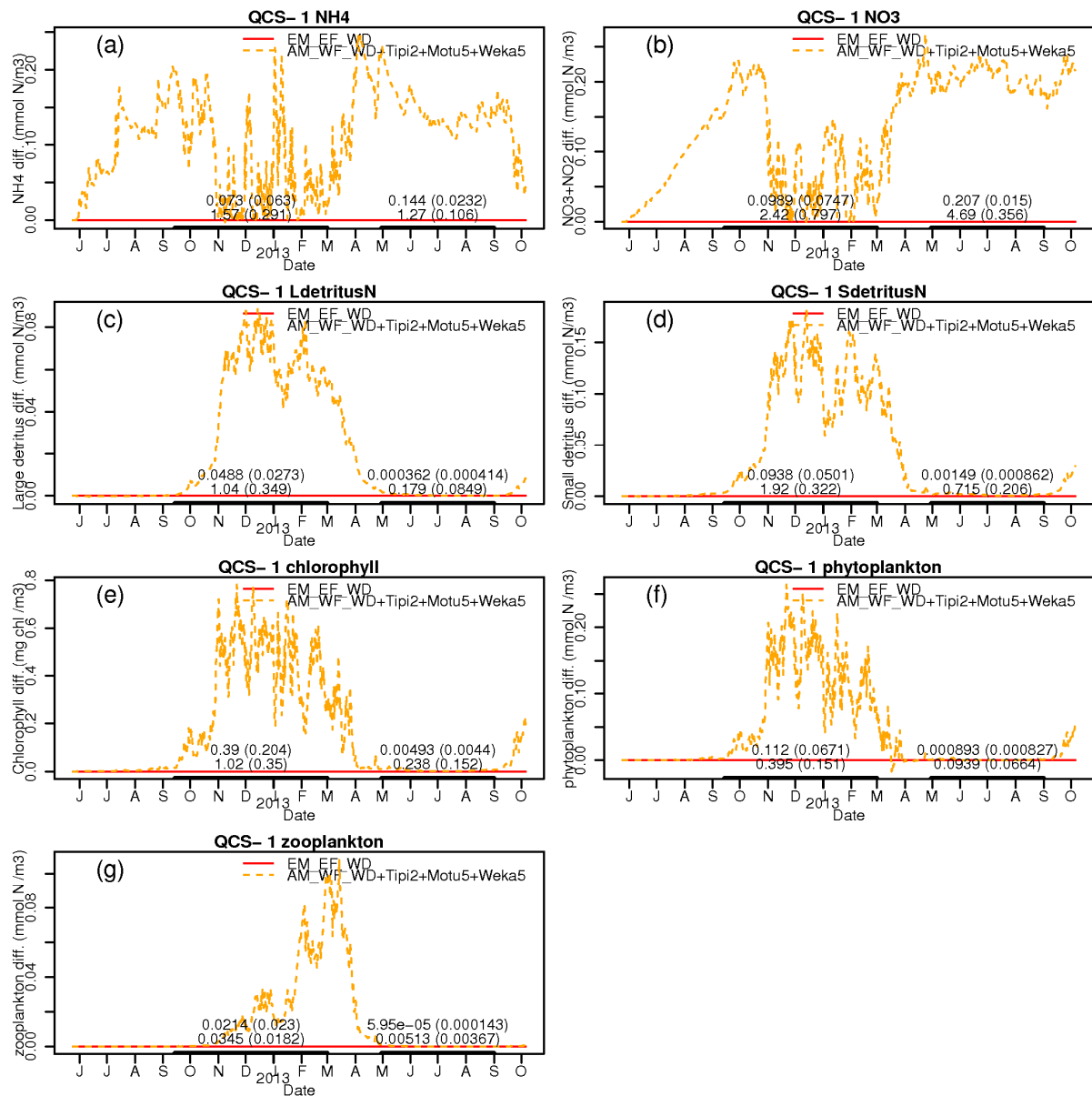


Figure E-1: Simulated dynamics of water-quality state-variables in the uppermost layer at station QCS-1. Dynamics are expressed as the concentration difference from a reference scenario (EM_EF_WD). A value in excess of 0.0 implies that the alternative scenario (AM_AF_WC+Tipi2+Motu5+Weka5) yields a concentration that is greater than the reference scenario (EM_EF_WD).

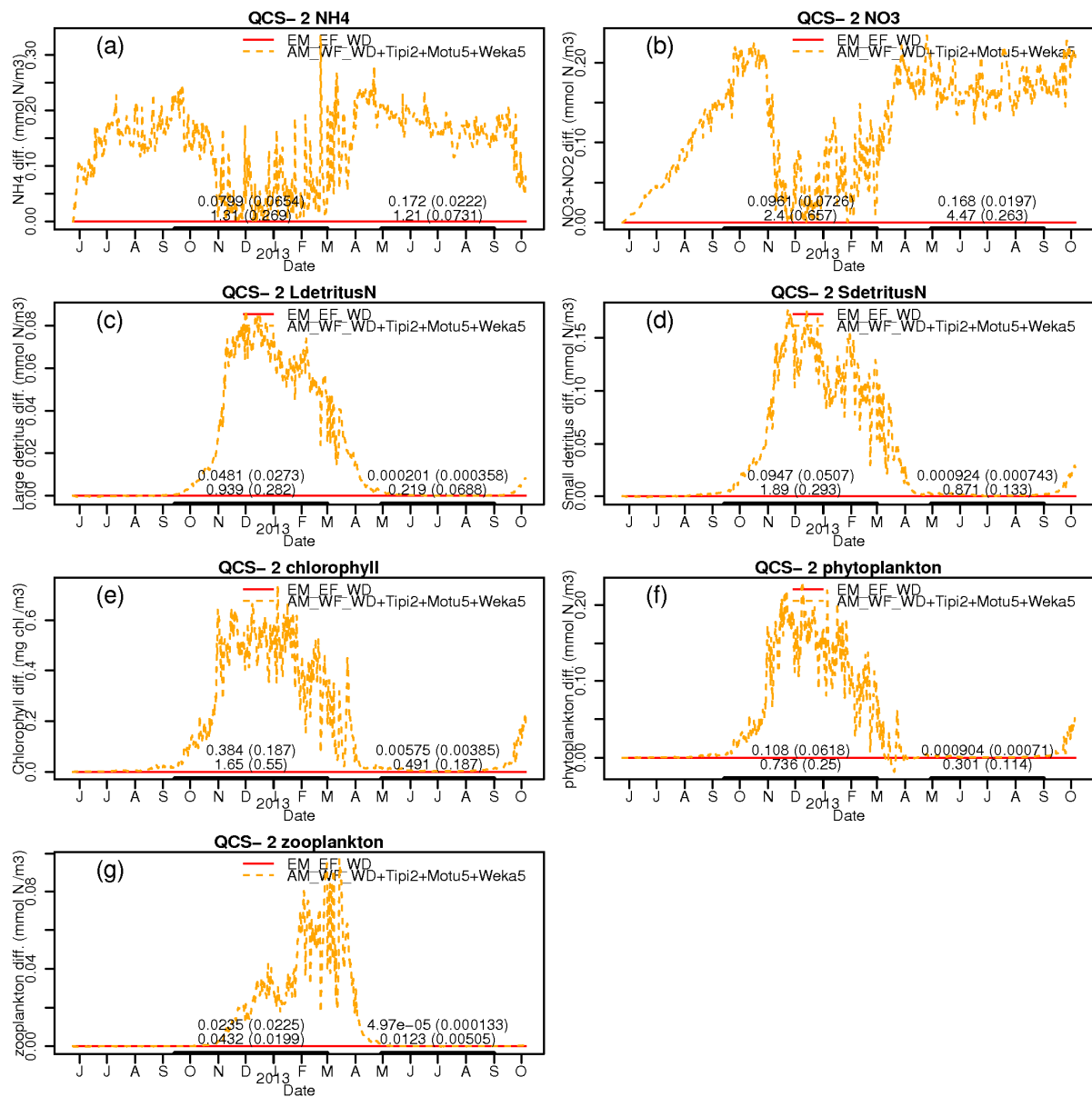


Figure E-2: Simulated dynamics of water-quality state-variables in the uppermost layer at station QCS-2 under differing single additional fish-farm scenarios. Dynamics are expressed as the concentration difference from a reference scenario (EM_EF_WD). A value in excess of 0.0 implies that the alternative scenario (AM_AF_WC+Tipi2+Motu5+Weka5) yields a concentration that is greater than the reference scenario (EM_EF_WD).

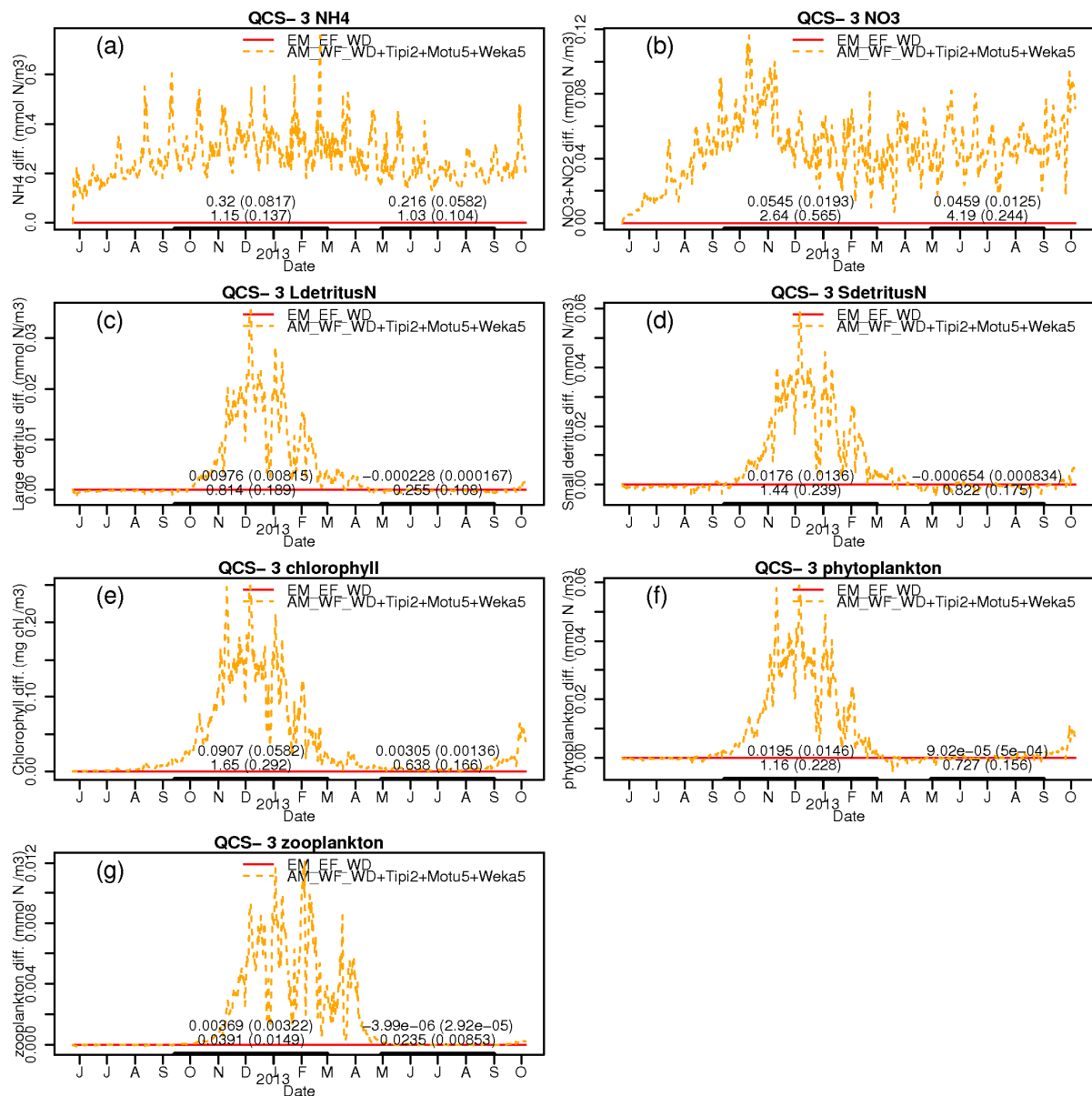


Figure E-3: Simulated dynamics of water-quality state-variables in the uppermost layer at station QCS-3 under differing single additional fish-farm scenarios. Dynamics are expressed as the concentration difference from a reference scenario (EM_EF_WD). A value in excess of 0.0 implies that the alternative scenario (AM_AF_WC+Tipi2+Motu5+Weka5) yields a concentration that is greater than the reference scenario (EM_EF_WD).

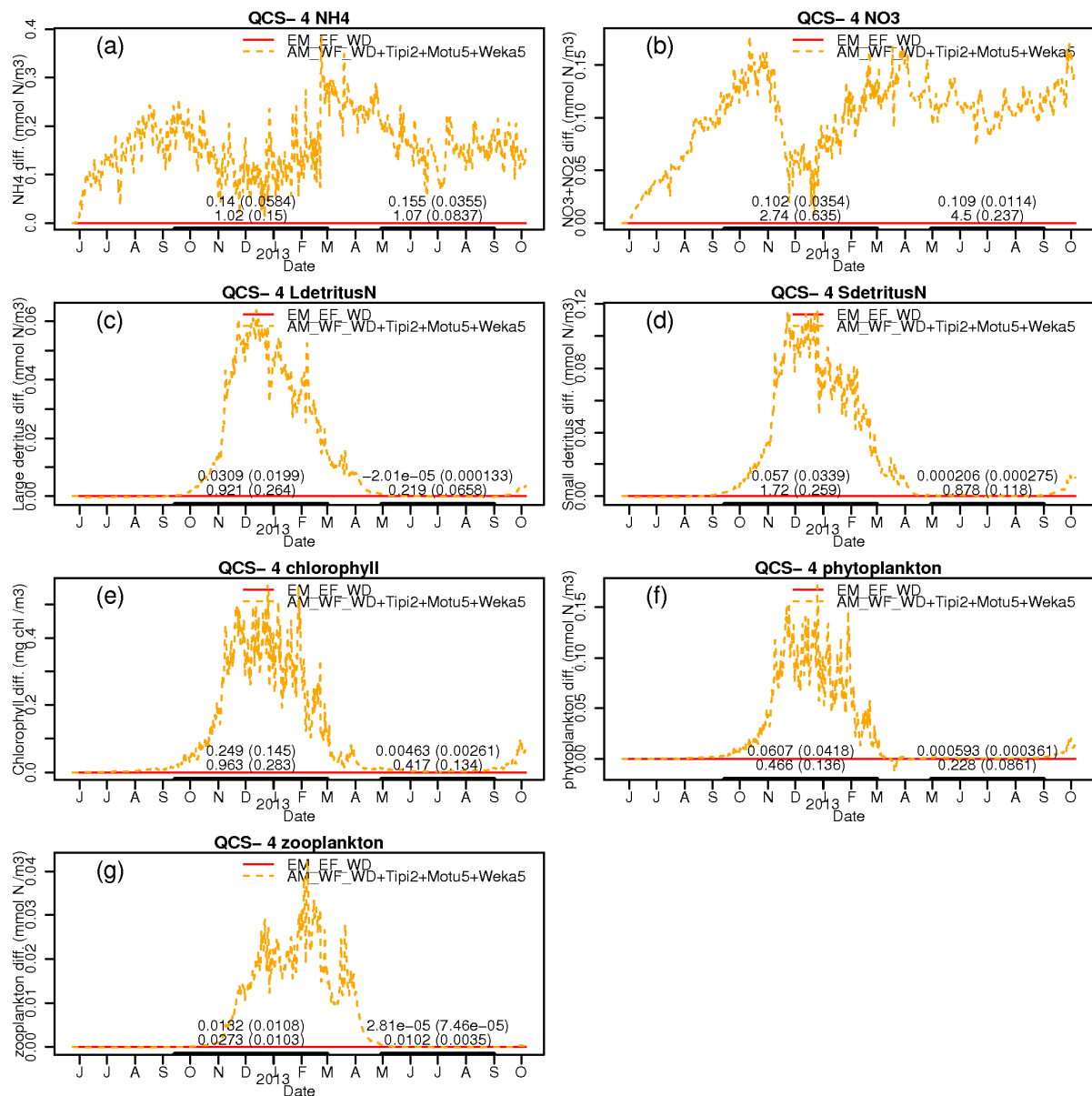


Figure E-4: Simulated dynamics of water-quality state-variables in the uppermost layer at station QCS-4 under differing single additional fish-farm scenarios. Dynamics are expressed as the concentration difference from a reference scenario (EM_EF_WD). A value in excess of 0.0 implies that the alternative scenario (AM_AF_WC+Tipi2+Motu5+Weka5) yields a concentration that is greater than the reference scenario (EM_EF_WD).

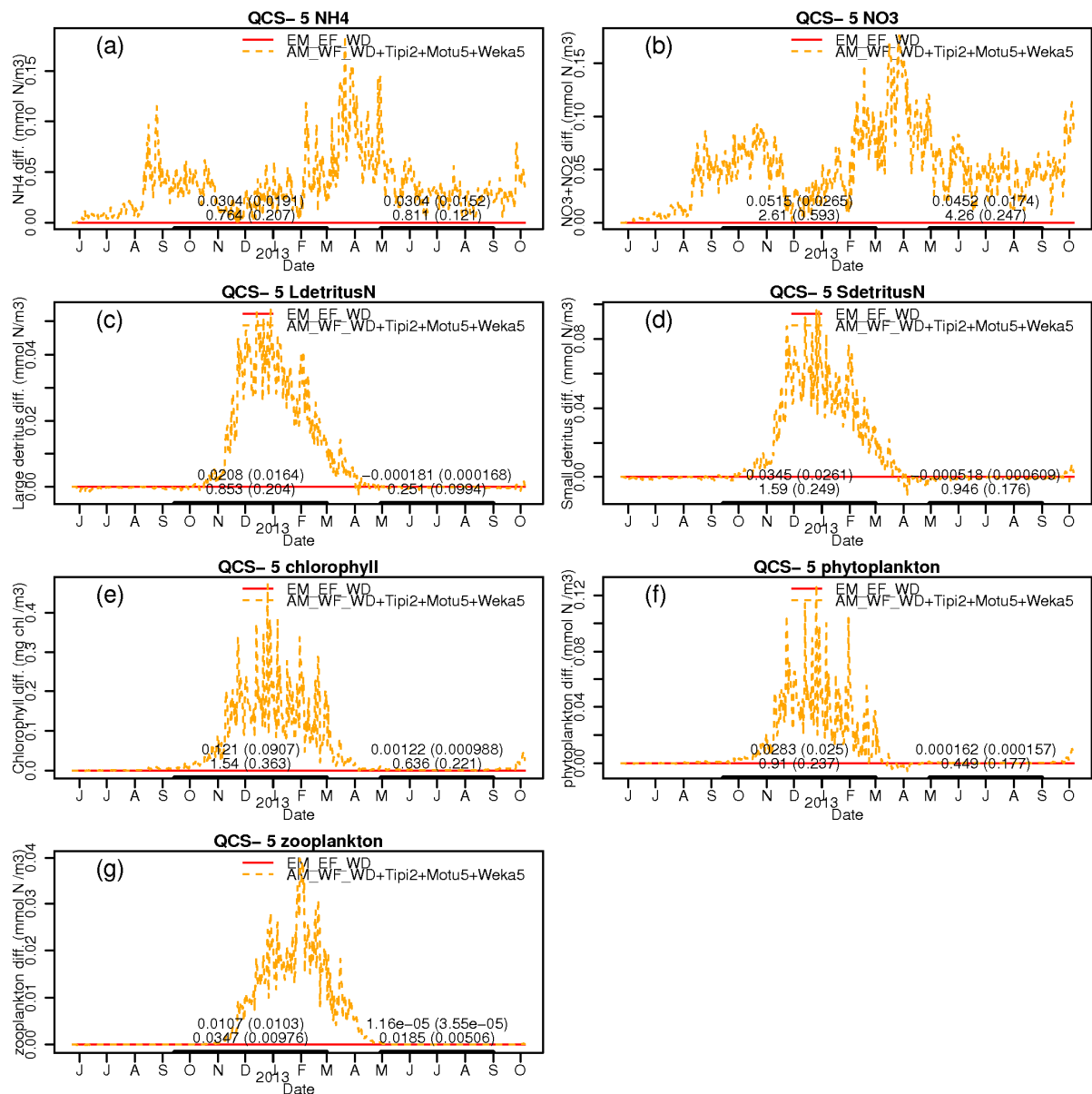


Figure E-5: Simulated dynamics of water-quality state-variables in the uppermost layer at station QCS-5 under differing single additional fish-farm scenarios. Dynamics are expressed as the concentration difference from a reference scenario (EM_EF_WD). A value in excess of 0.0 implies that the alternative scenario (AM_AF_WC+Tipi2+Motu5+Weka5) yields a concentration that is greater than the reference scenario (EM_EF_WD).